Russian Original Vol. 37, No. 5, November, 1974

May, 1975

SATEAZ 37(5) 1133-1222 (1974)

SOVIET ATOMIC ENERGY

АТОМНАЯ ЭНЕРГИЯ
(ATOMNAYA ENERGIYA)

TRANSLATED FROM RUSSIAN

CONSULTANTS BUREAU, NEW YORK

SOVIET ATOMIC ENERGY

Soviet Atomic Energy is a cover-to-cover translation of *Atomnaya Énergiya*, a publication of the Academy of Sciences of the USSR.

An agreement with the Copyright Agency of the USSR (VAAP) makes available both advance copies of the Russian journal and original glossy photographs and artwork. This serves to decrease the necessary time lag between publication of the original and publication of the translation and helps to improve the quality of the latter. The translation began with the first issue of the Russian journal.

Consultants Bureau journals appear about six months after the publication of the original Russian issue. For bibliographic accuracy, the English issue published by Consultants Bureau carries the same number and date as the original Russian from which it was translated. For example, a Russian issue published in December will appear in a Consultants Bureau English translation about the following June, but the translation issue will carry the December date. When ordering any volume or particular issue of a Consultants Bureau journal, please specify the date and, where applicable, the volume and issue numbers of the original Russian. The material you will receive will be a translation of that Russian volume or issue.

Subscription
$87.50 per volume (6 Issues)

Single Issue: $50
Single Article: $15

Prices somewhat higher outside the United States.

CONSULTANTS BUREAU, NEW YORK AND LONDON

227 West 17th Street
New York, New York 10011

4a Lower John Street
London W1R 3PD
England

Published monthly. Second-class postage paid at Jamaica, New York 11431.

Soviet Atomic Energy is abstracted or indexed in *Applied Mechanics Reviews, Chemical Abstracts, Engineering Index, INSPEC—Physics Abstracts and Electrical and Electronics Abstracts, Current Contents,* and *Nuclear Science Abstracts.*

SOVIET ATOMIC ENERGY

A translation of *Atomnaya Énergiya*

May, 1975

Volume 37, Number 5 November, 1974

CONTENTS

CONTENTS

(continued)

The Russian press date (podpisano k pechati) of this issue was 10/23/1974. Publication therefore did not occur prior to this date, but must be assumed to have taken place reasonably soon thereafter.

ARTICLES

EXTRACTION OF AMERICIUM, CURIUM, STRONTIUM, AND THE RARE EARTH ELEMENTS FROM AQUEOUS WASTE SOLUTIONS OF THE REPROCESSING OF SPENT FUEL CELLS OF VVÉR REACTORS

V. B. Shevchenko, V. S. Smelov,
A. G. Kozlov, V. V. Chubukov,
V. P. Lanin, and É. Ya. Smetanin

UDC 621.039.59

In this work we discuss questions of the theoretical substantiation of conditions providing for the quantitative extraction of strontium, americium, curium, and rare earth elements from aqueous solution and the systems of fractional separation of these elements on operations of their reextraction using di-2-ethylhexylphosphoric acid (D2EHPA). The successful practical utilization of the systems developed is illustrated by the example of the extraction and separation of strontium, americium, curium, and the rare earth elements from an aqueous waste solution from the regeneration of spent fuel cells of the VVÉR.

The distribution of elements between the organic and aqueous phases was monitored with the aid of the ratioisotopes ^{137}Cs, ^{22}Na, ^{86}Rb, ^{110}Ag, ^{133}Ba, ^{45}Ca, ^{90}Sr, ^{65}Zn, ^{54}Mn, ^{60}Co, ^{51}Cr, ^{63}Ni, ^{144}Ce, ^{241}Am, ^{244}Cm. The purification of D2EHPA was accomplished by a combination of two methods [1, 2].

Taking into consideration the possibility of the formation of complex compounds in the organic solution, and hydrolytic mixtures in the aqueous solution, as well as considering the dimerization of D2EHPA in the investigated diluents, the equation of extraction can be represented in the form

$$M(OH)_{z_b}^{m-z} + qA_b^- + nH_2K_{2(0)} \rightleftarrows M(OH)_z(A)_q(HK_2)_{m-z-q_0} + xH_b^+ \quad (1)$$

(here and henceforth HK is the D2EHPA monomer; A^- is the anion of the aqueous medium).

From the equation it follows that the thermodynamic constant of extraction is expressed as follows:

$$K = \frac{(M(OH)_z(A^-)_q(HK_2)_{m-z-q})(H^+)^x}{(M(OH)_z^{m-z})(A^-)^q(H_2K_2)^n}. \quad (2)$$

The indices denoting the phases are omitted. If we replace the activities of the compounds and ions by the concentration and assume that in an aqueous solution the concentration of various forms of the element can be considered negligible in comparison with the concentration of the free cations, then

$$K = \frac{E[H^+]^x}{[A^-]^q[H_2K_2]^n}, \quad (3)$$

where E is the distribution coefficient of the elements between the organic and aqueous phases. Solving this equation relative to E, after taking the logarithm, we obtain

$$\lg E = \lg K + q\lg[A^-] + n\lg[H_2K_2] - x\lg[H^+]. \quad (4)$$

At a constant concentration of hydrogen ions and anions of the aqeuous medium, Eq. (4) expresses the dependence of the distribution coefficient on the D2EHPA concentration:

$$\lg E = \lg K + n\lg[H_2K_2]. \quad (5)$$

Two more equations can be obtained analogously:

Translated from Atomnaya Énergiya, Vol. 37, No. 5, pp. 379-383, November, 1974. Original article submitted July 1, 1974.

TABLE 1. Indices n and x Obtained Experimentally in the Extraction of the Elements with D2EHPA

Element	n	x	Element	n	x
Na	2	1	Ba	2	2
Rb	2	1	Zn	1,5	2
Cs	2	1	Cr (III)	2	2
Ag	1,5	1	Mn (II)	2	2
Ca	2	2	Co (II)	2	2
Sr	2	2	Ni	2	2

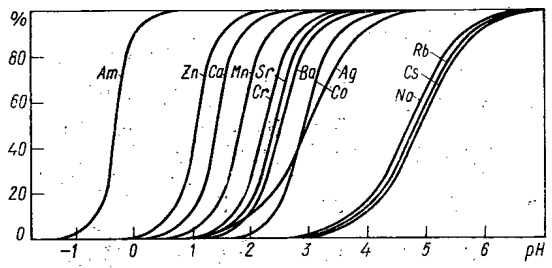

Fig. 1. Dependence of the percent extraction of the elements on the pH values.

$$\lg E = \lg K + q \lg [A^-] \quad \text{when } [H_2K_2] \text{ and } [H^+] - = \text{const} \tag{6}$$

and

$$\lg E = \lg K - x \lg [H^+] \quad \text{when } [H_2K_2] \text{ and } [A^-] - = \text{const.} \tag{7}$$

The construction of the corresponding dependences permits a determination of the indices n, q, and x, characterizing the process of interaction of the metal ion with D2EHPA.

The experimentally obtained dependences of E of most metals on the D2EHPA and hydrogen ion concentrations (diluent: n-decane, nitric acid medium, the ionic strength J is equal to 0.1) are cited in Table 1.

In an investigation of the influence of the nitrate ion concentration on extraction, it was established that the distribution coefficients remain practically constant within the interval of nitrate ion concentrations 0.01-0.1 M, i.e., q ≈ 0. From this it follows that the participation of nitrate ions in the processes under consideration is negligible, and it can be neglected.

For other diluents, as a rule, analogous values of n, q, and x were obtained. Exceptions are the dependences of the distribution coefficients of sodium, rubidium, and cesium on [D2EHPA] in the case of dilution of the latter with n-octane (in this case n = 1), as well as the dependences of E_{Zn} on D2EHPA when it is diluted with benzene, carbon tetrachloride, o-xylene, and chloroform (n = 2).

It should be noted that when the diluent of D2EHPA is replaced in the series of saturated hydrocarbons from hexane to tridecane, a small increase in the distribution coefficients is observed.

Assuming the existence of a dimer of D2EHPA and the extractable compounds in the form of uncharged complexes in organic solution, as well as assuming the absence of appreciable amounts of polynuclear complexes, considering the experimental results, the equations of extraction can be represented as follows:

for singly charged cations

$$M^+ + 2H_2K_2 \rightleftarrows M(HK_2)(HK)_2 + H^+; \tag{8}$$

for doubly charged cations

$$M^{2+} + 2H_2K_2 \rightleftarrows M(HK_2)_2 + 2H^+. \tag{9}$$

exceptions are silver and zinc, which are extracted by D2EHPA diluted with n-decane according to the equations

$$M^+ + 1.5H_2K_2 \rightleftarrows M(HK_2)\,HK + H^+; \tag{10}$$

$$M^{2+} + 1.5H_2K_2 \rightleftarrows MK_2 \cdot HK + 2H^+, \tag{11}$$

as well as alkali and alkaline earth metals, extracted by D2EHPA in n-octanol according to the equations

$$M^+ + HK \rightleftarrows MK + H^+; \tag{12}$$

$$M^{2+} + 2HK \rightleftarrows MK_2 + 2H^+. \tag{13}$$

When D2EHPA is diluted with n-octanol, it reacts with metals in the monomer state [3].

It is known that trivalent chromium is a readily hydrolyzable element. It has been established [4] that in the region of pH = 2-4.5, the partially hydrolyzed chromium cation $Cr(OH)^{2+}$ predominates, the

TABLE 2. Constants of Extraction of Elements at J = 0.1

Diluent	Na	Rb	Cs	Ag
n-Decane	$(8,5\pm0,8)\cdot10^{-4}$	$(7,3\pm0,7)\cdot10^{-4}$	$(6,5\pm0,7)\cdot10^{-4}$	$(1,4\pm0,2)\cdot10^{-2}$
Benzene	$(5,4\pm0,5)\cdot10^{-5}$		$(5,4\pm0,5)\cdot10^{-5}$	—
Carbon tetrachloride	$(3,2\pm0,3)\cdot10^{-4}$	$(2,3\pm0,2)\cdot10^{-4}$	$(1,4\pm0,2)\cdot10^{-4}$	—
o-Xylene	$(1,6\pm0,2)\cdot10^{-4}$	$(7,6\pm0,8)\cdot10^{-5}$	—	—
n-Octanol	$(2,9\pm0,2)\cdot10^{-4}$	$(2,7\pm0,3)\cdot10^{-4}$	$(2,1\pm0,1)\cdot10^{-4}$	—
Chloroform				

Diluent	Ca *	Sr	Ba	Zn
n-Decane	$(2,6\pm0,3)\cdot10^{-2}$	$(4,7\pm0,5)\cdot10^{-4}$	$(1,6\pm0,2)\cdot10^{-4}$	$(9,0\pm0,8)\cdot10^{-2}$
Benzene	$(2,9\pm0,3)\cdot10^{-5}$	$(5,2\pm0,5)\cdot10^{-6}$	$(3,1\pm0,3)\cdot10^{-6}$	$(5,0\pm0,2)\cdot10^{-2}$
Carbon tetrachloride	$(1\pm0,2)\cdot10^{-3}$	$(3,3\pm0,3)\cdot10^{-5}$	$(1,4\pm0,2)\cdot10^{-5}$	$(6,5\pm0,8)\cdot10^{-2}$
o-Xylene	—	—	—	$(6,0\pm0,5)\cdot10^{-2}$
n-Octanol	$(5,6\pm0,6)\cdot10^{-5}$	$(2\pm0,2)\cdot10^{-5}$	$(1,1\pm0,2)\cdot10^{-5}$	—
Chloroform				$(2,5\pm0,3)\cdot10^{-2}$

Diluent	Cr (III) †	Mn (II)	Co (II)	Ni †
n-Decane	$(2,4\pm0,4)\cdot10^{-3}$	$(8,6\pm0,7)\cdot10^{-3}$	$(6,0\pm0,9)\cdot10^{-5}$	$(3,9\pm0,6)\cdot10^{-6}$
Benzene	$(2,3\pm0,3)\cdot10^{-4}$	$(3,3\pm0,4)\cdot10^{-4}$	$(3,3\pm0,3)\cdot10^{-5}$	$(1,6\pm0,1)\cdot10^{-7}$
Carbon tetrachloride	$(2,8\pm0,2)\cdot10^{-4}$	$(1,2\pm0,1)\cdot10^{-3}$	$(3,5\pm0,4)\cdot10^{-5}$	$(5,7\pm0,3)\cdot10^{-7}$
o-Xylene	$(2,2\pm0,4)\cdot10^{-4}$	$(6,0\pm0,5)\cdot10^{-4}$	—	—
n-Octanol	—	—	—	—
Chloroform	$(1,6\pm0,3)\cdot10^{-4}$	$(1,6\pm0,2)\cdot10^{-4}$	$(2,5\pm0,4)\cdot10^{-5}$	$(1,3\pm0,1)\cdot10^{-7}$

* $J = 0,23$.
† $J = 0,05$.

instability constant of which is equal to $1.02\cdot10^{-10}$. From this the equation of the extraction of trivalent chromium into D2EHPA can be represented in the form

$$Cr(OH)^{2+} + 2H_2K_2 \rightleftharpoons Cr(OH)(HK_2)_2 + 2H^+. \quad (14)$$

Examples are known, indicating the extraction of such compounds. For example, the distance of hydrolyzed complexes of thorium, zirconium, bismuth, protactinium [7], and iron [8, 9] in solutions of D2EHPA has been established.

Table 2 presents the values of the constants of extraction of the investigated elements, calculated on the basis of the experimental principles obtained.

Some thermodynamic parameters of the extraction of rare earth elements by D2EHPA and questions of the influence of temperature on the distribution and separation coefficients of these elements were discussed in [5, 6].

Figure 1 presents the dependence of the percent extraction of the investigated metals on the pH value (the data on the distribution of americium were taken from [10]). From this dependence it follows that in the case of reextraction from D2EHPA, separation of americium, alkali, alkaline earth, and other elements by selection of the corresponding hydrogen ion concentration can be successfully accomplished.

Recently a number of principles determining the influence of the nature of the diluent on extraction with neutral phosphorus-containing compounds [11] and salts of amines [12, 13] have been established. It was shown that a linear dependence of the logarithms of the constants of extraction on the parameters of the diluent, characterizing the ability of electrophilic diluents to solvate the nucleophilic portions of the molecules of these extraction reagents, is observed. For extraction according to a cation exchange mechanism, which is associated with a substantial change in the polarity of the molecules in the organic phase, the nature of the dependence of the extraction constants on the nature of the diluent evidently will be somewhat different. The parameters of the diluents (PD) were taken from [12, 13]: n-decane (−1.0); o-xylene (1.0); carbon tetrachloride (1.8); benzene (2.5); chloroform (4.5). It should be noted that the diluents used in the work were purified according to the well known methods [14]. Figure 2 shows the dependence of the logarithm of the extraction constant on the PD. For comparison, the results of the influence of the nature

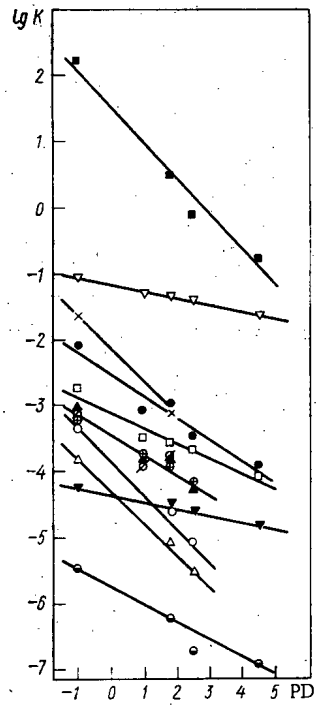

Fig. 2

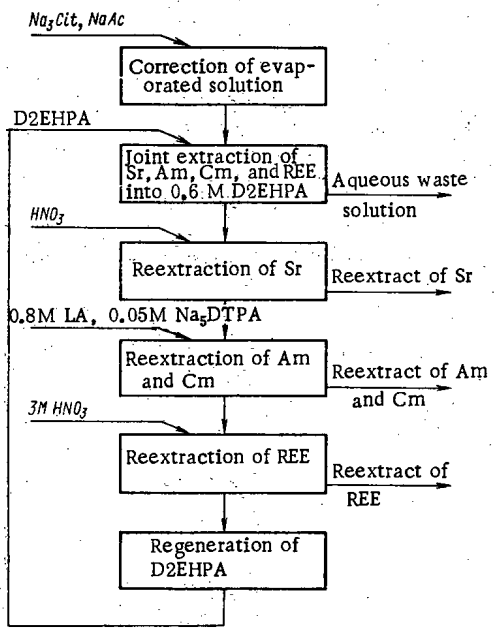

Fig. 3

Fig. 2. Dependence of the logarithm of the extraction constant on the parameter of the diluent (PD): ▲) Na; ϕ) Rb; ⊕) Cs; ○) Sr; △) Ba; ▽) Zn; ●) Mn (II); ▼) Co (II); ■) Am (III) when J = 0.1; ×) Ca when J = 0.23; □) Cr and ◒) Ni when J = 0.05.

Fig. 3. Principal technological scheme of the extraction of americium, curium, strontium, and the rare earth elements from aqueous waste solutions of the processing of spent fuel cells of VVÉR reactors.

TABLE 3. Distribution of Strontium, Americium, Curium, and the Rare Earth Elements Among Products of the Technological (Extraction) scheme, % of the Initial Value

Product	Sr	Am (III)	Cm (III)	REE (III)
Aqueous waste solution	2,5	3,0	3,0	3,0
Reextract of strontium	95,0	1,5	1,5	1,6
Reextract of americium and curium	0,08	92,0	92,0	0,015
Reextract of rare earth elements	0,04	1,0	1,0	94
Total balance	97,6	97,5	97,5	98,6

of the diluent on the extraction of americium, taken from [10], are cited, from which it follows that this dependence is satisfactorily expressed by a straight line. Moreover, the value of the constant decreases with increasing value of the PD, i.e., with increasing ability of the diluent to solvate polar molecules. A comparison of the results of the extraction of cations with the same charges shows that the selectivity of the process evidently increases with decreasing value of the PD, in other words, with decreasing solvating power of the diluent.

The results of theoretical investigations were used as the basis for developing a technological scheme of the isolation of americium, curium, strontium, and rare earth elements from the aqueous waste solution from extraction treatment of spent fuel cells of the VVÉR. (The scheme of extraction treatment of spent fuel cells of the VVÉR was described earlier [15, 16]). The studies [17, 18] were devoted to the questions of the separation of strontium and the rare earth elements, as well as the separation of americium and curium from the rare earth elements in extraction with a mixture of D2EHPA + TBP or with D2EHPA.

The aqueous waste solution was preliminarily evaporated to remove nitric acid. The final acidity of the evaporated solution was 0.2-0.3 M. In addition to fission products, it also contains corrosion products of the apparatus, the presence of which leads to serious complications during extraction. Iron, readily

extractable by D2EHPA [19], is quantitatively transferred to the organic solution, forming a gelatinous deposit, as a result of which the extraction process becomes unfeasable. To prevent the transfer of iron to the organic phase, a complex former (citrate ion) is introduced into the evaporated aqueous waste solution in an amount of about 120% of the stoichiometry. In addition to iron, other corrosion products, such as chromium and nickel, which are entirely extracted by D2EHPA at low acidity [20, 21], are also present in solution. Therefore, it is advisable to introduce a supplementary amount of the citrate ion to tie up these elements into strong inextractable complexes [22]. At the same time, sodium acetate is added to create pH = 4-4.5 in the solution. It was established that if the extraction of D2EHPA is performed four days after the pH is adjusted to the necessary value, then a supplementary amount of the citrate ion should not be introduced to tie up chromium, since such exposure of the solution at pH = 4-4.5 sharply reduces the extraction of chromium [20].

At pH = 4-4.5, a quantitative extraction of americium, curium, rare earth elements, and strontium is provided for (see Fig. 1).

The technological scheme includes the following basic operations (after evaporation and the correction of the solutions):

a) joint extraction of americium, curium, strontium, and the rare earth elements with a 0.6 M solution of D2EHPA in a hydrocarbon diluent;

b) the reextraction of strontium, conducted with dilute nitric acid (the basic requirement for successful performance of this operation is that the acidity of the reextract obtained should be about 0.1 M);

c) the reextraction of americium and curium; 0.8 M lactic acid (LA), containing 0.05 M sodium diethylenetriaminepentaacetate (Na_5DTPA) is used as the reextracting solution;

d) reextraction of the rare earth elements, performed with 3 M nitric acid.

Table 3 shows the experimentally obtained distribution of americium, curium, strontium, and the rare earth elements among products of the technological scheme tested (Fig. 3). From the results cited it follows that this technological scheme can ensure not only a high degree of extraction of the investigated elements, but also permits a number of successive selective reextractions of strontium, americium, curium, and the rare earth elements to be performed with a rather good yield (92-95% of the initial amount).

LITERATURE CITED

1. D. Peppard, J. Ferraro, and G. Mason, J. Inorg. and Nucl. Chem., 7, No. 3, 231 (1958).
2. V. S. Smelov and V. P. Lanin, At. Énerg., 25, No. 2, 157 (1968).
3. G. Mason, S. Lewey, and D. Peppard, J. Inorg. and Nucl. Chem., 26, 2271 (1964).
4. Yu. Yu. Lur'e and V. E. Genkin, Zavod. Lab., 32, No. 12, 1459 (1966).
5. J. Fidelis, Rep. Inst. Bad. Jadr. PAN, No. 1393 (1972), p. 20.
6. J. Fidelis, Rep. Inst. Bad. Jadr. PAN, No. 1394 (1972), p. 38.
7. D. Peppard and J. Ferraro, J. Inorg. and Nucl. Chem., 10, No. 3-4, 275 (1959).
8. C. Bake et al., III Intern. Conf. Geneva, Rep. USA No. 1550 (1965).
9. K. Kimura, Bull. Chem. Soc., Japan, 34, No. 1, 63 (1962).
10. E. S. Gureev et al., Third Geneva Conference, Reports of the USSR [in Russian], No. 347 (1964).
11. A. M. Rozen, Radiokhimiya, 10, No. 2, 273 (1968).
12. V. S. Shmidt and É. A. Mezhov, Radiokhimiya, 12, No. 1, 38 (1970).
13. V. S. Shmidt et al., Ibid., No. 5, p. 748.
14. A. Weisberger et al., Organic Solvents [Russian translation], Izd-vo Inostr. Lit., Moscow (1958).
15. V. B. Shevchenko et al., in: Transactions of the Symposium on High Energy Substances, Investigations in the Field of the Processing of Irradiated Fuel [in Russian], Vol. 1 Izd. ChKAÉ, Prague (1972), p. 259.
16. V. B. Shevchenko et al., Fourth Geneva Conference, Reports of the USSR [in Russian], No. 435 (1971).
17. R. Burns, W. Shul, and L. Bray, Nucl. Sci. and Engng., 17, No. 4, 566 (1963).
18. R. Lues et al., in: The Chemistry of the Extraction of Metals with Organic Solvents [Russian translation], Atomizdat, Moscow (1969), p. 292.
19. S. M. Karpacheva et al., Zhurn. Neorganich. Khimii, 12, No. 7, 1925 (1967).
20. V. S. Smelov and V. V. Chubukov, Radiokhimiya, 13, No. 3, 449 (1971).
21. V. S. Smelov and V. V. Chubukov, Radiokhimiya, 15, No. 4, 525 (1973).
22. V. V. Chubukov and V. S. Smelov, Radiokhimiya, 14, No. 1, 146 (1972).

Ge(Li)-DETECTORS FOR NATURAL RADIOACTIVITY ANALYSES

I. P. Shumilin

UDC 550.3:539.1.074.55:539.1.06

The possibility of using Ge(Li)-detectors for analysis purposes was investigated on the basis of an experimental study of the gamma spectra of uranous – uranic oxide, pitchblende (before and after heating at 1000°C), monazite, ^{210}Pb, ^{230}Tb, ^{234}Pa, and a radium calibration source. The samples were prepared on a silicate base and took the form of a 10 g mass of powder ground to a 200 mesh particle size.

The measurements were carried out on a 2048-channel pulse-height analyzer with detectors of volume 0.5 and 10 cm^3, giving a resolution of 0.5 and 2 keV at 100 keV level. The high resolution of the detector of volume 0.5 cm^3 is evident from Figs. 1 and 2, which show the gamma spectra of pitchblende and monazite at low energies.

The absolute error of the energy binding of the photopeaks obtained on the 0.5 keV resolution spectrometer did not exceed 0.1-0.2 keV, and in the case of the 2 keV resolution it amounted to 0.5-1.0 rel. %. On the basis of these data the spectrum of the natural radioactivity is differentiated into groups of elements between which, in the ore samples, indeterminate relationships may exist [1].

The radiation of the following groups was observed: thorium (^{232}Th, ^{228}Ra, ^{228}Ac, ^{228}Th, ^{224}Ra); thoron (^{220}Rn, ^{216}Po, ^{212}Pb, ^{212}Bi, ^{212}Po, ^{208}Tl); potassium (^{40}K); RaD (^{210}Pb, ^{210}Bi, ^{210}Po); radon (^{222}Rn, ^{218}Po, ^{214}Pb, ^{214}Bi, ^{214}Po, ^{210}Tl); radium (^{226}Ra); ionium (^{230}Th); uranium (^{238}U, ^{235}U, ^{234}U, ^{234}Th, ^{234}Pa, ^{231}Th);

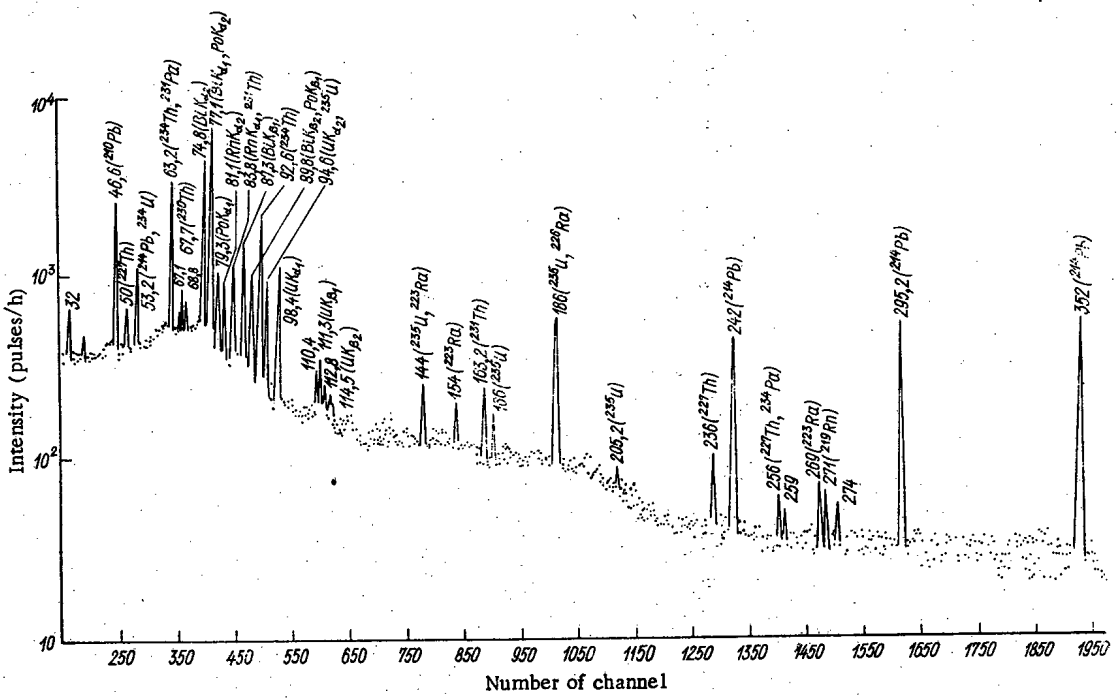

Fig. 1. Gamma spectrum of pitchblende sample.

Translated from Atomnaya Énergiya, Vol. 37, No. 5, pp. 384-389, November, 1974. Original article submitted April 25, 1973.

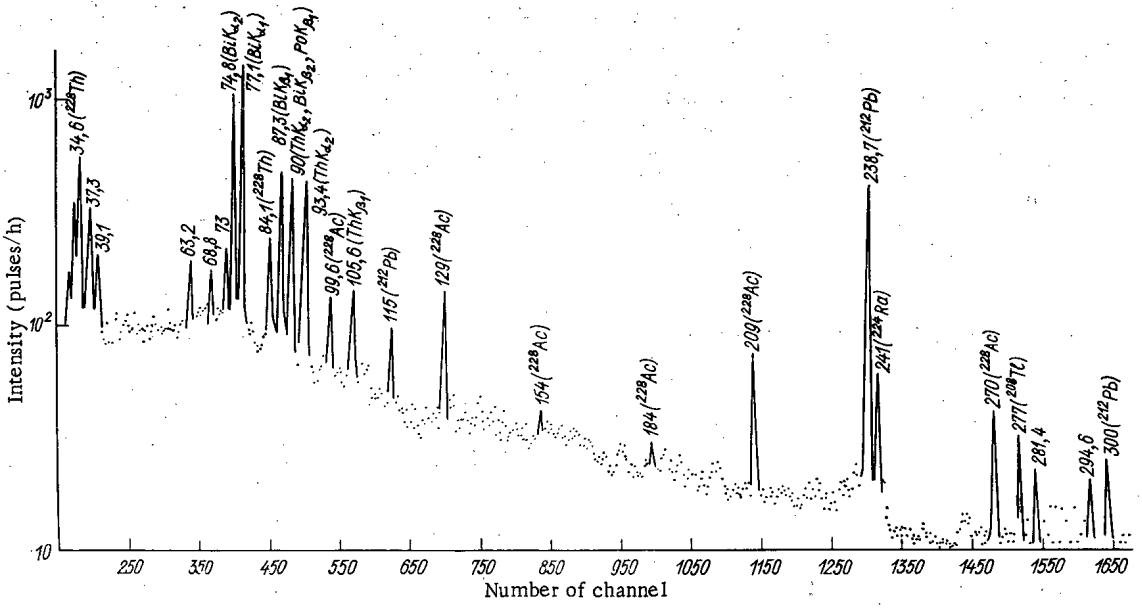

Fig. 2. Gamma spectrum of monazite sample.

and protactinium (^{231}Pa with decay products). Heating the pitchblende sample enabled the aforementioned differentiation to be effected with resolution of the gamma spectrum of the protactinium group without protactinium and actinium samples and without corrections for the effect of the real composition on the basis of the following formulas:

$$I_{Rn} = \frac{1}{1-n}(I_{SB} - I_{SA}) = 1.14\,(I_{SB} - I_{SA}); \quad (1)$$

$$I_{Pa} + I_{Io} + I_{Ra} + I_{RaD} = \frac{1}{1-n}(I_{SA} - nI_{SB}) - I_U = 1.14 I_{SA} - 0.14 I_{SB} - I_U, \quad (2)$$

where I_{Rn}, I_{Pa}, I_{Io}, I_{Ra}, I_{RaD}, I_U are respectively the gamma radiation intensities of the groups of radon, protactinium, ionium, radium (without decay products), RaD, and uranium (the uranous – uranic sample); I_{SB} and I_{SA} are the intensities of the gamma radiation from the standard pitchblende samples before and after heating; n is the quantity of radon remaining in the sample after heating relative to its initial amount (in the present case n = 0.123).

Formulas (1) and (2) are obtained on the basis of the known fact [1] that after heating at 1000°C the content of radon-group elements in the sample is reduced by around an order. The real composition of the sample and also the content of all other elements and their radiation remain unaffected. The following conclusions can be drawn from an analysis of the radiation spectra of the radioactive elements utilizing formulas (1) and (2) and the information in the literature [2-6] on the energies and yields of gamma quanta. For measurement on the spectrometer of resolution 0.5 keV (see Figs. 1 and 2) the most distinct lines are the $K_{\alpha_{1,2}}$ x-ray lines of ^{214}Bi (74.8 and 77.1 keV). These lines can be used to determine elements of the radon group in uranium ores that do not contain thorium, as a similar radiation is characteristic for elements of the thorium series. In complex ores radon is best determined from the lines of ^{214}Pb (242, 295.2, and 352 keV) and elements of the thorium series from the lines of ^{228}Ac (129 keV) and ^{212}Pb (238.7 keV). The possibility of determining ^{230}Th and ^{210}Pb is restricted to the lines 67.7 and 46.6 keV respectively. No other lines have been fixed in their spectrum.

The radiation of ^{234}U is characterized by a single line of low intensity (53.3 keV). It is very difficult to distinguish this line, however, as it coalesces in the one photopeak with the ^{214}Pb line (53.2 keV), which is an order greater in intensity.

Elements of the protactinium group can be determined through the ^{227}Th line (50 keV) and through the $K_{\alpha_{1,2}}$ x-ray lines of ^{219}Rn (81.1 and 83.8 keV). In the latter case, however, allowance must be made for the similar but less intense radiation of ^{222}Rn and also for the nuclear radiation of ^{231}Th (84.2 keV). ^{238}U can be determined through the intense energy lines at 92.6 and 63.2 keV, while ^{226}Ra can be determined via the photopeak in the region of 186 keV, formed as a result of the superposition of two intense lines of different energies belonging to ^{226}Ra (186.2 keV) and ^{235}U (185.8 keV).

TABLE 1. Results of Measurements on Radioactive Samples in Regions of Spectrum of Practical Interest for Analyses

Energy in photopeak (keV)	Elements giving rise to photopeak	Energy of quanta (keV)	Fractions of radiation in photopeak (a_i) (rel. units)	Uranium-radium standard (10% U)				Sample containing 4.2% U (radiation intensity in photopeak in uranium units, %)	
				before heating (K_{equ} = 100%)		after heating (K_{equ} Rn with Ra = 19%)			
				radiation intensity in photopeak (pulses/h)	intensity of scattered radiation under photopeak (pulses/h)	radiation intensity in photopeak (uranium units, %)	intensity of scattered radiation under photopeak (pulses/h)	before heating (K_{equ} = 100%)	after heating (K_{equ} Rn with Ra = 32%)
Detector volume 0.5 cm³, resolution 0.5 keV									
46,6	^{210}Pb(RaD)	46,6	1,00	6500	3200	9,70	1900	4,77	4,72
50,0	^{227}Th(RdAc)	50,0	1,00	600	3500	9,80	1800	4,81	4,80
53,2	^{234}U(UII) ^{214}Pb(RaB)	53,3 53,2	0,1 0,9	2100	3570	2,70	2000	4,87	1,89
63,2	^{234}Th(UX$_1$)	63,2	1,0	7900	5000	9,95	1870	4,60	4,60
67,7	^{230}Th(Io)	67,7	1,00	690	3900	9,85	1800	4,62	4,78
74,8	^{214}Pb(RaB)	74,8	1,00	13100	6700	2,20	2700	4,47	1,44
77,1	^{214}Pb(RaB)	77,1	1,0	22880	5900	2,10	2100	4,46	1,36
81,1	^{223}Ra(AcX) ^{226}Ra(Ra)	81,1 81,1	0,75 0,25	1370	2890	9,78	1540	4,23	4,30
83,8	^{223}Ra(AcX) ^{226}Ra(Ra) ^{231}Th(UY)	83,8 83,8 84,2	0,65 0,20 0,15	3460	4300	10,10	2000	4,33	4,27
92,6	^{234}Th(UX$_1$)	92,6	1,00	9000	3600	9,89	2400	4,16	4,12
186,0	^{235}U(AcU) ^{226}Ra(Ra)	185,8 186,2	0,40 0,60	2650	1750	10,20	500	4,15	4,15
242,0	^{214}Pb(RaB)	242,0	1,00	1500	770	1,80	250	4,16	1,41
295,2	^{214}Pb(RaB)	295,2	1,00	3000	350	2,00	100	4,30	1,45
352,0	^{214}Pb(RaB)	352,0	1,00	3500	500	1,90	170	4,20	1,25
129,0	^{228}Ac(MsThII)	129,0	1,00	520	420	—	—	—	—
238,7	^{212}Pb(ThB)	238,7	1,00	1900	320	—	—	—	—
Detector volume 10 cm³, resolution 2 keV									
144,0	^{235}U(AcU) ^{223}Ra(AcX)	143,8 144,0	0,70 0,30	5900	70200	10,10	19500	—	—
186,0	^{235}U(AcU) ^{226}Ra(Ra)	185,8 186,2	0,40 0,60	47000	85000	9,95	19000	—	—
270,0	^{223}Ra(AcX) ^{219}Rn(An) ^{214}Pb(RaB)	269,0 271,0 274,0	0,70 0,30	6450	45650	7,40	8270	—	—
1000,0	^{234}Pa(UX$_2$)	1000,0	1,00	500	4500	9,80	700	—	—
295,0	^{214}Pb(RaB)	295,0	1,00	63000	34000	1,16	6000	—	—
352,0	^{214}Pb(RaB)	352,0	1,00	96630	34100	1,30	5200	—	—
609,0	^{214}Bi(RaC)	609,0	1,00	47000	14000	1,20	2300	—	—
270,0	^{228}Ac(MsThII)	270,0	1,00	4850	11000	—	—	—	—
338,0	^{228}Ac(MsThII)	338,0	1,00	8800	9800	—	—	—	—
908,0	^{228}Ac(MsThII)	908,0	1,00	4460	2000	—	—	—	—
960,0	^{228}Ac(MsThII)	960,0	1,00	3000	2000	—	—	—	—

TABLE 1 (continued)

Energy in photopeak (keV)	Elements giving rise to photopeak	Energy of quanta (keV)	Fractions of radiation (a_i) in photopeak (rel. units, %)	Uranium-radium standard (10%U)				Sample containing 4.2% U (radiation intensity in photopeak in uranium units, %)	
				before heating (K_{equ} = 100%)		after heating (K_{equ} Rn with Ra = 19%)			
				radiation intensity in photopeak (pulses/h)	intensity of scattered radiation under photopeak (pulses/h)	radiation intensity in photopeak (uranium units, %)	intensity of scattered radiation under photopeak (pulses/h)	before heating (K_{equ} = 100 %)	after heating (K_{equ} Rn with Ra = 32%)
1600,0	^{228}Ac(MsThII)	1600,0	1,00	2300	1100	—	—	—	—
583,0	^{208}Tl(ThC″)	583,0	1,00	10500	7800	—	—	—	—
1460,0	^{40}K(K)	1460,0	1,00	75	15	—	—	—	—

Note. For elements of the thorium series and potassium the table cites the radiation intensity of thorium and potassium samples containing 10% thorium and 50% potassium respectively. In the case of measurements using the detector of volume 10 cm^3 the equilibrium coefficient of Rn with Ra after heating equals 12%.

Spectrometers with a resolution of 2 keV have very restricted possibilities for analyses in the low-energy region of the spectrum (30-120 keV). The ^{230}Th line (67.7 keV) is no longer resolved as it coalesces with the lines of the radon group (67.1 and 68.8 keV) and with the intense scattered radiation from quanta of higher energies. Neither is it possible to determine protactinium through the lines at 50, 81.1, and 83.8 keV, as they coalesce with the more intense lines of ^{214}Pb (53.2 keV) and with the x-ray lines of bismuth and polonium. The ^{234}Th photopeak at 92.6 keV is strongly distorted on account of the adjacent and coalescing (and four times more intense) x-ray emission of Bi + Po and the x-ray emission of radon, equal in intensity to 50% of the ^{234}Th radiation. Further distortions come from the $K_{\alpha_{1,2}}$ x-ray emission of uranium (94.6 and 98.4 keV), arising through the interaction of ^{238}U atoms with gamma quanta from other radioactive elements. For a 10 g sample containing 10% uranium in equilibrium with decay products, the composite intensity of the $K_{\alpha_{1,2}}$ lines of ^{238}U relative to the ^{234}Th line (92.6 keV) equals 60%. Variation of the uranium content and the decay products by a factor of m changes the ^{238}U x-ray intensity by a factor of m^2. All this considerably complicates the determination of uranium in this region of the spectrum.

Detectors of increased volume of resolution 2-3 keV enable the hard region of the spectrum to be utilized for analytical pruposes. The radon content in this case is best determined through the lines of ^{214}Pb (295, 352 keV) and ^{214}Bi (609 keV), while the thorium content is best determined through the lines of ^{228}Ac (338, 908, 960, 1600 keV) and ^{208}Tl (583 keV). Radium, as in the previous case, can be found from the 186 keV photopeak. Protactinium is best determined through the photopeak in the region of 270 keV formed as a result of the superposition of lines belonging to elements of the protactinium group ^{223}Ra (269 keV) and ^{219}Rn (271 keV), the thorium group ^{228}Ac (270 keV), and the radon group (274 keV). Uranium can be determined through the photopeak near 144 keV formed as a result of the superposition of the lines of ^{235}U (143.8 keV) and ^{223}Ra (144 keV) and through the line of ^{234}Pa (1000 keV). All remaining lines of the uranium and protactinium groups have an intensity less than 5% of that of the scattered radiation under the corresponding photopeaks, while some of them, in addition, coalesce into the one photopeak with more intense lines of other elements [for example, the lines of ^{234}Pa (256, 743, 767, and 787 keV) with the lines of ^{214}Bi (259, 742, 769, and 787 keV) and ^{227}Th (256 keV)].

All portions of the spectrum of interest for analytical purposes are indicated in Table 1. The contributions of the gamma radiation from radioactive elements to the photopeaks and the energies of the gamma quanta cited in the table were obtained from the results of measurements on the aforementioned samples and the radium calibration source and calculations using formulas (1) and (2).

The table also presents the results of measurements on samples of monazite, potassium, and five uranium samples with different equilibrium coefficients between the radon and radium.

The activity of the samples is expressed in the table in standard units through the relationship

$$A = (I/I_S)\, Q_S, \tag{3}$$

where A is the activity of the sample under analysis in uranium (thorium) units (%); I and I_S are respectively the radiation intensities of the sample under analysis and the standard, defined in terms of the areas under the corresponding photopeaks (pulses/h); Q_S is the uranium (thorium) content in the standard equilibrium sample (%).

When the photopeak characterizes the radiation intensity of a single element, the quantity A equals the content of this element in the sample expressed in units of the standard. If, however, the photopeak is made up out of the lines of several elements, then A corresponds to the content of these elements only in the particular case when the equilibrium between them is not disturbed (see Table 1).

A reliable determination of A in the low-energy region of the spectrum necessitates the introduction into the results of the measurements of a correction for the effect of the real composition of the use of standards close in composition to the samples being analyzed.

It can be seen from Table 1 that for analyses in the 40-80 keV region with a 10% uranium standard, the results of measurements on samples containing 4.2% uranium are 10-15% too high. Also, a comparison of the radiation spectra of the radium calibration source (a thin layer for gamma quanta) and the pitchblende sample shows that almost one half of the quanta with energies 50-60 keV are absorbed in the sample.

Error in the determination of scattered radiation intensity under the photopeaks makes a significant contribution to measurement error. The error is reduced greatly by heating the samples before the measurements, as this results in a sharp drop in the intensity of the scattered radiation.

If radioactive equilibrium between the elements whose radiation gives rise to the photopeak is violated, the results of the analyses must be calculated by solving a linear system of k equations [1]:

$$A_i = \sum_{i=1}^{i=k} a_i Q_i, \tag{4}$$

where A_i is the activity of the sample in the regions of the spectrum chosen for the analysis (calculated via formula (3)); k is the number of radioactive groups whose radiation gives rise to the photopeak; a_i are coefficients characterizing the contributions of the radiation of these groups to the corresponding photopeaks for equilibrium between the groups (rel. units); Q_i is the content in the sample of the elements being determined in units of the standard (%).

In particular, in the determination of U, Ra, and Pa via the lines 92.6, 186, and 83.8 keV using the detector with 0.5 keV resolution, we find on the basis of the data in Table 1 that the set of equations and formulas for computing the results of the analyses have the form:

$$A_{186} = 0.4Q_U + 0.6Q_{Ra};$$
$$A_{83.8} = 0.15Q_U + 0.20Q_{Ra} + 0,65Q_{Pa};$$
$$Q_U = A_{92.6};$$
$$Q_{Ra} = 1.66A_{186} - 0.66A_{92.6};$$
$$Q_{Pa} = 1.54A_{83.8} - 0.51A_{186} - 0.03A_{92.6}.$$

In the determination of U, Ra, Pa, Rn, and Th via the lines 144, 186, 270, 352, and 338 keV using the detector of volume 10 cm^3, it is necessary to know the contribution of thorium radiation to the 270 keV photopeak relative to the contribution of the uranium – radium standard (from the tabulated data this ratio equals 4850/6450 = 0.75) and to calculate the thorium content from the 338 keV photopeak. Under these conditions we find on the basis of the data in Table 1 that the set of equations and analysis formulas have the form:

$$A_{270} = 0.7Q_{Pa} + 0.3Q_{Rn} + 0.75Q_{Th};$$
$$A_{186} = 0.4Q_U + 0.6Q_{Ra};$$
$$A_{144} = 0.7Q_U + 0.3Q_{Pa};$$
$$Q_{Th} = A_{338};$$
$$Q_{Rn} = A_{352};$$
$$Q_{Pa} = 1.43A_{270} - 0.43A_{352} - 1.07A_{338};$$
$$Q_U = 1.43A_{144} + 0.18A_{352} - 0.61A_{270} + 0.46A_{338};$$
$$Q_{Ra} = 1.67A_{186} - 0.96A_{144} + 0.41A_{270} - 0.12A_{352} - 0.31A_{338}.$$

For the heated pitchblende sample (see Table 1) $A_{338} = 0$; $A_{352} = 1.3\%$; $A_{270} = 7.40\%$; $A_{186} = 9.95\%$; $A_{144} = 10.10\%$. The content of radioactive elements in the sample is thus: $Q_{Th} = 0$; $Q_{Rn} = 1.3$; $Q_{Pa} = 10.02\%$; $Q_U = 10.17\%$; $Q_{Ra} = 9.8\%$.

The equations and formulas for the other regions of the spectrum specified in Table 1 are derived in a similar manner.

In this manner, Ge(Li)-detectors can be used for the analysis of radioactive ores and the products of their industrial treatment. The sensitivity of the analyses can be considerably enhanced by increasing the mass of the investigated material and the size of the detectors.

LITERATURE CITED

1. E. I. Zheleznova, I. P. Shumilin, and B. Ya. Yufa, Radiometric Methods of Analyzing Natural Radioactive Elements [in Russian], Nedra, Moscow (1968).
2. V. A. Bobrov, Laboratory Gamma-Spectrometric Analysis of Natural Radioactive Elements [in Russian], Nauka, Novosibirsk (1941).
3. B. S. Dzhelepov, V. O. Sergeev, and L. K. Pekker, Decay Schemes of Radioactive Nuclei [in Russian], Izd. AN SSSR, Moscow—Leningrad (1963).
4. R. P. Kogan, I. M. Nazarov, and N. D. Fridman, Fundamentals of Gamma-Spectrometry of Natural Materials [in Russian], Atomizdat, Moscow (1969).
5. P. Dumesnil and C. Andrieux, Industr. Atomiques, No. 14 (1970).
6. D. Williams, "The gamma-ray spectra of pitchblende and monazite (10-200 keV) obtained with a lithium-drift germanium detector," Electronic and Applied Physics Division, Atomic Energy Research Establishment, Harwell (1966).

DEACTIVATABILITY OF CERTAIN PAINT AND VARNISH COATINGS CONTAMINATED WITH ^{237}Np, ^{241}Am, AND $^{242+244}Cm$

I. I. Tsameryan, D. S. Gol'dshtein, and É. I. Atamanova

UDC 667.6

The use of transuranium elements, which has been expanding with each passing year, leads to the necessity of using readily deactivated paint and varnish coatings for the surfaces of room, equipment, and individual parts of individual protection facilities. However, at the present time only studies on the evaluation of the deactivatability of paint and varnish coatings in the case of contamination with plutonium are known [1, 2]; there are no data in the literature on the evaluation of the deactivatability of paint and varnish materials contaminated by other transuranium elements.

TABLE 1. Brief Characterization of the Investigated Paint and Varnish Coatings

Paint or varnish coating, brand	All-Union State Standard or Technical Specification	Characteristics
Varnish KhS-76	All-Union State Standard 9355-60	Solution of the resin SVKh-40 (copolymer of vinylidene chloride with vinyl chloride) in a mixture of organic solvents
Enamel KhVÉ-4001, white	Interrepublican Technical Specifications 6-10-951-70	Solution of the resin SVKh-40 in a mixture of organic solvents with addition of pigments
Enamel KhSÉ-1, white	All-Union State Standard 7313-55	Solution of perchlorovinyl and alkyd resins in a mixture of organic solvents with an addition of pigments and plasticizer
Enamel KhV-1100, white	All-Union State Standard 6993-70	Solution of perchlorovinyl and alkyd resins in a mixture of organic solvents with an addition of pigments and plasticizer
Varnish ÉP-55	All-Union Technical Specification GIPI-4 No. 4031-64	Solution of epoxide resin É-41 in organic solvents
Enamel ÉP-56, white	Technical Specification 6-10-1243-72	Solution of epoxide resin É-41 in organic solvents with addition of pigments and fillers
Spackle ÉP-00-10	All-Union State Standard 10277-62	Mixture of epoxide resin É-40 with pigments, fillers, plasticizer, and organic solvents
Mixture of spackle ÉP-00-10 and varnish ÉP-55		Mechanical mixture of spackle with varnish in a 1:1 ratio
Enamel PF-115, white	All-Union State Standard 6465-63	Solution of pentaphthalic resin PFL-64 in organic solvents with addition of pigments
Enamel ÉT-147, white	All-Union Technical Specification No. N4 2031-67	Suspension of pigments in a solution of chlorosulfurated polyethylene in toluene

Translated from Atomnaya Énergiya, Vol. 37, No. 5, pp. 390-392, November, 1974. Original article submitted December 11, 1973.

TABLE 2. Deactivatability of Paint and Varnish Coatings, Contaminated with ^{237}Np, ^{241}Am, and $^{242+244}Cm$

Coating	Residual activity according to cycles of contamination and washing, %																									
	^{237}Np, pH = 0,1					^{241}Am, pH = 2,8					^{241}Am, pH = 0,1					$^{242+244}Cm$, pH = 3					$^{242+244}Cm$, pH = 0,1				
	I	II	III	IV	V	I	II	III	IV	V	I	II	III	IV	V	I	II	III	IV	V	I	II	III	IV	V
Varnish KhS-76	0,02	0,07	0,07	0,1	0,1	0,01	0,01	0,02	0,03	0,03	0,1	0,1	0,1	0,1	0,1	0,01	0,02	0,07	0,07	0,07	0,1	0,1	0,1	0,2	0,2
Enamel KhVE-4001	7	7	6	9	9	0,4	2	2	3	4	10	11	16	16	20	0,6	2	3	3	5	10	10	14	14	15
Enamel KhS-1	0,9	7	10	12	15	0,04	2	2	2	2	4	12	15	15	20	0,07	0,5	0,5	0,5	0,7	5	15	15	15	15
Enamel KhV-1100	13	35	40	40	45	0,2	10	13	20	20	6	12	14	15	20	0,5	10	16	17	17	7	12	12	20	20
Varnish EP-55	20	35	40	50	55	0,03	0,07	0,2	0,3	0,3	6	10	10	11	12	0,02	0,1	0,2	0,2	0,2	3	4	4	4	7
Enamel EP-56	20	35	35	40	45	0,01	0,4	0,6	1	1	10	20	30	35	35	0,01	0,5	1	2	5	7	15	15	25	30
Spackle EP-00-10	20	40	40	55	60	2	5	7	8	8	4	6	7	8	8	2	3	4	6	6	2	5	7	7	7
Mixture of spackle EP-00-10 and varnish EP-55	18	50	40	40	60	0,7	3	5	6	10	1	3	8	8	10	0,1	0,2	1	4	5	0,9	3	9	9	10
Enamel PF-115	5	8	8	10	10	0,4	10	20	50	50	15	20	30	40	55	0,2	10	20	30	35	20	25	50	65	70
Enamel ET-147	15	20	20	20	20	0,1	5	15	15	15	3	5	8	8	10	0,5	5	10	10	10	3	6	7	7	7

Note. Roman numerals denote cycles of contamination and washing.

The present work was devoted to a study of the deactivatability of certain paint and varnish materials in the case of their contamination with nitric acid solutions of ^{237}Np, ^{241}Am, and $^{242+244}Cm$.

The contaminating solutions of these isotopes were prepared with pH values at which they are most difficult to remove from polymer materials: solutions of americium with pH 2.8 [3], curium with pH = 3 [4], and neptunium with pH = 0.1 [5]. In addition, considering that in the previous investigations with plutonium, a poor deactivatability of a number of paint and varnish coatings was noted when they were contaminated by nitric acid solutions with pH = 0.1 [2], we decided to use nitric acid solutions of americium and curium with pH = 0.1 for the contamination of the coatings.

The samples were prepared for the experiment by the application of enamels and varnishes onto metallic plates with dimensions 40 × 50 mm and exposed for two to three weeks for the formation of a film. In this case attention was paid to complete painting of the samples on all sides, so that there would be no possibility of contact of the metallic base with the solution during the treatment. For contamination of the sample, five drops of the contaminating solution were applied in its center (circle 300 mm in diameter). After drying for 18 h, the initial activity of the samples was determined with a PS-349-2 scintillation attachment with a scalar instrument.

Deactivation of the samples was performed in 0.5 liter glass vessels with a jacket into which water was delivered from a TS-24 thermostat to maintain constancy of the selected temperature of deactivation. The investigated samples, fixed in special cassette holders, were immersed in a detergent solution, which was mixed with a glass mixer, rotated by an electric motor.

The deactivatability was investigated in five repetitions of the cycle of contamination and washing, using an oxidation—reduction method: first treatment – 5% Na_2CO_3 + 0.1% $KMnO_4$ + 0.4% $(NaPO_3)_6$; second treatment – 0.3 N HNO_3 + 0.2% NaF + 0.2% $H_2C_2O_4$ + 0.5% "Novost'." Each treatment was conducted for 10 min at 30-35°C, followed by rinsing for 5 min. This method was used earlier for an evaluation of the deactivatability of materials contaminated with plutonium [2] and showed high effectiveness in the case of removal of neptunium, americium, and curium from the polymers [3-5].

After deactivation, the samples were dried and their residual activity determined; it was expressed in percent of the initial activity. In each experiment we used five samples of the investigated material; two to three series of monotypic experiments were conducted. The selected methods permitted a satisfactory reproducibility of the results to be obtained.

Table 1 presents a brief characterization of the investigated paint and varnish coatings.

In an examination of the results of the investigations (Table 2), it should be noted that the best deactivatability with respect to neptunium, americium, and plutonium is possessed by a coating based on the varnish KhS-76. Although the deactivatability of this coating is somewhat reduced for a contaminating solution with pH = 0.1, however, for all three isotopes it remains very high during all five cycles of contamination and washing. In all cases the initial contamination of the coating can be reduced no less than 500-1000-fold during the process of deactivation.

The results obtained are explained primarily by the substantially greater chemical stability of the copolymer SVKh-40 in comparison with other investigated film-forming coatings. However, the deactivatability of a coating based on the copolymer SVKh-40 deteriorates substantially when it is filled with pigments (see the results on the enamel KhVÉ-4001).

In the case of contamination with neptunium, satisfactory results of deactivation could not be obtained for any coating other than the varnish KhS-76. In the best case, for the enamels KhVÉ-4001 and PF-115, the initial contamination can be reduced 10-fold after the fifth cycle. The enamel PF-115, although washed free of neptunium just like the enamel KhVÉ-4001, is poorer than all the coatings tested in deactivation after contamination with americium and curium. Moreover, on the enamel PF-115, a swelling was formed at the site of application of the contamination, and during treatment, the color of the coating changed. The chemically stable enamel KhSÉ-1 is readily washed free of neptunium after the first contamination; however, by the fifth cycle its residual activity reaches 15%.

Coatings based on epoxide resins, which have found wide use in work with radioactive substances, are very poorly washed free of neptunium. These coatings are considerably better freed of americium and curium than of neptunium.

The deactivatability of the enamels KhVÉ-4001, KhSÉ-1, and ÉP-56 and the varnish ÉP-55 with respect to americium and curium depend greatly on the pH of the contaminating solution. In the case of contamination with nitric acid solutions of americium and curium with pH equal to 2.8 and 3, respectively, quite satisfactory deactivatability of the indicated paint and varnish coatings is noted, especially for the enamel KhSÉ-1 and the varnish ÉP-55.

Thus, on the basis of the results of our investigations we can recommend the varnish KhS-76, which is a solution of the resin SVKh-40 in a mixture of organic solvents, for use as the outer layer of the protective coating of surfaces in work with neptunium, americium, and curium.

LITERATURE CITED

1. P. Walker, J. Oil and Color Chemists Assoc., 49, No. 2, 117 (1966).
2. L. M. Nosova and D. S. Gol'dshtein, in: Medico-Technical Problems of Individual Protection of Man [in Russian], No. 2, Izd. Minzdrav SSSR, Moscow (1969), p. 99.
3. I. I. Tsameryan and D. S. Gol'dshtein, in: Medico-Technical Problems of Individual Protection of Man [in Russian], No. 10, Meditsina, Moscow (1972), p. 89.
4. I. I. Tsameryan, Ibid., p. 106.
5. I. I. Tsameryan, in: Medico-Technical Problems of Individual Protection of Man [in Russian], No. 15, Meditsina, Moscow (1974), p. 120.

ENERGY MODULATION OF PROTON BEAM FROM A LINEAR ACCELERATOR

I. M. Kapchinskii and V. I. Bobylev

UDC 621.384.643

In carrying out certain methods of multiturn proton injection into a circular accelerator or storage ring, it is necessary to change the average energy of the particles at the exit of the linear accelerator-injector in an almost linear fashion during a current pulse. In principle, particle energy can be changed simultaneously with beam debunching. For this purpose, the frequency of the buncher voltage must be shifted with respect to the frequency of the accelerating field in the injector by an amount

$$\Delta f = \Delta\varphi/2\pi\tau, \tag{1}$$

where τ is the length of the proton current pulse; $\Delta\varphi$ is the phase spread of the used portion of the voltage variation in the debuncher. The value of $\Delta\varphi$ is determined by the tolerance in the linearity of the modulation law. For example, for a permissible relative error in the rate of change of the average momentum,

$$\delta = \Delta \frac{d}{dt}\left(\frac{\Delta p_{av}}{p_{av}}\right) \Big/ \frac{d}{dt}\left(\frac{\Delta p_{av}}{p_{av}}\right)_{max},$$

equal to 0.1 and a beam pulse length $\tau = 15$ μsec, we obtain $\Delta\varphi = 0.90$ rad and $\Delta f = 9.54$ kHz.

In the variables $\psi = \varphi - \varphi_S$, $g = (p - p_S)/p_S$ (φ and p are the phase and momentum of a particle), let the phase volume of the beam at the exit of the linear accelerator be bounded by the ellipse

$$\frac{\psi^2}{\Psi_0^2} + \frac{g^2}{G_0^2} = 1. \tag{2}$$

Then at the exit of the debuncher the phase volume is enclosed by the curve

$$g = k\sin(\psi + \varphi_0) - k_0\psi \pm \frac{\nu}{1+a^2\nu^2}\sqrt{(1+a^2\nu^2)\,\Psi_0^2 - \psi^2}, \tag{3}$$

where

$$\left.\begin{aligned} \nu = G_0/\Psi_0;\ a = \frac{2\pi}{\gamma^2}\cdot\frac{l}{\beta\lambda};\\ k = \frac{U_D T_D}{\beta^2\gamma E_0};\ k_0 = \frac{a\nu^2}{1+a^2\nu^2}; \end{aligned}\right\} \tag{4}$$

l is the drift length to the debuncher; U_D and T_D are the voltage amplitude and the flight-time factor in the debuncher gap; E_0 is the rest energy of a particle; β and γ are the relative velocity and energy of the particles; λ is the wavelength of the hf field in the linear accelerator; φ_0 is the instantaneous value of the phase of the hf field in the debuncher for which the synchronous particle passes through the center of the debuncher gap,

$$\varphi_0(t) = 2\pi\Delta f\left(t - \frac{\tau}{2}\right). \tag{5}$$

The parameter k is positive if the particle bunch arrives in the debuncher on the rising portion of the sinusoidal voltage and is negative for the descending portion.

For the following evaluations, we limit ourselves to a linear rise of the debuncher voltage. Then the condition for optimal debunching has the form $k = k_0$. In this case, the phase volume of the beam at the debuncher exit is enclosed by the ellipse

Translated from Atomnaya Énergiya, Vol. 37, No. 5, pp. 393-395, November, 1974. Original article submitted November 23, 1973.

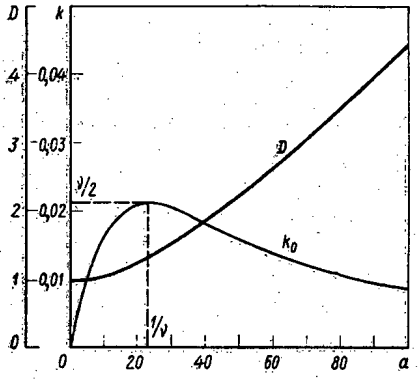

Fig. 1

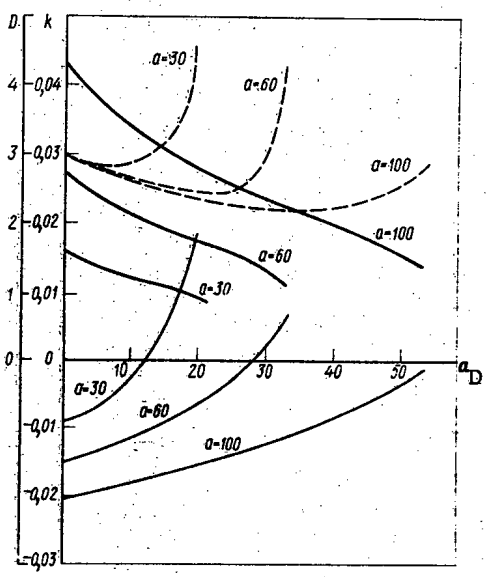

Fig. 2

Fig. 1. Dependence of the parameter k_0 and of the debunching factor on relative drift length.

Fig. 2. Dependence of the parameters k_D and k_M and of the debunching factor on the relative distance between modulator and debuncher (light solid lines give values of k_D; light dashed lines, values of k_M).

$$\frac{\psi}{\psi_к^2}+\frac{(g-k\varphi_0)^2}{G_к^2}=1, \tag{6}$$

where

$$\Psi_к=D\Psi_0,\quad G_к=G_0/D, \tag{7}$$

$$D=\sqrt{1+a^2\nu^2}. \tag{8}$$

The function $k_0(a)$ is shown in Fig. 1. We consider the case $\nu = 0.043$, which corresponds to the I-2 linear accelerator at ITEF. Below the curve for optimal debunching, $k < k_0$; the ellipse of the debunched beam is not "drawn out" as far as the canonical axes; the voltage amplitude in the debuncher gap is less than optimal. Above the curve for optimal debunching, $k > k_0$ corresponding to too high a voltage amplitude in the debuncher. The heavy line represents the dependence of the debunching factor D on the relative drift length a. In selecting debuncher parameters, one usually assigns a value to the debunching factor, which uniquely determines the drift length and the optimal voltage in the gap. The maximum value of k_0 corresponds to the point $a = 1/\nu$; $k_{0max} = \nu/2$. It is clear from Fig. 1 that $a > 1/\nu$ always when $D \geqslant 1.5$ so that the optimal voltage in the debuncher decreases when the drift length increases.

If one must achieve debunching and modulation simultaneously in a debuncher, the parameter k is given by the requirement imposed on the modulation,

$$\frac{dg_{av}}{g_{av}}=k\frac{d\varphi_0}{dt},$$

and cannot be determined from a given value of the debunching factor.

Let the value of k determined by the requirement for energy modulation be lower than k_{0max}. In principle, the functions of debunching and modulation can be combined in a single debuncher. However, the debunching factor cannot be selected independently in this case. If $k > k_{0max}$ because of modulation requirements, the debunching and modulation functions cannot generally be combined in a single debuncher and one should install a sequence of two single-gap resonators on the beam line (this case is encountered in practice).

We consider the transformation of the phase volume of the beam during successive passages through two single-gap resonators. Let a_M be the relative distance from the linear accelerator to the first single-gap

resonator (modulator) and a_D the relative distance between the modulator and the second single-gap resonator (debuncher), the frequency of which is the same as the frequency of the linear accelerator. The frequency of the field in the modulator is shifted with respect to the accelerating field in the injector. The total drift length up to the debuncher is $a = a_M + a_D$. Let k_M and k_D be the corresponding parameters of the modulator and debuncher (see Eq. (4)) which are determined by the voltage amplitudes in the gaps. Then the transformation of the coordinates ψ and g from the exit of the injector to the exit of the debuncher is given by the matrix equation

$$\begin{pmatrix} \psi + a_D k_M \varphi_0 \\ g - K\varphi_0 \end{pmatrix}_{db} = \begin{pmatrix} a_{11} a_{12} \\ a_{21} a_{22} \end{pmatrix} \begin{pmatrix} \psi \\ g \end{pmatrix}_{la}, \tag{9}$$

where φ_0 is the instantaneous value of the phase of the hf field in the modulator gap for which the synchronous particle passes through the center of this gap; K is the modulation coefficient characterizing the shift in the average momentum of the particles, $dg_{av}/dt = K(d\varphi_0/dt)$; it is given by

$$K = (1 - a_D k_D)\, k_M. \tag{10}$$

The subscripts "db" and "la" refer respectively to debuncher and linear accelerator.

The matrix elements for the transformation (9) are

$$a_{11} = 1 - a_D k_M;\ a_{12} = -a + a_M a_D k_M;$$
$$a_{21} = k_D + k;\ a_{22} = 1 - a k_D - a_M K.$$

In this case, the condition for optimal debunching takes the form

$$\frac{a_{11}}{a_{22}} = -\nu^2 \frac{a_{12}}{a_{21}}. \tag{11}$$

The phase volume of the beam at the exit of the debuncher for optimal debunching is bounded by the ellipse

$$\frac{(\psi - a_D k_M \varphi_0)^2}{\Psi_K^2} + \frac{(g - K\varphi_0)^2}{G_K^2} = 1. \tag{12}$$

The semiaxes of the ellipse are given by Eqs. (7) and the debunching factor is determined by the more general expression

$$D = \nu \sqrt{\frac{a - a_M a_D k_M}{K + k_D}}. \tag{13}$$

In the particular case where there is no modulator, $k_M = 0$ and Eq. (13) reduces to Eq. (8).

With the installation of two single-gap resonators, the modulation coefficient and the debunching factor can be assigned independently. For given values of K and D, appropriate device parameters k_M, k_D, a, and a_D are selected which correspond to optimal debunching. The values of these parameters turn out to be completely acceptable for practical realization.

In the usual device containing a single debuncher, the condition $k_D > 0$ must always be satisfied. It is clear from Eq. (10) that in a modulator—debuncher system where $k_D > 0$, the debuncher decreases the modulation of the average energy determined by the resonator with shifted frequency. In precisely this case, however, the choice $k_D < 0$ is possible and the most efficient use of both resonators is ensured. The physical significance of the choice $k_D < 0$ is particularly obvious when the distance between the gaps in modulator and debuncher is negligibly small. Setting $a_D = 0$, we find $k_M = K$, $k_D = k_0 - K$, and $D = \sqrt{a/k_0}$. If the assigned modulation coefficient K is greater than the maximum permissible value k_{0max}, the negative value of k_D makes it possible to reduce the angle of rotation of the ellipse during debunching to an optimal value.

The device parameters k_D and k_M are given by the expressions

$$\left.\begin{aligned} k_D &= \frac{A - \sqrt{\Delta}}{2a_D}; \\ k_M &= \frac{k}{1 - a_D k_D}. \end{aligned}\right\} \tag{14}$$

The following notation was introduced in Eqs. (14):

$$A = 2k_0 K a_D^2 - (2K - k_0)\, a_D + 1; \tag{15}$$

$$\Delta = (1 - k_0 a_D)^2 - \frac{4Kk_0^2}{a^2\nu^2}(1 + Ka_D)\, a_D^3 \tag{16}$$

The choice of $k_D < 0$ makes it possible to reduce the required voltage amplitude in the modulator. The dependence of the parameters k_D and k_M on the relative distance between modulator and debuncher is represented respectively in Fig. 2 by the light solid lines and dashed lines for various values of the total drift length. The heavy lines give similar relationships for the debunching factor. The curves are drawn for the case $K = 0.03$ and $\nu = 0.043$. If $D \approx 4$ when $a = 100$ and $k \approx 0.01$ for a single debuncher (see Fig. 1), we obtain $k_M = 0.03$, $k_D \approx -0.02$, and $a_D \approx 0$ in a modulator—debuncher system for $k = 0.03$ when $D \approx 4$ and $a = 100$. As the modulator is brought closer to the linear accelerator, the parameters k_M and k_D first fall in absolute magnitude and then begin to increase; however, the debunching factor falls monotonically as the distance between modulator and debuncher is increased. Because of the demodulating effect of the debuncher, it is impossible to bring the modulator as close to the linear accelerator as desired. There is a maximum permissible value of a_D which is determined by the change in the sign of the discriminant (16).

Thus a system of two sequentially arranged single-gap resonators makes it possible to modulate the average energy of a beam efficiently over a current pulse while maintaining optimal conditions for debunching. The system parameters are given by Eqs. (13) and (14).

MULTIPLE-TURN INJECTION INTO A 76 GeV PROTON SYNCHROTRON

Yu. M. Ado, V. I. Zaitsev, and M. F. Ovchinnikov

UDC 621.384.634

The first indications as to the possibility of multiple-turn injection into the Institute of High-Energy Physics proton synchrotron (operating at an energy of 76 GeV) were given in [1]. * On studying this problem further a slightly different method was adopted [2], but hardly any changes were required in the systems originally designed for introducing the beam.

The introduction of multiple-turn injection enables us to make fuller use of the phase volume of the annular accelerator and to store a greater number of particles without increasing the pulse current of the injector. According to [3], 90% of the injected beam occupies a radial phase space of $\pi \cdot 2$ cm $\cdot$ Mrad. According to measurements carried out in the accelerator accepting the existing distortions of the orbit and using the nominal accelerating voltage, the amplitudes of the betatron oscillations of the particles exhibiting a maximum deviation of their momentum from the equilibrium value are radially limited by the phase space $\pi \cdot (4 \pm 0.5)$ cm $\cdot$ Mrad. Thus by using two- and three-turn injection in the radial direction the number of assimilated particles may be considerably increased.

Here we shall give a brief description of the method and present some of the experimental results obtained with the accelerator.

Arrangement for Introducing the Beam into the Annular Accelerator

For introducing the beam into the accelerator we use a system of deflecting condensers [4, 5]. The disposition of the equipment is shown in Fig. 1. The chamber of the annular accelerator contains five condensers for deflecting the beam in a radial direction. In the condenser E_1, lying outside the aperture of the chamber, the voltage is kept constant. The parameters of the condenser are so chosen as to be able to change the injection angle by up to 31.5 Mrad. The voltage on the condensers E_2-E_5, embracing the working section of the chamber, is capable of being removed in a time much shorter than the beam rotation (revolution) time. The deflection angle of the particle beam in the condensers may reach 4.5 mrad. Each condenser plate has an independent supply source. This enables us to remove the voltage from each plate in a specific time interval, which is equivalent to having a stepped change in the deflecting electric field.

Method of Multiple-Turn Injection

The method of achieving two-turn injection is illustrated in Fig. 2. The center of the beam is injected at the point A_1 in the phase plane with coordinates r_i, r_i'. In contrast to single-turn injection, the initial conditions for introducing the beam are not completely compensated by the fields of the condensers E_2, E_3 (r_k, r_k'); hence in the first turn the beam executes coherent oscillations around the equilibrium orbit (point O). The amplitude and initial phase of the oscillations correspond to point A in the injection azimuth. After one turn with the condensers disconnected, the beam falls into one of the points of the selected phase trajectory indicated in Fig. 2, the particular point which it strikes being governed by the

*The initial 60 GeV version of the accelerator was considered.

Translated from Atomnaya Énergiya, Vol. 37, No. 5, pp. 396-399, November, 1974. Original article submitted December 24, 1973.

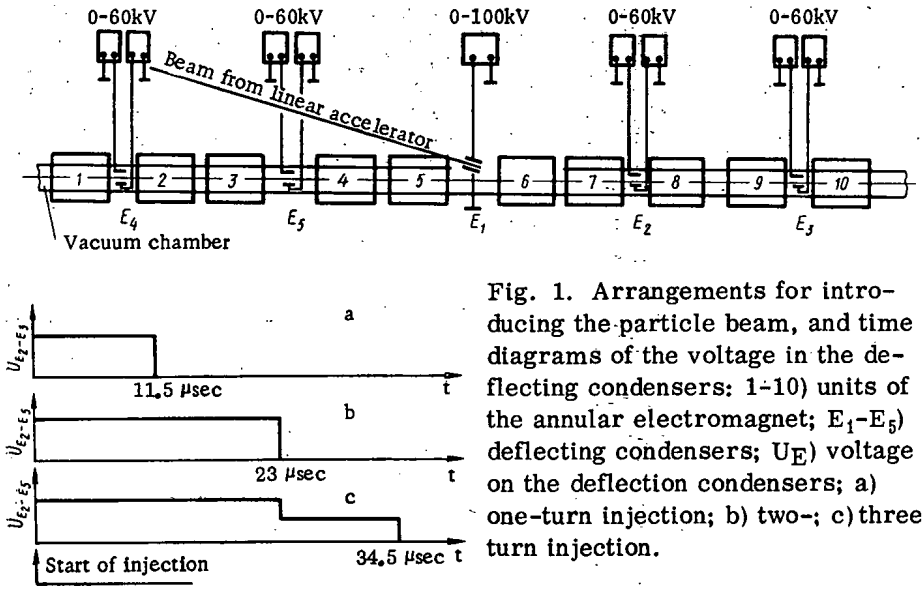

Fig. 1. Arrangements for introducing the particle beam, and time diagrams of the voltage in the deflecting condensers: 1-10) units of the annular electromagnet; E_1-E_5) deflecting condensers; U_E) voltage on the deflection condensers; a) one-turn injection; b) two-; c) three-turn injection.

value of Q_r. The action of the fields of the condensers E_4, E_5 (r_B, r'_B) lies in displacing the center of the beam to the point B_1, and its coordinates are determined by the relation

$$\begin{pmatrix} r_1 - r_B \\ r_1 - r'_B \end{pmatrix} = M(Q_r) \begin{pmatrix} r_1 - r_K \\ r'_1 - r'_K \end{pmatrix},$$

where $M(Q_r)$ is the rotation matrix. The voltages on the condensers are chosen such that, for a specified amplitude of the coherent oscillations, the centers of the emittances corresponding to two rotations of the beam may lie symmetrically on the phase trajectory. The same figure shows the manner in which the beam fills the phase plane for $Q_r = 9.8$; the calculation allows for the real shape of the emittance. The fairly wide range of variation of the deflection angles in the entry condensers enables us to inject the beam over the period of two turns equally effectively for a variety of frequencies of the betatron oscillations. After executing the second turn, the voltage on the plates is rapidly removed, ensuring the capture of the stored

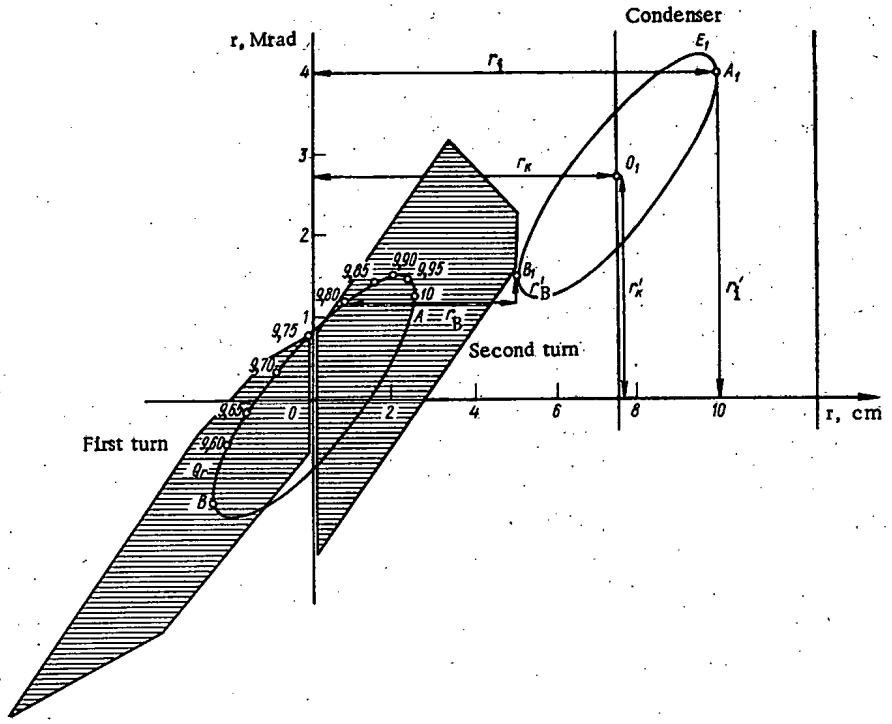

Fig. 2. Scheme of two-turn injection for $Q_r = 9.8$ (shaded region indicates the manner in which the particles fill the phase plane).

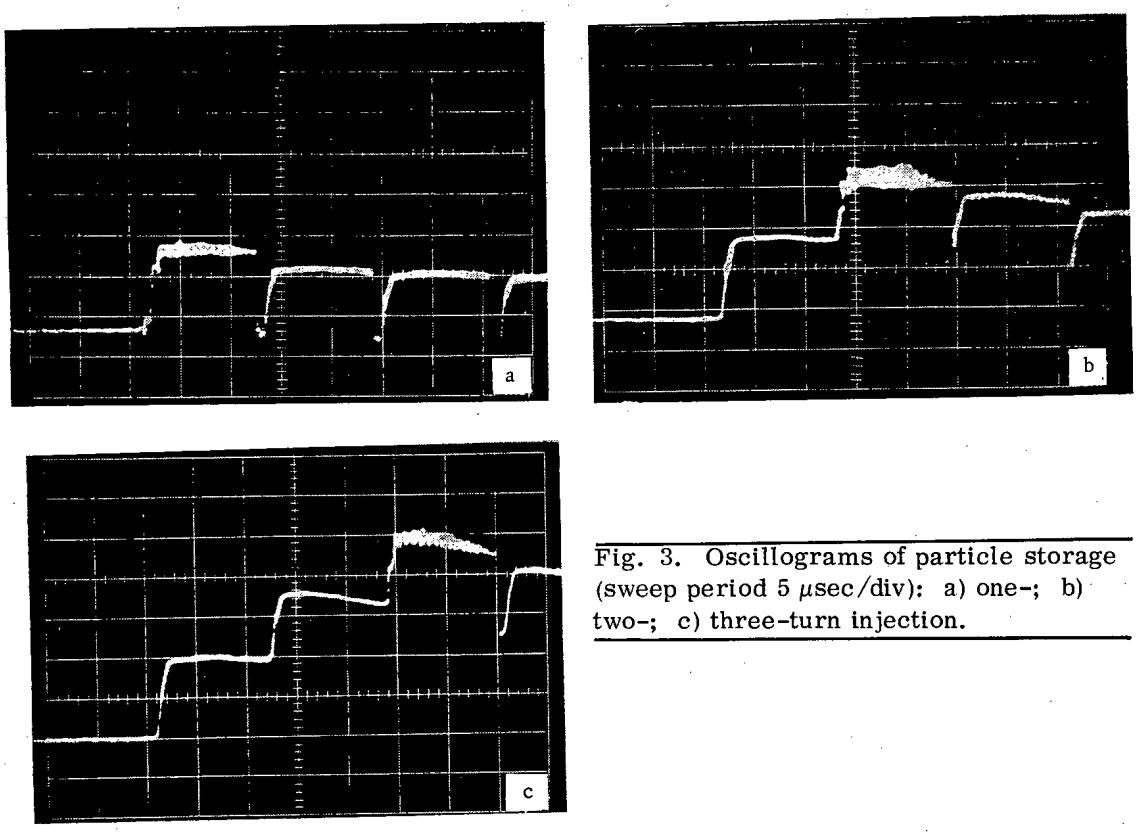

Fig. 3. Oscillograms of particle storage (sweep period 5 μsec/div): a) one-; b) two-; c) three-turn injection.

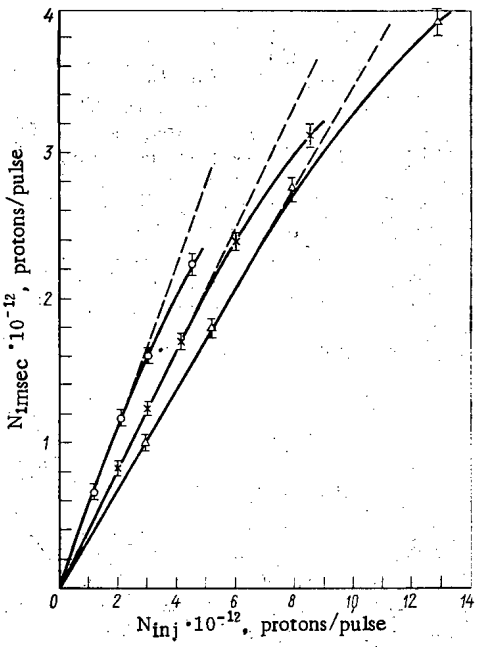

Fig. 4. Number of particles captured into the acceleration mode as a function of the number of injected particles for various number of injection turns: —○—) one; —×—) two; —Δ—) three.

beam by the magnetic field of the accelerator. If the voltage on the pulse condensers is kept constant for three turns, three-turn injection may also be effected. However, the contribution of each of the turns to the stored intensity will then depend on Q_r. If the voltage on the entry condensers is changed sharply after two turns, the phase plane will be filled more evenly and the emittances of the beams will lie on the phase trajectory at intervals of $2\pi/3$. For this form of injection the amplitudes of the coherent oscillations are identical for all the turns. This eliminates the dependence of the beam entry efficiency on Q_r and enables us to obtain the maximum number of stored particles over a fairly wide range of variation of the particle betatron oscillation frequencies.

Experimental Results

The storage of particles for various modes of injection is indicated in Fig. 3, which illustrates the oscillograms of the beam signals taken from a sensor placed in the chamber of the annular accelerator. The number of stored particles is approximately 90% of the number of injected particles for two-turn injection and 80% for three. The main losses occur at the inner plate of condenser E_1 and at the walls of the chamber in the inlet section, where in addition to the deflection of the beam from the equilibrium orbit (due to the coherent oscillations) there is also a distortion of the particle trajectories by the fields of the condensers.

Figure 4 illustrates the intensity of the accelerated beam as a function of the number of particles introduced into the accelerator chamber for various numbers of turns. These relationships were plotted for a constant emittance of the injected beam and for a momentum spread of the particles equal to $\Delta P/P \leq \pm 3 \cdot 10^{-3}$. The intensity was measured 1 msec after injection. The amplitude of the coherent oscillations at

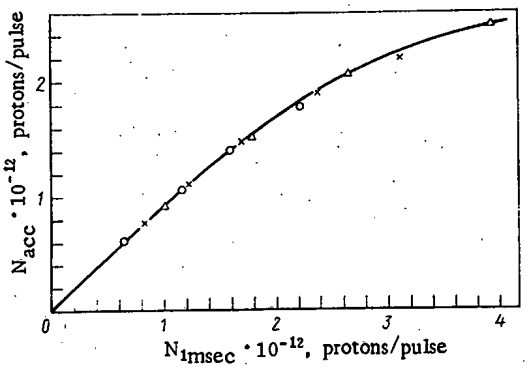

Fig. 5. Number of particles accelerated to the final energy as a function of the number of particles captured into the acceleration mode: ○) one turn; ×) two; Δ) three.

the point of injection was 2.5 cm for two- and 2 cm for three-turn injection. These values were chosen from the condition that the acceptance should be filled with the maximum number of particles. For small injection currents the number of particles captured into the acceleration mode depends linearly on the number of injected particles. The capture coefficient N_{1msec}/N_i for one-turn injection was 0.55; for two and three-turn injection it equalled 0.40 and 0.35 respectively. In the case of one-turn injection, the number of captured particles coincides with the number of particles in stable phases of the accelerating voltage. With increasing number of injection turns, particles with betatron oscillation amplitudes lying outside the acceptance limits are lost. The capture coefficient then obtained coincides with the calculated value [2] within the limits of stable operation of the accelerator. An increase in the density of the injected beam leads to additional losses, associated, as it would appear, with the action of the intrinsic field of the particle beam. It should be noted that, on increasing the number of injection turns, the deviation from linearity takes place at considerably greater values of N_i. This may be explained by a decline in the influence of the space charge of the particle beam on the betatron motion as the number of turns increases (and the particle density diminishes).

We see from Fig. 5 that the increment in the intensity of the beam accelerated to the final energy slows down as the number of injected particles increases. The measurements were made for various numbers of injection turns. The remaining accelerator parameters were kept constant. The deviations from the resultant curves due to the instability of the selected accelerator parameters are no greater than ±3%. The losses during the acceleration period reach 30-40% for an intensity of $(2.3\text{-}2.5) \cdot 10^{12}$ protons/pulse. These results also show that the particle losses during the acceleration time depend very little on the manner in which the acceptance is filled during injection.

Multiple-turn injection is being introduced at the present time.

The authors are grateful to A. A. Naumov for constant interest in the work, É. A. Myaé and E. F. Troyanov for useful discussions, and V. A. Beketov, A. D. Ermolaev, and A. G. Nevskii for help in the measurements.

LITERATURE CITED

1. D. Koshkarev, Intern. Conf. on High-Energy Accelerators and Instruments, CERN (1959), p. 656.
2. Yu. M. Ado, V. I. Zaitsev, and M. F. Ovchinnikov, Preprint Inst. High.-En. Phys., 73-11, Serpukhov (1973).
3. D. A. Demikhovskii, É. A. Myaé, and E. F. Troyanov, At. Énerg., 29, No. 4, 272 (1970).
4. S. N. Boiko et al., Electrophysical Apparatus, No. 9 [in Russian], Atomizdat, Moscow (1971), p. 3.
5. V. I. Zaitsev et al., in: All-Union Conf. on Charged-Particle Accelerators, Vol. 1 [in Russian], Izd. VINITI, Moscow (1970), p. 503.

ANALYTICAL REMOTE AND LABORATORY CONTROL OF THE REPROCESSING OF FUEL ELEMENTS FROM NUCLEAR POWER STATIONS

A. E. Klygin, A. N. Kononov, and V. G. Pastukhov

UDC 621.039.59:66.012

For a detailed analysis of the state of control of a radiochemical process by extraction technology [1-5], it is convenient to divide all types of control into three groups: laboratory control, by the method of sampling the medium being analyzed with subsequent analysis in the laboratory; remote analytical control by automatic instruments directly in the technological lines and apparatus [6, 7] and general technical control of the level, consumption, temperature, pressure, and evacuation of the technological media, carried out by industrial instruments [8, 9].

Analytical Remote Control

Uranium Control. All solutions requiring uranium concentration (C) measurements can be divided into several groups.

First Group – Solutions with C > 5 g/liter, containing a large quantity of different elements (up to several tens of g/liter) and creating a high γ-radiation exposure dose rate (EDR) (up to several tens of R/sec). The leading products of dissolution, mixing, and filtration processes belong to this group.

Second Group – Solutions with C > 5 g/liter with a relatively low EDR (up to 0.1 R/sec) and containing almost no salts of other elements. Extracts and reextracts belong to this group.

Third Group – Solutions with C < 1 g/liter, creating a considerable EDR (up to several tens of R/sec) and containing several tens of g/liter of salts of various elements. This group includes aqueous raffinates of the first extraction cycle, solutions from the washing of organic solutions, and discard solutions subject to burial.

Fourth Group – Solutions with C < 1 g/liter and with a relatively low EDR, not containing salts. Organic raffinates (recirculated organic solutions), decantates, mother liquors, condensates, and certain discard solutions belong to this group.

A number of physical and physicochemical methods can be used in principle for remote measurements of the uranium concentration: γ-absorption; x-ray (absorption, fluorescence); measurement of the β-radiation albedo; recording of the intrinsic γ-radiation; recording of the intrinsic α-radiation; exposure to moderated neutrons; densitometric; the rate of propagation of ultrasonics; spectrophotometric; potentiometric and multiparametric.

Production solutions differ in the great diversity of the concentrations to be measured and the presence of interfering impurities, and therefore it is not possible to control the uranium concentration by means of only one of these methods.

Gamma-absorptiometric instruments, characteristic of a high selectivity toward the majority of components and differing in the simplicity of the equipment design [10, 14], are found to have the greatest application for the measurement of uranium concentration in solutions of the second group. The principal nuisance factor is the γ-background (greater than 0.01 R/sec).

Translated from Atomnaya Énergiya, Vol. 37, No. 5, pp. 401-407, November, 1974. Original article submitted July 1, 1974.

For solutions with an enhanced EDR and with the addition of ballast salts (first group), the multiparametric method of [15, 16] can be used. Spectrophotometric instruments are used preferably and mainly for measurements of the valence state of uranium, for example U(IV) in the presence of U(VI) [17-20]. In order to determine the concentration of ^{235}U, the neutron irradiation method [21, 22] has the greatest application.

The main problem of uranium control is the development of methods of determining it in small concentrations within the range of 5-100 mg/liter, and which are suitable for the design of automatic instruments. There are data in the literature [23] about the feasibility in principle of using an x-ray fluorescence method for this purpose. However, there are no data on the incorporation of suitable instruments into the operation.

The most promising method for measurements of low ^{235}U concentrations is the γ-spectrometric method, based on the recording of the 184 keV line, and the neutron irradiation method. However, it is necessary to solve complex problems for their application: in the first case, to find a way of reducing the effect of fission products (^{241}Am, ^{144}Ce, etc.) and in the second case to design a simple and cheap apparatus utilizing strong sources of moderated neutrons [24, 25].

Control of Plutonium, Neptunium, and Americium. During reprocessing of fuel elements, the main problem is the separation and purification not only of uranium but also of plutonium, and also neptunium and americium, which are most valuable products and which are accumulated during irradiation of the fuel elements. The purpose of analytical control of these elements is for control in the process and, for plutonium also observance of nuclear safety standards. Taking into account the types of products of the technological process and the feasibilities of methods of remote control, all solutions of the elements can be divided according to concentration into three groups: first group, $C > 0.1$ g/liter; second group $0.1 \geq C > 2 \cdot 10^{-3}$ g/liter, and the third group, $C \leq 0.2 \cdot 10^{-3}$ g/liter. Refined solutions of these elements belong to the first group; the starting solution of the uranium cycle and certain solutions of the refined cycle belong to the second group and raffinates, recycled organic, waste and other discard solutions belong to the products of the third group.

Various methods can be used for the remote control of these valuable elements [26, 27]. Plutonium control can be effected on the basis of the (α, n) reaction at concentrations of 0.05 to 0.1 g/liter; by recording secondary fast neutrons for concentrations of 0.05 to 0.1 g/liter; by γ-spectrometric methods for concentrations of $0.1 \cdot 10^{-3}$ g/liter; by the α-count method for concentrations of $(0.05 \text{ to } 0.1) \cdot 10^{-3}$ g/liter; the calorimetric method (in a special vessel) for measuring the total quantity; the spectrophotometric method for concentrations of 0.1 g/liter. The α-count method can be used for monitoring neptunium concentrations greater than $(10\text{-}20) \cdot 10^{-3}$ g/liter and the spectrometric method for concentrations greater than $(20\text{-}50) \cdot 10^{-3}$ g/liter; the (α, n)-reaction method can be used for monitoring americium concentrations greater than $(1 \text{ to } 5) \cdot 10^{-3}$ g/liter, the γ-spectrometric method for concentrations greater than $(5\text{-}20) \cdot 10^{-6}$ g/liter, the γ-radiation method for concentrations greater than $(1 \text{ to } 2) \cdot 10^{-6}$ g/liter and the spectrometric method for concentrations greater than $(10\text{-}20) \cdot 10^{-13}$ g/liter.

For monitoring plutonium concentrations in solutions of the first group and americium in solutions of the first and second groups, the (α, n)-reaction method is the most preferable; this is distinguished by the high selectivity towards interfering components and simplicity of the equipment design [28-37]. The main limitation in this case is the γ-background ($\lesssim$1000 R/h). For monitoring plutonium and americium in solutions of the second and third group, the most promising method is the α-count method [32-35], which has a high sensitivity with excellent selectivity toward the many elements in solution. This method is most promising also for monitoring neptunium in products of the first group.

The spectrometric method may find application mainly for monitoring all the elements mentioned, in the products of the first group and partially of the second group. It is used preferably when it is necessary to determine the concentrations of different valence types [17-20]. The γ-spectrometric method has shown no great prospects up to now because of the effect of fission product elements.

The most promising trends in the determination of small concentrations of plutonium and americium is the development of methods for α-counting and α-spectrometry of the liquid [36].

Control of the γ-Radiation Exposure Dose Rate (EDR). The magnitude of the EDR in the products of radiochemical processing varies over a wide range from 10-100 down to 10^{-7} R/sec. The measurement accuracy when determining the EDR, as a rule does not play the same role as in the determination of the concentration of the elements. In the majority of cases, an estimate is required of the magnitude of the

degree of purification and therefore an error of 20-50% is quite acceptable. The EDR is determined remotely by measuring the flux of γ-quanta from the medium being monitored [37-39]. The methods used differ in respect of the arrangement of the sensors (inside the apparatus, at the side, in the technological line), the type of detectors used (ionization chambers, photomultipliers, gas-filled counters), and the method of eliminating the effect of external and adsorbed background.

The EDR can be measured by these methods over almost the entire range of values. A well-known difficulty is the measurement of solutions with EDR of 10^{-4} to 10^{-7} R/sec. Over this range, the external and adsorbed backgrounds start to exert a strong effect. At the same time, there are no methods which permit radically to reduce the background effect, especially for intraequipment positioning of the sensor. Thus, the most difficult problem of controlling the EDR is the development of methods for measuring small EDR values (10^{-4} to 10^{-7} R/sec).

Nitric Acid Control. The concentration of nitric acid in technological solutions varies within the limits of 0-8 M. Conductimetric, potentiometric (by the pH value), multiparametric, and densitometric methods can be used for remote control; the nuclear magnetic resonance method can also be used. The most useful are the multiparametric and conductimetric methods. The latter is most applicable for simple solutions, in particular, for the majority of aqueous solutions in extraction technology (excluding starting solutions), where the principal and only interfering component is uranium. However, its concentration is comparatively low, whilst the acid concentration is quite high [40-44].

The multiparametric method can be used conveniently in the simplest version – two-parametric, and mainly for starting products. This method differs from the others in complexity of equipment and its accuracy is not high as it depends on the errors of certain instruments, which occur in the assembly of apparatus [45].

The accuracy of present-day industrial instruments (conductimeters, densimeters, and pH-meters) is low and therefore the problem of remote control of nitric acid is to design instruments with increased accuracy.

Laboratory Control of Radiochemical Production

Production solutions, for which no remote monitoring methods exist, are analyzed predominantly in the laboratory. In consequence of the high β- and γ-activity of the irradiated nuclear fuel solutions, the analysis is carried out in special chambers or boxes. Therefore, in laboratory analysis, preference should be given to methods which provide for the use of the simplest devices but which permit quite accurate results to be obtained with the minimum volumes of the samples. In addition, it is desirable that the methods be versatile and quite rapid.

Determination of Uranium. For an accurate determination of uranium in the highly-radioactive starting solutions, it is advisable to use the isotopic dilution method with mass-spectrometric completion of the analysis [46]. The most suitable tracer atoms for introducing into the sample are ^{233}U. The method permits the uranium content to be determined with an error not exceeding 1 rel.%. It has been necessary to develop a simple and rapid coulometric method for determining uranium.

A relatively high concentration of uranium in other technological products can be determined by the volumetric method based on the reduction of uranyl to U(IV) with Mohr's salt in a phosphoric acid medium with subsequent oxidation of surplus reducing agent with nitric acid or sodium nitrite, and by titration of the uranium with ammonium vanadate [47] with potentiometric determination of the end point [48]. The error of the determination is ±2 to 3 rel. %.

With small uranium concentrations in discard solutions and in solutions with a high content of plutonium and neptunium, it is advisable to measure by the extraction-photometric method. The method is based on the extraction of uranyl diethyldithiocarbaminate with amyl acetate [49] from solutions with pH = 7.5, containing hydrazine chloride (1 M), hydrazine hydrate (1.3 M), and complexon III (0.1 to 0.5 mole /liter). The uranium is reextracted with a $5 \cdot 10^{-3}$% solution of arsenazo III in an acetate buffer solution with pH = 5.5, containing complexon III (75 g/liter), and the uranium is determined spectrophotometrically. The sensitivity of the method is 0.5 mg/liter. The coefficient of variation when determining 1 to 20 mg/liter of uranium does not exceed 8 rel. %.

TABLE 1. Remote Analytical Control Methods

Method, and its physicochemical basis	Range of determination	Effect of γ-background	Principal special features of the method	Principal limiting factors; possible instrumental error	Range of application
			Uranium monitoring		
Gamma-absorption; measurement of radiation attenuation of external source	1-500 g/liter	Depends on type and size of source, design of sensor and conditions of measurement	High selectivity toward the majority of constituents; simplicity of design of apparatus	Permissible EDR equal to 0.01 R/sec; $\Delta \approx 3\%$	Aqueous and organic media, including multiconstituent; lower limit of determination ~ 1 g/liter
Spectrophotometric; selective absorption of light by valence electrons	1-400 g/liter	No effect (with a high γ-background of the medium, the lifetime of the sensor is reduced)	Selectivity toward valence types; radioactive radiations do not affect	Effect of chemical conversions of element; effect of other elements, possessing spectral absorption; error in determining light absorption ~ 2%	Determination of U(IV) in the presence of U(VI); intra-apparatus determination of uranium in products with elevated γ-background
"Short exposure" method; measurement of fast fission reactions of ^{235}U when irradiated with moderated neutrons from an external source	$\geq$ 50-100 mg g/liter w.r.t. ^{235}U	Determined by the type of neutron detector chosen	Selective measurement of ^{235}U in the presence of other uranium isotopes	Rapid decay of source; absence of selectivity toward ^{239}U $\Delta \approx 2\%$	Determination of ^{235}U in the products from fuel-element reprocessing
Two-parametric; measurement of two independent parameters of the medium, with subsequent solution of a system of equations	0.900 g/liter	No effect	Measurements are possible with varying acid concentrations	Low selectivity toward macroconstituents; $\Delta \approx 5$-10%	Three-constituent, highly-active solutions
Ultrasonic; measurement of the velocity of propagation of ultrasound in the medium	3-5 g/liter	No effect	Radioactive radiations do not affect	Absence of selectivity to other constituents; $\Delta \approx 5\%$	Measurement of uranium ($C > 3$ to 5 g/liter) in highly-active media, with constant composition of other constituents
			Control of plutonium		
(α, n)-Reaction method; recording of neutrons formed by the $^{18}O(\alpha, n)^{21}Ne$ reaction	$\geq (10\text{-}50)\cdot 10^{-3}$ g/liter	Determined by the type of neutron detector	Slight dependence on chemical composition; simplicity of design of apparatus	Effect of α-active isotopes; low sensitivity; $\Delta \approx 5\%$	Determination of plutonium concentration in solutions with $C \geq$ 20-100 mg/liter

Declassified and Approved For Release 2013/02/21 : CIA-RDP10-02196R000400040003-4

α-Count method; measurement of intensity of α-radiation from the liquid	$\geq (20\text{-}50)\cdot 10^{-6}$ g/liter	No effect	High sensitivity; γ- and β-radiation have no effect	Effect of sorption on surface of detector	Measurement of plutonium concentration in discard solutions
Spectrophotometric; selective absorption of light by valence electrons	$\geq$0.1-0.2 g g/liter	No effect	Selectivity toward valence states of plutonium; unaffected by radioactive radiations	Effect of chemical conversions of elements; effect of other elements having absorption spectra; effect of suspensions and emulsions; $\Delta \approx 2\%$	Selective determination of valence states of plutonium; determination of plutonium in the products with elevated γ-EDR
Monitoring of γ-EDR of medium					
Recording of γ-EDR from the body of the apparatus by means of chambers	10^{-5}-10^{-2} B/sec	-	-	$\Delta \approx 2\%$ -	Operative control of purification factors
Determination of specific γ-activity of products in the technological lines, according to recordings of the γ-ray intensity from the body of the cuvette by means of counters and photomultipliers	10^{-7}-10^{-2} r/sec	-	-	$\Delta \approx 5\%$	The same
Monitoring of nitric acid					
Conductimetric; based on measurment of specific electrical conductivity	0-400; 400-900 g/liter	No effect	Simple apparatus design	High selectivity toward macrocomponents; $\Delta \approx 2.5\%$	Two-component solutions with a small amount of impurities
Two-parametric; measurement of two independent parameters of the medium with subsequent solution of a system of equations	0-300 g/liter	No effect	Measurements are possible at varying concentrations; radioactive radiations have no effect	Low selectivity toward macrocomponents	Three-component, highly-radioactive solutions from extraction technology
Potentiometric, by pH-value	0-100 g/liter	No effect	Simplicity of apparatus	Effect of macrocomponents of medium $\Delta \approx 0.1$ pH	Highly-radioactive solutions with small acid content.

Declassified and Approved For Release 2013/02/21 : CIA-RDP10-02196R000400040003-4

In the report on the work carried out by agreement with the International Atomic Energy Agency [50], the use is discussed of the chromatographic extraction of uranium with a running film of 5% TBP solution in CCl_4 for the subsequent determination of uranium by the photometric or luminescence method. The sensitivity of the photometric method is 2.5 μg per sample; the coefficient of variation for uranium concentrations of 100 mg/liter is 3%.

The method of chromatographic extraction of uranium on columns with TBP-sorbent is very convenient. The coefficient of variation in determining 0.02 to 1 g/liter of uranium amounts to 3%.

Determination of Plutonium and Neptunium. Among the numerous and well-known present-day methods for determining the transuranic elements [51-54], may be distinguished methods with an acceptable error in measuring large quantities or with the required limit of detection for the analysis of discard solutions.

The plutonium in the VVÉR fuel elements has a variable isotopic composition. It consists of a mixture of the isotopes ^{238}U to ^{242}U. Its specific α-activity can very from $1 \cdot 10^6$ to $1 \cdot 10^7$ dis/min · μg. Therefore, a radiometric method can be used only when data are available on the specific activity of the plutonium.

The specific α-activity of plutonium can be determined by the data from mass-spectrometric and α-spectrometric analysis of its isotopic composition. However, this can be done considerably more rapidly and simply by the separation of plutonium and other α-emitters by the anion-exchange chromatographic method with subsequent coulometric determination of the plutonium concentration in a pure solution of it and by measurement of the α-activity of this solution.

In the report [55], it is recommended that a column with a diameter of 5.5 mm be used for this purpose, filled with 1 g of 1X4 Dowex anionites or Dowex 2X8 (50-100 mesh) in nitrate form, washed with a 7 M solution of nitric acid. During filtration through the column of a solution containing ≥80 μg Pu(IV) in 7.0 M nitric acid, the plutonium is securely retained in the column, whilst all other α-emitting actinides existing in other valence states, can be eluted from the column almost without residue with a 7-8 M solution of nitric acid. The plutonium separated in this way from the other actinides is washed from the column with a hot 0.3 M solution of nitric acid.

Solutions containing more than 0.1 g/liter of plutonium can be analyzed by a coulometric or spectrophotometric method after oxidation of the plutonium to Pu(VI) [52]. The coefficient of variation of these methods does not exceed ±0.5%.

Chromatographic separation of plutonium from technological and discard solutions with its subsequent recording by means of an immersed α-detector is a very convenient and efficient method for determining small quantities of plutonium [51]. The coefficient of variation for a plutonium content of 3 to 5 μg per aliquot does not exceed 5%; the sensitivity of the method is 10 μg/liter; the duration of a single determination is 20-25 min.

Among the most sensitive methods for determining neptunium is the spectrophotometric method based on the formation of colored compounds of Np(IV) with arsenazo III [53, 56] and arsenazo M [57]. If necessary, preliminary separation of Np(IV) is carried out with extraction chromatography by methods similar to those for the separation of Pu(IV). For a more accurate determination of neptunium in solutions with high content, the coulometric method with controllable potential is used [53].

Determination of Nitric Acid. A rapid and reliable method of determining the concentration of acid is required for the efficient control of the technological process, which will permit its determination in the presence of hydrolyzing ions in both the aqueous and organic phases. One of these methods is potentiometric titration up to the original pH-value of a solution of potassium oxalate, added as a complexing agent [58, 59]. In order to use this method successfully, it is necessary to establish at what pH values the oxalate solution masks each of the hydrolyzing ions occurring in the solution to be analyzed. It is found that a solution of ammonium oxalate at pH = 6.0 forms simple complexes with Fe^{3+}, Fe^{2+}, Al^{3+}, UO_2^{2+}, Ni^{2+}, Cu^{2+}, PuO_2^{2+} and other ions which, with their simultaneous presence in solution, permits the concentration of acid to be determined by the potentiometric titration method up to the initial value of pH = 6.0. For the titration, and aliquot of the aqueous or organic solution to be analyzed is taken (for example, TBP + synthene), containing 0.002 to 1.0 mg-eq of acid, 50 ml of a 4% solution of ammonium oxalate at pH = 6.0, and is titrated (with stirring) with alkali up to the original value of pH = 6.0. For an acid concentration of 0.01 M and above, the coefficient of variation amounts to 2.5%. The time of a single determination is ~5 min.

The potentiometric method of titration up to a defined pH value can be automated by the use of a pH-meter in conjunction with an automatic titration unit.

Thus, the data available in the literature on methods of analytical control are essentially sufficient for designing instruments for the laboratory and remote analytical monitoring of the process of extraction reprocessing of fuel elements.

LITERATURE CITED

1. M. Benedict and T. Pickford, The Chemical Technology of Nuclear Materials [Russian translation], Atomizdat, Moscow (1960).
2. S. Stoller and S. Richards, Reprocessing of Nuclear Fuel [Russian translation], Atomizdat, Moscow (1964).
3. V. B. Shevchenko, The Chemical Technology of Irradiated Nuclear Fuel [in Russian], Atomizdat, Moscow (1971).
4. V. B. Shevchenko (editor), Reprocessing of Fuel from Power Reactors [in Russian], Atomizdat, Moscow (1972).
5. Yu. G. Mitskevich and L. S. Bogatova, Automatic Control of Radiochemical Factories by Technological Processes [in Russian], Atomizdat, Moscow (1970).
6. V. V. Boiko et al., Pribory i Sistemy Upravleniya, No. 9, 3 (1967).
7. B. V. Shelemin, Automatic Analyzers of the Composition of Radiochemical Media [in Russian], Atomizdat, Moscow (1965).
8. A. A. Balashov et al., Systems and Means of Automating Radiochemical Processes [in Russian], Gosatomizdat, Moscow (1963).
9. G. N. Balasanov, Simulation and Optimization in Automated Control Systems [in Russian], Atomizdat, Moscow (1972).
10. Budmen et al., in: Proceedings of the Second Geneva Conference [in Russian], Izbr. Dokl. Inostr. Uchenykh, Atomizdat, Moscow, 5, 422 (1958).
11. R. Connaly, Nucleonics, 17, No. 12, 98 (1959).
12. S. Broderick, Analyt. Chem., 34, No. 2, 295 (1962).
13. A. M. Drobiz, in: Automation of Chemical Processes [in Russian], OKBA Goskhimkomiteta, Moscow, No. 1 (1959).
14. L. K. Tototchenko, Radioactive Isotopes in Instrument Design [in Russian], Atomizdat, Moscow (1960).
15. A. M. Drobiz, in: Automation of Chemical Processes [in Russian], OKBA Goskhimkomiteta, Moscow, No. 4 (1959).
16. R. B. Popov, Problems of the Development of Scientific Instrument Design in the USSR [in Russian], Optipribor, 27 (1966).
17. R. Canning and P. Dixon, Analyt. Chem., 27, No. 6, 877 (1955).
18. C. Francois, Analyt. Chem., No. 1, 50 (1958).
19. R. Keil et al., Z. Anal. Chem., 244, No. 3, 165 (1969).
20. F. Scott and R. Dierks, Analyt. Chem., 32, No. 2, 268 (1960).
21. C. Nilson, Nucl. Instrum. and Methods, 13, No. 2, 183 (1961).
22. V. K. Bogatyrev et al., Atomnaya Énergiya, 28, No. 2, 111 (1970).
23. G. Baumgartel and L. Finsterwalder, Kerntechnik, No. 8, 347 (1970).
24. V. O. Vyazemskii et al., The Scintillation Method in Radiochemistry [in Russian], Atomizdat, Moscow (1961).
25. N. Kinnon et al., Nucleonics, 20, No. 1, 72 (1962).
26. W. Maeck et al., Analyt. Chem., No. 12, 1775 (1961).
27. F. Elliott and A. Pearson, Nucleonics, 21, No. 5, 78 (1963).
28. D. Cartwight and M. Todd, Nucl. Power, 6, No. 66, 79 (1961).
29. V. V. Ivanova et al., Atomnaya Énergiya, 7, No. 2, 166 (1959).
30. I. A. Serdyukova et al., Izv. AN SSSR. Ser. Fiz., 21, No. 7, 1017 (1957).
31. V. K. Bogatyrev et al., Zavodsk. Laboratoriya, No. 2, 208 (1970).
32. Bisby, Nucl. Power, 7, No. 74, 59 (1962).
33. J. Chabert, Nucl. Appl., 6, No. 1, 56 (1969).
34. A. N. Kononov et al., in: Trudy Vsesoyuz. Ob'ed. Moskov. Inzhen. Fiz. Inst. [in Russian], No. 1, Chelyabinsk (1971).
35. N. V. Chukichev et al., Pribory i Tekhnika Éksperimenta, No. 2 (1963).

36. J. Janguy, Rep. CEA-R-3422, Saclay (1968).
37. W. Abson and W. Loosemore, Rep. AERA-R-4552, 1 (1965).
38. G. V. Gorshkov, "Gamma-radiation of radioactive substances," Izv. LGU (1956).
39. V. Oxair and D. Andrews, Nucl. Appl., 6, No. 3, 225 (1969).
40. V. I. Eliseev, in: Automation of Chemical Processes [in Russian], No. 3, NIITÉKhIM, Moscow (1973), p. 35.
41. Yu. A. Gabuniya et al., Pribory i Sistemy Upravleniya, No. 9, 38 (1967).
42. P. D. Demchenko et al., Priborostroenie, No. 7, 3 (1966).
43. Yu. P. Zhukov, High-Frequency Electrodeless Conductimetry [in Russian], Énergiya, Moscow (1968).
44. A. B. Rozenblit, in: Automatic Control and Methods of Electrical Measurements, Proceedings of the Fifth All-Union Conference [in Russian], Vol. 2, Nauka, Novosibirsk (1966), p. 105.
45. T. A. Slepyan and S. M. Karpacheva, Radiokhimiya, 2, No. 3, 369 (1960).
46. D. Waldron (editor), in: Advances in Mass Spectrometry [Russian translation], IL, Moscow (1963).
47. V. K. Markov et al., Uranium, Methods of Determination [in Russian], Atomizdat, Moscow (1960).
48. L. Bakosh and L. Andrash, Zhurn. Anal. Khim., 20, 820 (1965).
49. Investigations in the Field of Geology, Chemistry and Metallurgy [in Russian], Izd. Akad. Nauk SSSR, Moscow, 21 (1955).
50. V. K. Markov and M. I. Krapivin, Report of a Research Contract with the IAEA [in Russian], No. 880/RI/RB (1971).
51. Analytical Method for the Determination of Plutonium, PG-Report-210 (W), UKAEA, Risley (1961).
52. M. S. Milyukova et al., Analytical Chemistry of Plutonium [in Russian], Nauka, Moscow (1965).
53. V. A. Mikhailov, Analytical Chemistry of Neptunium [in Russian], Nauka, Moscow (1971).
54. B. F. Myasoedov et al., Analytical Chemistry of the Transplutonium Elements [in Russian], Nauka, Moscow (1972).
55. V. K. Markov, Report of a Research Contract with IAEA [in Russian], No. 882 CF (1971).
56. S. B. Savvin, Reagents of the Arsenazo-Thoron Group [in Russian], Atomizdat, Moscow (1972).
57. Yu. P. Novikov, M. N. Margolina, and B. F. Myasoedov, Zhurn. Anal. Khim., 29, 698 (1974).
58. J. Booman et al., Analyt. Chem., 30, No. 2, 284 (1958).
59. Edzava Mapssi et al., Japan Analyst, 17, No. 10, 1273 (1968).

METHODS OF ESTIMATING THE RELIABILITY OF NUCLEAR REACTOR INSTALLATIONS

I. Ya. Emel'yanov, A. I. Klemin, and E. F. Polyakov

UDC 621.039.515:621.039.564

The problem of ensuring the high reliability of equipment, systems, and reactor installations as a whole is especially pronounced in the extensive development of nuclear power. It is impossible to create economical, competitive, and safe atomic power installations without solving this problem. Domestic and foreign experience indicates that a powerful means of increasing the efficiency of efforts to ensure the reliability of components is the use of quantitative reliability analysis at all stages of their manufacture and application. Such analysis allows optimization of the structure of the installation with respect to the criterion of reliability as well as effective determination of weak points and choice of measures to eliminate them.

In the last decade quantitative methods of estimating the reliability both of separate subsystems and of nuclear power installations have been developed strongly in all those countries which produce atomic energy. This accelerated development was made possible to a large degree by progress in the mathematical theory of reliability and in computational technique.

From the standpoint of modern reliability theory, a nuclear power installation, as well as its separate components (e.g., the control and safety rods, the emergency reactor cooling system, etc.), represents a complex technical system which is characterized by these specific properties:

1) structural overdesign (with spares) so that in the event of failure of individual components the system may be kept workable in the majority of cases;

2) functional overdesign, a consequence of which is the possibility of running the installation at reduced power in the event of failure of individual equipment elements;

3) the presence of a large spectrum of failures significantly differing in probability of occurrence and consequences (loss and time needed for its correction);

4) regular systematic preventive maintenance (SPM) during operation when defects and disturbances are removed as potential causes of equipment failure, as a consequence of which the reliability is increased;

5) repairability (ease of maintenance), that is the capability of eliminating equipment failure by emergency repairs over the entire lifetime of the installation.

Reliability calculations for such systems are usually done on an electronic computer. The present article gives a review of the basic ideas and methods and a brief description of the computer programs used in foreign and domestic practice for calculating the reliability of nuclear power installations and their subsystems. In addition, a method proposed by the authors for estimating the reliability of such installations (including an atomic electric power plant), which is a generalization and extension of existing analytic approaches, is presented. This method is convenient for engineering applications, especially at the stage of choosing a final version for the structure of an installation.

There are practically no publications on methods of calculating the reliability of nuclear power installations in the domestic literature, and the remaining foreign publications in periodicals often either

Translated from Atomnaya Énergiya, Vol. 37, No. 5, pp. 408-416, November, 1974. Original article submitted September 18, 1973; revision submitted May 23, 1974.

do not consider the entire variety of specific factors inherent in a nuclear power installation or contain only the basic ideas of the calculation without concrete details which significantly impede their practical application.

In what follows we shall refer to a nuclear power installation as a system, first for brevity, and also since these methods are useful for estimating the reliability of individual subsystems of the installation.

Summary of the Basic Concepts, Ideas, and Methods

The reliability problem assumes an estimate of the reliability of the elements* which comprise the system and an estimate of the so-called structural reliability of the system (that is, a calculation of its reliability based on the known logical relationships among the elements in the system and on the known indices of their reliability taking maintenance into account). The latter aspect is considered in the present paper.

An estimate of the structural reliability of the system begins with an engineering analysis of it during which the functional relationships between elements are replaced by logical relationships. First the notions of breakdown and workable states of the system are strictly formulated. Then, on the basis of these notions of failure or successful operation, a logical scheme is constructed and those combinations of various states of the elements are defined which lead to states of the system which are of interest.

The most common methods of logical representation of the states of the system during an analysis of their reliability are the relay-contact circuit (RCC), sometimes called the structural diagram of the system for reliability analysis and the "logical tree." In an RCC the electrical contacts represent elements and the wires joining the elements represent the logical relations, AND and OR, between the elements. In recent years, as evidenced in the material from conferences devoted to the problems of reliability and safety in reactor engineering† and in periodical publications [1, 2], there has been extensive development of the techniques for constructing logical trees. In this case, if the event of interest is a failure of the system then the tree is called a "failure tree."

An example of the construction of the simplest RCC and failure tree is given in Fig. 1.

The system (see Fig. 1) fails when elements 1 and 2 together, or 1, 3, and 4 together, or all four elements fail. This is shown in Fig. 1a and b.

The state of the system may be conveniently described with the aid of the so-called functions of logic algebra (FLA) which denote the failure of an element or of the system by the digit 1 and operation by the digit 0. According to the rules of mathematical logic all states of the system in Fig. 1 may be written out with the help of the following FLA:

$$Y(x_1, x_2, x_3, x_4) = x_1 \Lambda [x_2 \mathrm{V} (x_3 \Lambda x_4)] = (x_1 \Lambda x_2) \mathrm{V} (x_1 \Lambda x_3 \Lambda x_4). \quad (1)$$

Here x_i denotes one of the possible states of an element. Either $x_i = 1$ or $x_i = 0$. Λ is the symbol for the product of events and V, for the sum of events.

The condition that the system fails to operate is written in the form

$$Y(x_1, x_2, x_3, x_4) = 1. \quad (2)$$

The final goal of system reliability analysis is to determine certain quantitative indices. The probability $P\{Y(x_1, \ldots, x_n) = 1\}$ is usually regarded as the basic index.

For a system composed on nonrepairable elements

$$P\{Y(x_1, \ldots, x_n) = 1\} = F_0(t), \quad (3)$$

where $F_0(t)$ is the integral distribution law for the time of failure-free operation of the system. In this case, the probability $P\{x_i = 1\} = F_i(t)$ is the integral distribution law for the time of failure-free operation of the i-th element.

*By "element" we shall mean any component of the system whose structure is not considered in analyzing the reliability of the system as a whole.

†Conference of specialists in the reliability of mechanical components in nuclear safety systems in reactors, Riso, Denmark, September 24-26, 1969; Conference on the application of quantitative analysis of complex systems to the problems of safety of nuclear installations, Munich, FRG, May 26-28, 1971, etc.

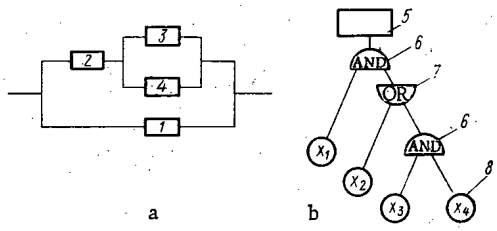

Fig. 1. Structural diagram (RCC) of a system (a) and failure tree (b): 1-4) elements; 5) failure of the system (final failure); 6) logical element AND (product of events); 7) logical element OR (sum of events); 8) failure of the i-th element (initial failure).

For a system composed of repairable elements,

$$P\{Y(x_1, \ldots, x_n) = 1\} = 1 - K_{P_0}(t) = Q_0(t), \tag{4}$$

where $Q_0(t)$ is the coefficient of system unpreparedness at time t (complement with respect to unit preparedness coefficient). In this case $P\{x_i = 1\} = 1 - K_{P_i}(t)$ is the coefficient of unpreparedness of an element at time t.

The reliability coefficients of the system, in accordance with Eqs. (3) and (4) are determined by reducing the FLA to a form for which it is possible to apply the basic formulas of probability theory. As a rule, the FLA reduces to one of two normal forms [3]: the disjunctive normal form (DNF), which is the sum of the products of events and the conjunctive normal form (CNF) which is the product of the sums of events.

Thus, the FLA for Y (see Eq. (1)) is written in the DNF. Using the distributive law, it is easy to reduce it to the CNF,

$$Y = x_1 \wedge (x_2 \vee x_3) \wedge (x_2 \vee x_4). \tag{5}$$

Using an expansion theorem [3], it is possible to write an arbitrary FLA in the so-called complete disjunctive normal form (CDNF):

$$Y(x_1, \ldots, x_n) = \mathrm{V}_1 x_1^{\alpha_1}, \ldots, x_n^{\alpha_n}, \tag{6}$$

where

$$x^{\alpha} = \begin{cases} x \text{ confirmation, if } \alpha = 1; \\ \bar{x} \text{ negation, if } \alpha = 0; \end{cases}$$

and V_1 means that sums of events are taken corresponding to those "sets" of $\alpha_1, \ldots, \alpha_n$ for which Y = 1.

For example, the FLA in Eq. (5) is written in CDNF in the following way:

$$Y = (x_1\bar{x}_2x_3x_4) \vee (x_1x_2\bar{x}_3\bar{x}_4) \vee (x_1x_2\bar{x}_3x_4) \vee (x_1x_2x_3\bar{x}_4) \vee (x_1x_2x_3x_4). \tag{7}$$

As for an FLA in the CDNF, it is said that it is orthogonal, since the logical product of any two products of events entering into it is zero. This property of the CDNF permits direct transformation from an FLA to a probability function using the formula for the probability of a sum of nonsimultaneous events:

$$P(\mathrm{V}K_i) = \sum_{i=1}^{n} P(K_i), \tag{8}$$

where K_i is the i-th product of events from the FLA written in CDNF.

Thus, for a system whose FLA takes the form of Eq. (7),

$$P[Y(x_1, \ldots, x_4) = 1] = F(t) = P(\mathrm{V}K_i) = (1 - F_2(t))\,F_1(t)\,F_3(t)\,F_4(t) + F_1(t)\,F_2(t)\,[1 - F_3(t)]\,[1 - F_4(t)]$$

$$+ F_1(t)\,F_2(t)\,F_4(t)\,[1 - F_3(t)] + F_1F_2F_3\,[1 - F_4(t)] + F_1(t)\,F_2(t)\,F_3(t)\,F_4(t) = F_2\,[F_1 + F_3F_4 - F_1F_3F_4]. \tag{9}$$

One of the widely used approaches for estimating reliability based on these concepts is the shortest path of successful operation (SPSO) and critical element group (CEG). The latter term is also called the minimum cross section for system failures. The SPSO is the minimum number of elements of the system which, when operating normally together, will ensure successful functioning of the system as a whole. The failure of even a single element of the SPSO means failure of the given SPSO. The system will work if at least one shortest path functions. This condition for workability may be written in the form of the following FLA:

$$\overline{Y}(x_1, \ldots, x_n) = \overset{i^*}{\underset{i=1}{\mathrm{V}}} \Phi_i, \tag{10}$$

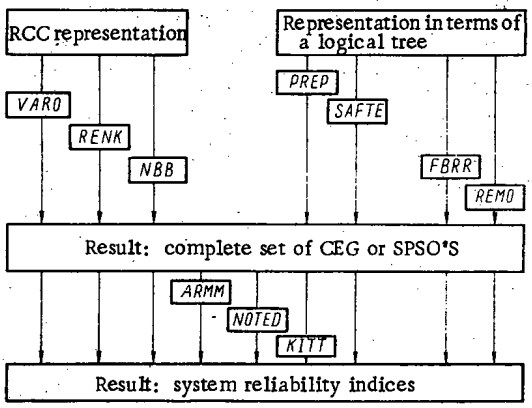

Fig. 2. Reliability computation programs.

where $\Phi_i = \Lambda \bar{x}_{k_i}$ is the event of normal functioning of the i-th SPSO; $\bar{x}_{k_i}$ is the workable state of the k-th element in the i-th SPSO. The CEG is the minimum number of elements whose simultaneous failure signifies failure of the system as a whole.

The condition for breakdown of the system consists of failure of even one CEG:

$$Y(x_1, \ldots, x_n) = \overset{i^*}{\underset{i=1}{\vee}} O_i = \overset{i^*}{\underset{i=1}{\vee}} \Lambda x_{k_i}. \qquad (11)$$

The condition for workability of the system, written in the form of Eq. (10), or nonworkability in the form of Eq. (11) permits transformation to a probability function upon use of the formula for the probability of the sum of simultaneous events:

$$P\{\bar{Y}(x_1, \ldots, x_n) = 1\} = P\left(\overset{i^*}{\underset{i=1}{\vee}} \Phi_i\right) = \sum_i P(\Phi_i) - \sum_i \sum_j P(\Phi_i \Lambda \Phi_j) + (-1)^{i^*-1} P(\Phi_1 \Lambda \Phi_2 \ldots \Lambda \Phi_{i^*}); \qquad (12)$$

$$P\{Y(x_1, \ldots, x_n) = 1\} = P\left(\overset{i^*}{\underset{i=1}{\vee}} O_i\right) = \sum_i P(O_i) - \sum_i \sum_j P(O_i \Lambda O_j) + \ldots (-1)^{i^*-1} P(O_1 \Lambda O_2 \ldots \Lambda O_{i^*}). \qquad (13)$$

Examination of an experiment applying these methods and the associated computer programs for estimating reliability allows us to draw the following general conclusions:

1. A reliability estimate of a system usually consists of two steps: analysis of the corresponding form of the logical representation of the system to isolate the CEG or SPSO and calculation of the reliability indices using the entire set of CEG or SPSO's. For complex systems (with a large number of elements) both these stages may be carried out by separate computer programs.
2. The calculation of the reliability of elements and the system as a whole, as well as isolation of the CEG and SPSO may be carried out analytically or by the method of statistical trials (Monte-Carlo). Both approaches may be applied in a single program [4].

Brief Description of Computer Programs for Reliability Estimates Developed in Other Countries

A general representation of the characteristics of computer programs for estimating system reliabilities is shown in the diagram of Fig. 2 (constructed from material in [5]).

The programs VARO, RENK, NBB, SAFTE, FBRR, and REMO combine the two stages: isolation of CEG or SPSO and calculation of the system reliability indices. The programs ARMM and NOTED carry out the second stage of an estimate of reliability. The programs PREP and KITT use a technique based on the so-called kinetic theory of failure trees [1]. With PREP and KITT, the two stages of reliability are distinguished. The programs VARO, RENK, and NBB, as follows from Fig. 2, require the logical representation of the system in the RCC-form. VARO uses the technique of compiling tables of states. It examines successively combinations of m failing elements out of n elements (n is the total number of elements in the system, and m = 1, 2, ..., k). The CEG's are isolated from these combinations, the probabilities of failure of the CEG's are calculated and these are then combined. If the CEG failures are not simultaneous events this gives only an approximate estimate for the desired probability of failure of the system. If the probabilities of failure of all the elements of the system are of one order the quantity m may be limited to a few units (because of the relatively small probability of failure of the large number of different independent elements). RENK is also based on the method of constructing tables of states given an exponential distribution law for the time until failure of the elements and their inability to be repaired. NBB yields upper and lower estimates for the reliability of a system based on the RCC representation.

In all the above listed programs an analytic approach is used. In the programs PREP, SAFTE, FBRR, and REMO a logical representation of the system in the form of failure trees is used.

PREP has two modifications: COMBO and FATE. In COMBO a deterministic algorithm for isolating the CEG is carried out by means of constructing tables of states, while in FATE the CEG is isolated by statistical trials.

The program SAFTE, based on the Monte-Carlo method, has three modifications. SAFTE-1 is used to estimate the reliability indices for systems consisting of repairable elements with spares. The resulting output characteristics are differential and integral distribution laws for the time until first failure of the system, the mean time of failure-free operation of the system, and the mean maintenance time. It is assumed that following repairs, every element of the system returns to its initial state (that is, repair is equivalent to replacing an element by a new one). SAFTE-2 is used to estimate the reliability indices of a system with emergency back up consisting of $N \leq 500$ nonrepairable elements. The program calculates the differential and integral distribution laws for the time until system failure, the mathematical expectation value of the time until failure, and its dispersion. SAFTE-3 calculates the probability of failure of the system at time t (coefficient of unpreparedness) assuming a known duration of maintenance. Using SAFTE-3 it is possible to estimate the reliability of the back-up systems and for statistical modelling to apply direct and "weighted" selection. SAFTE-3 is intended for systems containing up to 2000 elements. FBRR is a variant of SAFTE. REMO is also based on the Monte-Carlo method.

KITT uses the CEG and data on the reliability indices of the separate elements (repairable and nonrepairable) as input data. An analytic approach is used in the program. The output consists of the failure flow parameter and the preparedness (unpreparedness) coefficient.

An analytic approach, based on successive applications of Bayes' rule to a system of nonrepairable elements, is used in ARMM. The Weibull law is used as the distribution law for the time until failure.

In the program NOTED, which is based on the analytic approach of [6], the criterion for workability is described with the help of the SPSO. Various laws for the reliability of elements are used taking into account their back-up arrangements.

Thus the logical tree system predominates as a means of representing the workability (nonworkability) state. The reliability indices are calculated about equally often by means of the method of statistical trials and by analytic means.

When the Monte-Carlo method is used the real system operation is replaced by a mathematical model in the form of a succession of chance failures (recoveries) of the elements and of the system as a whole. The merit of this method is that it allows an estimate to be made of the reliability of a system with any given algorithm of operation. In this case it is possible to more fully take account of certain system peculiarities (in particular the variation in element failures) than when using analytic methods.

However, the feasibility of the method of statistical trials is limited by a number of inadequacies. The most important of these is the very large sensitivity of the method to the probability of an event and to the number of elements in the system. For highly reliable and complex systems an estimate of the reliability with acceptable accuracy may be obtained only by use of large amounts of machine time. In connection with this, the authors of [4, 7] propose methods which allow a reduction in the dispersion of the calculated result (and, thus, of the computing time). One of these methods is the method of statistical trials with a weight factor or with sampling according to importance [4, 7, 8].

Of the domestic papers on analytic methods of computing reliability of reactor plants, works [9-11], which are devoted to estimating the reliability of control and safety rods, should be especially noted. They use an approach differing in principle from those considered above. It is based on the theory of Markov and semi-Markov processes, the theory of bulk maintenance, and graph theory.

This approach is most effective when applied to systems of control and safety rods and of control and measuring instruments and automation equipment, whose elements may be considered as practically nonaging if cleaning and replacement are taken into account.

An answer to the question of which method is to be preferred (the method of statistical trials or the analytic method) evidently is not unique and depends on the concrete conditions, the nature of the problem to be solved, the complexity of the system being considered, etc. Statistical modelling is reasonable as an instrument for correcting analytic methods (to clarify the correctness of the basic assumptions made, etc.) but not for engineering calculations. The latter must be carried out using a more "mobile" method which yields a rapid, acceptably accurate, and sufficiently complete estimate of system reliability. The present paper proposes a variant of such a method.

Engineering Method of Estimating the Reliability of Reactor Installations

A failure tree will be used as a logical representation of the nonworkability state of the system. The resulting tree is digitized and fed into the memory of a computer. A complete listing of the CEG for the system is carried out deterministically on a computer using the program VYBOR KGÉ ("CHOICE OF CEG"). This program permits analysis of a system with up to 200 elements in about one minute on a type M-220 computer.

The reliability indices of the systems are calculated under the following basic assumptions: failures of elements of the system (initial failures) are independent events; equipment maintenance (planned and emergency) leads to complete recovery of the properties of an element.

A differential approach is used in this technique, i.e., events are considered which occur over a small time interval dt. The probabilities of such events are proportional to the interval dt. Thus, the probabilities of simultaneous occurrence of two or more independent events, proportional to $(dt)^2$, $(dt)^3$, etc., may be neglected.

Along with a failure tree, the initial data must include the reliability and ease of maintenance* characteristics of all the elements of the system, in particular: the differential distribution laws for the time until failure of the elements, f(t), and the time for emergency repair (replacement), g(t). The form of these laws may be arbitrary.

This method allows inclusion of planned-preventive maintenance (PPM) of the individual elements and systems (for example, planned repair of an atomic electric power plant) within the framework of the following assumptions:

1) planned-preventive, current (CM), and capital (CAM) maintenance of the system include the CM and CAM of elements and replacement of elements over a definite lifetime;

2) the time intervals between current (T_s^{CM}) and capital (T_s^{CAM}) repairs of an element and of the system (T_0^{CM} and T_0^{CAM}), and between replacements of an element over a definite lifetime (T_s^P) are determinable, plannable-in-advance quantities;

3) the time intervals between current and capital maintenance on the s-th element are multiples of the intervals between CM on the system;

4) the duration of system shutdowns during CM and CAM is determined by the number and types of elements repaired or replaced during the given PPM of the system;

5) all elements may be referred to several groups, each of which is served by its own maintanance staff;

6) the duration of PPM on the system elements is characterized by the mathematical expectation of the corresponding random quantities: the replacement time of an element over its lifetime, the time for its CM or CAM ($\Delta\bar{T}_s^P$, $\Delta\bar{T}_s^{CM}$, $\Delta\bar{T}_s^{CAM}$):

$$\Delta\bar{T}_s^i = \int_0^\infty t_s^i f_s^i(t)\,dt;\ t = \text{P, CM, CAM.} \tag{14}$$

The planned shutdown time of the system, ΔT^{PPM}, is defined in the framework of the above assumptions.

The quantity ΔT^{PPM} is used in calculating such complex reliability indices of the system as the technical utilization factor and the installed power utilization coefficient (see Eqs. (29) and (33), respectively).

*It should be noted that ease of maintenance (defining the duration of emergency and planned repairs) of atomic power station equipment takes on a special significance: it often is the defining factor in reliability. This creates a need for special studies to increase the ease of maintenance of equipment and for careful accounting of this characteristic in evaluating the reliability indices of reactor installations and their subsystems.

Estimating the Reliability of Elements. For each element of the system the failure flow parameter (average number of failures in a small unit time interval after time t), $\omega(t)$,† and the coefficient of unpreparedness, q(t), are calculated according to Eqs. (15) and (16) at the computing grid points in time between two successive PPM's on the system, t^l_{PPM} and t^{l+1}_{PPM} (or between t = 0 and the first system PPM):

$$\omega(t) = \tilde{f}(t - t^l_{PPM}) + \int_{t^l_{PPM}}^{t} \omega(t'')\,dt'' \int_{t''}^{t} g(t' - t'')\, f(t - t')\,dt'; \tag{15}$$

$$q(t) = 1 - K_P(t) = \tilde{F}(t - t^l_{PPM}) - \int_{t^l_{PPM}}^{t} \omega(t'')\,dt'' \int_{t''}^{t} g(t' - t'')\{1 - F(t - t')\}\,dt'. \tag{16}$$

Evaluation of the quantities $\tilde{f}$ and $\tilde{F}$ depends on whether a planned servicing of a given element has been carried out in a system PPM prior to the given time interval. If repair or replacement of the element were planned (and carried out) for this system PPM,‡ then

$$\tilde{f}(t - t^l_{PPM}) = f(t - t^l_{PPM}). \tag{17}$$

If the repair (or replacement) of an element was not planned for this system PPM, then

$$\tilde{f}(t - t^l_{PPM}) = \{1 - K_P(t^l_{PPM})\}\, f(t - t^l_{PPM}) + K_P(t^l_{PPM})\, f^*(t - t^l_{PPM}), \tag{18}$$

where f(t) is the differential distribution law for the time until failure for an element which is in working order up to the time of the beginning of a system PPM, t_{PPM}. $f^*(t - t^l_{PPM})$ is defined by the following relationships:

$$f^*(t - t^l_{PPM}) = -\frac{dP^*(t - t^l_{PPM})}{dt}; \tag{19}$$

$$P^*(t - t^l_{PPM}) = \frac{K_{P_{op}}(t^l_{PPM},\ t - t^l_{PPM})}{K_P(t^l_{PPM})}; \tag{20}$$

$$K_{P_{op}}(t^l_{PPM},\ t - t^l_{PPM}) = 1 - \tilde{F}(t - t^{l-1}_{PPM}) + \int_{t^{l-1}_{PPM}}^{t^l_{PPM}} \omega(t'')\,dt'' \int_{t''}^{t^l_{PPM}} g(t' - t'')\{1 - F(t - t')\}\,dt', \tag{21}$$

where $K_{P_{op}}$ is the coefficient of operational preparedness.

Eq. (15) is solved for the general case of arbitrary (nonexponential) distribution laws by the method of finite sums [12] on a time interval between successive system PPM's. Advancing successively from t = 0 in time steps we find the reliability coefficients of an element. This procedure is repeated for all the elements.

Estimating the Reliability of a CEG. The coefficient of unpreparedness of the l-th CEG is

$$Q_l(t) = \prod_{s=1}^{k} q_{sl}(t), \tag{22}$$

where s = 1, 2, ..., k is the index number of an element in the l-th CEG.

The failure flow parameter of an individual CEG, $\omega_l(t)$, is calculated on the basis of the formula for the total probability with the assumption that only one of the elements of the CEG may fail in a time interval dt:

$$\omega_l(t) = \sum_{\nu=1}^{k} \omega_{\nu_l} \prod_{\substack{s=1 \\ s \neq \nu}}^{k} q_{sl}(t). \tag{23}$$

The indices for all the CEG's in the system (l = 1, 2, ..., r) may be estimated using Eq. (22) and (23).

†We note that here and in the following the failure flow parameter is defined on a time axis which includes the periods of operation and emergency shutdowns of a component; that is, it is a complicated index which characterizes the freedom from failure and ease of maintenance of the piece. The derivation of Eqs. (15) is analogous to the derivation of $\omega(t)$ in [3], but is carried out taking the finite recovery time into account (i.e., recovery is not "instantaneous").

‡This is established by successive testing of the computed time steps from the grid of the system PPM and that of the element PPM.

Estimating the Reliability of the System. The probability of finding the system in a failure state at an arbitrary time t, $Q_0(t)$, is determined from Eq. (13) for the probability of the sum of failures of all the CEG's:

$$Q_0(t)=\sum_{l=1}^{r}Q_l(t)-\sum_{l=1}^{r-1}\sum_{j=l+1}^{r}\prod^{l,j}q(t)+\ldots(-1)^{r-1}\prod_{l,j,\ldots,k}^{1,\ldots,r}q(t), \tag{24}$$

where the symbol $\prod q(t)$ denotes the product of the unpreparedness coefficients of all the elements in the given l, j, ..., k CEG (if one and the same element appears in two or more CEG's, it enters this product only once).

Calculation of Eq. (24) for a system composed of a large number of elements and CEG's is fairly laborious. By successively limiting the expression for $Q_0(t)$ to terms with even or odd indices it is possible to obtain a sequence of upper and lower estimates for $Q_0(t)$ which converge to the exact value of $Q_0(t)$. The highest and lowest estimates are

$$Q_{0\max}(t)=\sum_{l=1}^{r}Q_l(t);\quad Q_{0\min}(t)=\sum_{l=1}^{r}Q_l(t)-\sum_{l=1}^{r-1}\sum_{j=l+1}^{r}\prod^{l,j}q(t). \tag{25}$$

In several cases (for example, when the system contains nonrecoverable elements for which $Q_l(t) \to 1$ at large t) the upper estimate in Eq. (25) may be ≥ 1. In this case $Q_{0_{max}}$ is more conveniently evaluated using the formula [13]:

$$Q_{0\max}(t)=1-\prod_{l=1}^{r}[1-Q_l(t)]. \tag{26}$$

Since usually $q(t) \ll 1$, Eqs. (25) and (26) yield a fairly good approximation to the exact value of Eq. (24).

The preparedness coefficient of the system, $K_{P_0}(t) = 1 - Q_0(t)$.

It is convenient to use the formulas for the upper and lower estimates for the failure flow parameter of the system $\omega_0(t)$:

$$\begin{gathered}\omega_{0\max}(t)=\sum_{l=1}^{r}\omega_l(t);\\ \omega_{0\min}(t)=\sum_{l=1}^{r}\omega_l(t)-\sum_{l=1}^{r-1}\sum_{j=l+1}^{r}\omega(t,\ l,\ j)\prod^{l,j}q(t)-\sum_{l=1}^{r}\sum_{\substack{s=1\\ s\neq l}}^{r}\omega(t,\ s,\ l)\prod^{s}q(t),\end{gathered} \tag{27}$$

where $\omega(t,\ l,\ j)$ is the failure flow parameter of a "fictitious CEG" composed of elements common to the l-th and j-th CEG's; $\omega(t,\ s,\ l)$ is the failure flow parameter of a fictitious CEG formed from the l-th CEG after removing those elements in common with the s-th CEG. $\omega(t,\ l,\ j)$ and $\omega(t,\ s,\ l)$ are evaluated according to Eq. (23); $\prod^{l,j} q(t)$ is the product of the coefficients of those elements which are not common to the l-th and j-th CEG's; and $\prod^{s} q(t)$ is the product of the unpreparedness coefficients of all the elements of the s-th CEG.

The mean values of the preparedness coefficient and failure flow parameter of the system may be obtained from the formulas

$$\overline{K}_{P_0}=\frac{\int_0^T K_{P_0}(t)\,dt}{T};\quad \overline{\omega}_0=\frac{\int_0^T \omega_0(t)\,dt}{T}, \tag{28}$$

where T is the utilization time (or calendar time after deduction of planned shutdown time).

The technical utilization coefficient of the system is defined as the ratio of the total working time of the system to the calendar working time

$$K_{t.u.}=\frac{t_u^W}{t_{cal}}=\overline{K}_{P_0}\left(1-\frac{\sum\Delta T^{PPM}}{t_{kal}}\right), \tag{29}$$

In order to calculate the utilization coefficient for an installed power N_{nom} it is necessary to consider in succession several failure trees for the system corresponding to partial and total failures and to

TABLE 1. Actual and Calculated Values of the Reliability Indices for the Beloyarsk Atomic Power Station

Reliability index	First plant		Second plant	
	actual value of index	calculated upper and lower estimates	actual value of index	calculated upper and lower estimates
ω_0	$2{,}56\cdot10^{-3}$	$2{,}76\cdot10^{-3}$; $2{,}53\cdot10^{-3}$	$2{,}43\cdot10^{-3}$	$2{,}67\cdot10^{-3}$; $2{,}55\cdot10^{-3}$
K_{P_0}	0,783	0,771; 0,759	0,866	0,908; 0,900
$K_{u.i.p.}$	0,764	0,751; 0,739	—	—

calculate the corresponding reliability indices for each. Each preceding failure state must be chosen to be wider and include the succeeding states within it; for example,

$$\begin{aligned} &1)\ N \leqslant N^0 = N_{nom};\ Q_0^0 = P\{N \leqslant N^0\} = 1; \\ &2)\ N \leqslant N^1 < N^0;\ Q_0^1 = P\{N \leqslant N^1\}; \\ &\ldots\ldots\ldots\ldots\ldots\ldots\ldots\ldots \\ &\ldots\ldots\ldots\ldots\ldots\ldots\ldots\ldots \\ &k+1)\ N \leqslant N^k < N^{k-1};\ Q^k = P\{N \leqslant N^k\}. \end{aligned} \tag{30}$$

It is clear that $Q_0^0 - Q_0^1 = P\{N^0 \geq N > N^1\}$ is the probability that the system works at a power satisfying the condition $N^0 \geq N > N^1$; that $Q_0^1 - Q_0^2 = P\{N^1 \geq N > N^2\}$, etc.

The average available power of the plant at time t may be written in the form

$$N_{avail}(t) = \sum_{i=1}^{k} [Q_0^{i-1}(t) - Q_0^i(t)]\, N_{av}^{i-1,\,i}, \tag{31}$$

where $N_{av}^{i-1,i}$ is some average power within the range $N^{i-1} \geq N > N^i$.

The average available power over the utilization period t_u is given by

$$\overline{N}_{avail} = \frac{\int_0^{t_u} N_{avail}(t)\, dt}{t_u}. \tag{32}$$

The utilization coefficient for the installed power is

$$K_{u.i.p.} = \frac{N_{avail}\, t_u}{N_{nom}\, t_{cal}} = \frac{\overline{N}_{avail}}{N_{nom}}\left(1 - \frac{\sum \Delta T^{PPM}}{t_{cal}}\right). \tag{33}$$

An Example: Exponential Model. Statistical information on the reliability of the elements of an atomic power plant is often inadequate so it is sometimes necessary to assume exponential reliability laws for all the elements although some of them have different laws from an exponential. On the other hand, in the initial fairly extended operating period of an installation, with appropriate planned-preventive maintenance of its elements, their reliability laws may be very close to exponential. In other words, the particular case in which the laws f(t) and g(t) may be considered as exponential is of no small practical interest. In this case the method described above becomes significantly simpler. In particular, the basic equation (15) is solved analytically for any time t and simple formulas are obtained for $\omega(t)$ and $K_P(t)$.

An algorithm for an exponential model calculation of the reliability of reactor installations has been carried out with the program OSNOVA-1 ("BASIS-1") for a type M-220 computer. To test the program it was used to calculate the reliability indices of the first and second plants at the Beloyarsk Atomic Power Station. A test of the method and the program was made by comparing the actual reliability indices of the first and second plants (obtained by analysis of the respective statistical information on plant operations) with the indices calculated using the program OSNOVA-1. The actual reliability indices of the individual equipment elements were used as initial data. Comparisons were made of three indices: the failure flow parameter, ω_0, the preparedness coefficient, K_{P_0}, and the installed power utilization coefficient, $K_{u.i.p.}$ * The actual values of these indices were compared with the upper and lower calculated estimates for both plants.

The initial statistical data on the reliability of individual elements of equipment and data on the first and second plants are taken, respectively, for the periods from July 1, 1967 to December 31, 1971 and from December 29, 1967 to December 31, 1970. These periods were chosen as they corresponded to the most reliable statistical data.

As is clear from Table 1, good agreement is obtained between calculated and actual values of the reliability indices of the first and second plants of the Beloyarsk Atomic Power Station. Thus, the difference between the lower calculated and the actual values of the preparedness coefficient and of the installed power utilization coefficient does not exceed 5% (in this case it should be noted that the 90% confidence

*The mean values of these reliability indices were compared over the time interval considered.

interval for the actual values taken is several percent). Based on the results obtained, it may be assumed that the calculated upper and lower estimates of the reliability indices differ insignificantly from one another. This situation is rather satisfying, since it eliminates the need to do the calculations with the exact formulas for Q_0 and ω_0 and leads to a significant economy in machine time. This test of the exponential method on the example of calculating the reliability indices of a real object showed that it may be a convenient and sufficiently accurate means of analyzing the reliability of reactor installations.

CONCLUSIONS

1. Domestic and foreign experience indicate that quantitative analysis of the reliability of reactor systems during their development is a rather effective means of increasing their reliability.

2. The introduction of quantitative reliability analysis into engineering practice is impeded because of inadequately developed engineering methods applicable, in particular, to reactors for atomic power stations.

3. A variant of the engineering technique for estimating the structural reliability of reactors is proposed. This method enables calculations to be made of the reliability of a broad class of installations and their subsystems during the design stage with satisfactory accuracy and generality.

4. A particular (simplified) case of this method, the exponential model, was considered. Based on the example of a calculation of the reliability of the reactors in the first and second units of the Beloyarsk Atomic Power Station it was shown that this model can give a good approximation to the actual situation, is simple, and is conveniently applied.

LITERATURE CITED

1. W. Vesely, Nucl. Engng. and Design, 13, No. 2, 337-360 (1970).
2. G. Mieze, Kerntechnik, 12, No. 9, 377-387 (1970).
3. I. A. Ryabinin, Elements of the Theory and Computation of the Reliability of Marine Electrical Power Systems [in Russian], Sudostroenie, Leningrad (1971).
4. E. Dressler, Kerntechnik, 4, No. 12, 574-581 (1972).
5. A. Colombo, Survey and Critical Analysis of Programs for System Reliability Computation. Commission of the European Communities, CCR, Ispra, Italy (1971).
6. E. Woodcock, The Calculation of Reliability of Systems. The Program NOTED. UKAEA-AHSB(S), R117 (1968).
7. B. Garrik, Nucl. Engng. and Design, 13, No. 2, 245-321 (1970).
8. J. Spanier and E. Gelbard, The Monte-Carlo Method and Neutron Transport Problems [Russian translation], Atomizdat, Moscow (1972).
9. P. I. Popov and V. G. Terent'ev, Reliability of Automated Systems [in Russian], Izd. MIFI, Moscow (1966).
10. P. I. Popov and A. P. Cherenkov, Avtomatika i Telemekhanika, No. 9, 143-151 (1968).
11. P. I. Popov and A. P. Cherenkov, in: Control of Nuclear Power Stations [in Russian], Vol. 4, Atomizdat, Moscow (1970), pp. 119-133.
12. B. P. Demidovich et al., Numerical Methods in Analysis [in Russian], Nauka, Moscow (1967).
13. R. Barlow and F. Proshan, Mathematical Theory of Reliability [Russian translation], Sovetskoe Radio, Moscow (1960).

ABSTRACTS

EFFECTIVE BOUNDARY CONDITIONS AT THE SURFACE OF AN ABSORBING ROD

R. A. Peskov and O. B. Samoilov

UDC 621.039.51.12

The effect of neutron absorption and scattering on the form of the boundary condition at the surface of a control rod is taken into account in calculating the neturon flux in the surrounding medium in the diffusion approximation. One-group effective boundary conditions (EBC) are found for a gray cylindrical rod containing a neutron source and located in a scattering and absorbing medium with a distributed source. A procedure for calculating the EBC from the neutron balance is based on the requirement of a correct description of neutron leakage from the medium. The source in the medium is taken to be uniform or having a radial variation described by a logarithmic function or a Bessel function. The effect of the nonuniformity of a source distributed linearly or exponentially is analyzed in plane geometry.

A number of approximate formulas are obtained for calculating the EBC. A comparison is made with the results of exact numerical calculations of other authors [1, 2]. We recommend the following approximate expression for the EBC at the surface of a black rod without an internal source located in a medium with a uniform source:

$$\gamma_1 = \left[\frac{1}{\Sigma_t}\cdot\frac{d(\ln\varphi)}{dr}\right]^{-1}_{r=r_0} \approx \frac{4}{3} - r_0\Sigma_t\cdot\frac{0.577+0.046\Sigma_s/\Sigma_t}{0.225+r_0\Sigma_t+0.18\,(\Sigma_s/\Sigma_t)^2},$$

where φ is the neutron flux, r_0 is the radius of the rod, Σ_t is the total macroscopic cross section, and Σ_s is the scattering cross section. This expression is not in error by more than 2%. For $\Sigma_s = \Sigma_t$ it agrees with the Flatt [3] approximation and has the correct limits for $r_0\Sigma_t = 0$;

$$r_0\Sigma_t \to \infty,\quad \frac{\Sigma_s}{\Sigma_t} = 1;\quad r_0\Sigma_t \to \infty,\quad \frac{\Sigma_s}{\Sigma_t} = 0.$$

Our results are useful for refining calculations of control rod effectiveness in the multigroup diffusion approximation.

LITERATURE CITED

1. L. Ya. Isakova, Atomnaya Énergiya, 25, No. 3, 229 (1968).
2. G. Pomraning, Nucl. Sci. and Engng., 16, No. 2, 239 (1963).
3. N. Flatt, Nucl. Sci. and Engng., 22, No. 1, 87 (1965).

Original article submitted February 7, 1974.

MONITORING METHODS FOR TITANIUM TRITIDE AEROSOLS

L. F. Belovodskii, V. K. Gaevoi, V. I. Grishmanovskii, N. A. Mishin, and G. L. Tokarev

UDC 546.821-138:539.1.04+539.1.07

Neutron generators with Ti – T targets produce contamination of the air and working surfaces by particles of Ti – T, the amount of which may be determined by complicated and laborious methods such as

Translated from Atomnaya Énergiya, Vol. 37, No. 5, pp. 417–418, November, 1974.

autoradiography or combustion of filters bearing the Ti – T particles over CuO, with subsequent measurement of the resulting tritium oxide with a liquid scintillation counter. *

To determine Ti – T in air and on working surfaces we have used simpler methods and apparatus for analyzing filters or other such units.

Pyrolysis. The specimen containing Ti – T is fired for 10 min in a quartz tube evacuated to 10^{-1} torr at 1000°C; the gas is passed through a filter into an evacuated ionization chamber to measure the activity of the T.

Chemical Decomposition. The sample is placed in a Lucite vessel and is treated with a mixture of concentrated HF (20%) and HNO_3 (1%) in distilled water. The time for treatment of the Ti – T is 5-7 min. The resulting gas is passed through a drying system to the ionization chamber.

One can detect $3 \cdot 10^{-7}$ Ci if one uses these methods with a Kaktus instrument for the measurement.

Determination of Ti – T from the x-Rays from the Beta Particles of T. Here the filter is used with an end-window counter; the amount of T in the sample (Ci) is determined from the count rate, N, counts /min, from the x-rays via $Q = \alpha N$, where α is a coefficient of proportionality to be determined by experiment. It is found that α is constant for sample activities up to 10^{-4} Ci and is $0.58 \cdot 10^{-7}$ Ci · min/pulse for the SI-2B counter. If the times of measurement for sample and background are 30 min each, the limit of detection with an SI-2B counter in a DS-000 lead castle is $5.2 \cdot 10^{-7}$ Ci of T when ±20% coefficient of variation is accepted. The limit can be improved to 10^{-8} Ci if one uses specimens of FPP cloth treated with dioxan and 2-channel system with a coincidence circuit such as the URB-1. One can use as a detector for the x-rays a scintillation plastic based on polystyrene with 2% PPO and 0.2% POPOP. The treated filter is placed between two plastic disks and around these are placed the photomultipliers of the counting system.

One can determine similarly the contamination of air and working surfaces with other compounds of T, such as Zr – T.

Original article submitted February 18, 1974.

THERMODYNAMIC PROPERTIES OF THORIUM – ANTIMONY ALLOYS

V. A. Kadochnikov, A. M. Poyarkov, V. A. Lebedev, I. F. Nichkov, and S. P. Raspopin

UDC 669.755.298+541.134

Within the interval 666-820°C, the emf of the galvanic cell

$$Th_{sol} | KCl - NaCl + 3 \text{ wt.\% } ThCl_x || KCl - NaCl + 3 \text{ wt.\% } ThCl_4 | Th - Sb_{(L+ThSb_2)}$$

varies with the temperature according to the equation

$$E = 0.827 - 0.201 \cdot 10^{-3} T,$$

where E is expressed in volts. On the basis of this equation we calculated the partial enthalpies and entropies of thorium in the intermetallic compound $ThSb_2$, at equilibrium with saturated solutions. Within the temperature interval studied, these values are constant and equal to: $\Delta\bar{H}_{Th} = -76.3 \pm 1.8$ kcal/g-atom; $\Delta\bar{S}_{Th} = -18.5 \pm 1.7$ entropy units/g-atom, respectively.

The measured values of the emf of the cell

$$Th - Sb_{(L+ThSb_2)} | KCl - NaCl + 3 \text{ wt.\% } ThCl_4 | Th - Sb_{(L)}$$

permitted a determination of the activity coefficient and solubility of thorium in antimony. It was established that the activity coefficient of thorium does not depend on the concentration of the solution, but its temperature variation is described by the equation: $\log \gamma_{Th} = -0.02 - 9.83 \cdot 10^3 T^{-1}$.

*J. Biro and I. Feher, Assessment of Airborne Radioactivity, Vienna, IAEA (1967), p. 501.

The dissolution of α-thorium in antimony is accompanied by a substantial exothermic effect ($\Delta\bar{H}^{excess}_{Th}$ = −44.9 ± 3.7 kcal/g-atom), whereas the excess of entropy of thorium is practically unchanged ($\Delta\bar{S}^{excess}_{Th}$ = 0.1 ± 3.5 entropy units/g-atom).

The activation of thorium in liquid antimony is characterized by substantial negative deviations from Raoult's law. The solubility of thorium is described by the equation: $\log x_{Th} = 4.07 - 6.82 \cdot 10^3\, T^{-1}$, and at 700 and 800°C it is 0.22 and 1.0% by weight, respectively.

Original article submitted February 27, 1974.

INTERACTION OF LIQUID ALUMINUM WITH A $KCl - NaCl - UCl_3$ MELT

V. I. Sal'nikov, V. A. Lebedev,
I. F. Nichkov, S. P. Raspopin,
and L. M. Polyakov

UDC 669.715.298

Within the temperature interval 700-800°C the reaction of liquid aluminum with a $KCl - NaCl - UCl_3$ melt was studied:

$$Al + U^{3+}_{KCl-NaCl} \rightleftarrows Al^{3+}_{KCl-NACl} + U(Al).$$

An empirical equation for the temperature dependence of the conditional equilibrium constant of this reaction was obtained according to the experimental data:

$$\lg K^* = \frac{1805}{T} - 4.318 \pm 0.195.$$

It was shown that the experimental values of the conditional equilibrium constant are in good agreement with those calculated according to the known thermodynamic characteristics of the state of U^{3+} and Al^{3+} ions in a melt of $KCl - NaCl$ and uranium atoms in liquid aluminum alloys.

Original article submitted March 4, 1974.

CALCULATION OF ABSORBED GAMMA DOSE FROM A PLANE SOURCE WITH ARBITRARY ANGULAR AND ENERGY DISTRIBUTIONS

Yu. N. Lazarev and Yu. I. Chernukhin

UDC 539.122.173.001.2

We describe a semianalytical method for calculating the absorbed dose at distances ≥10 mfp from a plane gamma source with arbitrary angular and energy distributions. This quantity can be found rather easily if an exact solution is known for the dose $F_P^D(z, r, \lambda_0)$ from a point monodirectional monochromatic source (PMMS). Here z and r are the coordinates of the detector in a cylindrical coordinate system with its axis along the direction of the radiation, and λ_0 is the wavelength of the radiation. For example the dose recorded by a detector placed on the axis which passes through the center of the polar coordinate system ρ, φ perpendicular to the source plane can be written in the form

$$F_{PL}^D(z, r=0) = \int d\lambda_0 \int \rho d\rho d\varphi \int \sin\theta' d\theta' d\varphi' f(\rho, \varphi, \theta', \varphi, \lambda_0) F_P^D(\sqrt{z^2+\rho^2}\cos\beta, \sqrt{z^2+\rho^2}\sin\beta, \lambda_0), \quad (1)$$

where $f(\rho, \varphi, \theta', \varphi', \lambda_0)$ is the radiation source, and

$$\cos\beta = \frac{z}{\sqrt{z^2+\rho^2}}\cos\theta' + \frac{\rho}{\sqrt{z^2+\rho^2}}\sin\theta'(\varphi-\varphi').$$

The exact expression for $F_P^D(z, r, \lambda_0)$ is not known, and therefore approximate expressions for it are of great practical interest.

Since F_{PL}^D can be obtained by integrating F_P^D it is expected that even a crude approximation of F_P^D which takes account only of the most important moments in its functional behavior will provide a rather accurate value of F_{PL}^D.

Doses at large distances from a PMMS can be described approximately by using the fact that $F_P^D(z, r, \lambda_0)$ is a rapdily decreasing function of r. Thus F_P^D must correctly describe the dose at small r, and must give the value

$$F_\infty(z, \lambda_0) = 2\pi \int_0^\infty dr r F_P^D(z, r, \lambda_0) \quad (2)$$

as accurately as possible.

For r = 0 the main contribution to the dose comes from singly-scattered gamma rays (we consider only scattered gamma radiation) since a photon leaving the axis along which the source radiates has an infinitely small probability of returning to the axis, and photons scattered at zero angle can only be singly-scattered. This is confirmed by numerical calculations [1, 2]. Consequently

$$\lim_{r\to 0} 2\pi r F_P^D(z, r, \lambda_0) \approx [2\pi r F_P^{(1)D}]_{r=0}, \quad (3)$$

where $F_P^{(1)D}(z, r, \lambda_0)$ is the dose of singly-scattered gamma radiation from a PMMS. By using this approximation we can write

$$F_P^D(z, r, \lambda_0) = \frac{A(z)}{2\pi r}\frac{\exp\left\{-(\alpha\mu_0 r + b)\frac{r}{2z}\right\}}{\alpha\mu_0 r + b}[1 + B(z)\mu_0 r]. \quad (4)$$

Here $[2\pi r(\alpha\mu_0 r + b)]^{-1}\exp\{-(\alpha\mu_0 r + b)(r/2z)\}$ is the functional dependence characterizing the dose from singly-scattered gamma rays. It is obtained within the framework of the following approximations:

Translated from Atomnaya Énergiya, Vol. 37, No. 5, pp. 419-421, November, 1974. Original letter submitted June 27, 1973; revision submitted June 4, 1974.

TABLE 1. Absorbed Dose from a PMMS ($MeV \cdot cm^{-3}/kV \cdot sec^{-1}$)

$\mu_0 z$	$\mu_0 r$	E_0, MeV		
		2	4	10
6,97	0,61	$\frac{0,91 \cdot 10^{-7}}{2,39 \cdot 10^{-7}}$	$\frac{5,25 \cdot 10^{-8}}{8,33 \cdot 10^{-8}}$	$\frac{2,65 \cdot 10^{-8}}{2,38 \cdot 10^{-8}}$
6,76	1,81	$\frac{1,53 \cdot 10^{-8}}{3,6 \cdot 10^{-8}}$	$\frac{5,54 \cdot 10^{-9}}{5,4 \cdot 10^{-9}}$	$\frac{1,12 \cdot 10^{-9}}{0,71 \cdot 10^{-9}}$

TABLE 2. Absorbed Dose from a Plane Anisotropic Source ($\cdot 10^{-6}$ $MeV \cdot cm^{-3}/kV \cdot sec^{-1}$)

n	E_0 = MeV			E_0 = MeV		
	I	II	III	I	II	III
0	1,00	1,07	0,89	1,05	1,00	0,90
1	0,90	0,89	0,81	0,95	—	0,82
2	0,82	0,86	0,75	0,86	—	0,75

$$\mu(\lambda) \approx \mu_0 + \mu_1(\lambda - \lambda_0); \quad g(\lambda) \approx g_0 + g_1(\lambda - \lambda_0);$$
$$\alpha = 1 + \frac{\mu_1}{\mu_0};$$
$$\left(\frac{\lambda_0}{\lambda}\right)^2 K(\lambda, \lambda_0) \approx \exp\left(-b\sqrt{\frac{\lambda - \lambda_0}{2 - \lambda + \lambda_0}}\right); \tag{5}$$
$$b \approx \frac{2.6}{\sqrt{\lambda_0}},$$

where $\mu(\lambda)$ is the absorption coefficient of the medium, $g(\lambda)$ is the energy absorption coefficient of the detector material, and $K(\lambda, \lambda_0)$ is the gamma-ray scattering kernel.

The coefficients A(z) and B(z) in Eq. (4) are determined by using requirements (2) and (3) imposed on the function F_P^D:

$$A(z) = b\,[2\pi r F_P^{(1)D}]_{r=0} = abE_0 g_0 \gamma e^{-\mu_0 z}; \tag{6}$$
$$E_0 = \frac{0.511}{\lambda_0};$$
$$B(z) = \frac{\alpha}{b} \cdot \frac{\mu_0 \alpha \frac{F_\infty}{A} - V(y)}{\frac{\sqrt{4\pi}}{y}[1 - \Phi(y)]\, e^{y^2} - V(y)};$$
$$y^2 = \frac{b^2}{8\alpha\mu_0 z};$$
$$V(y) = -\ln 2y - 0.2886 + \sum_{n=0}^{\infty} y^{2n+1}\left[\frac{\sqrt{\pi}}{n!\,(2n+1)} - \frac{2^n y}{(2n+1)!!\,(n+1)}\right]; \tag{7}$$
$$\gamma = 2\left\{\frac{1 - \exp\left[-b\sqrt{\frac{t}{2-t}}\right]}{b} + \varkappa\frac{2 - \left[1 + \left(1 + b\sqrt{\frac{t}{2-t}}\right)^2\right]e\left[-b\sqrt{\frac{t}{2-t}}\right]}{b^3}\right\};$$
$$\Phi(y) = \frac{2}{\sqrt{\pi}}\int_0^y d\omega e^{-\omega^2}; \quad \varkappa = 2\frac{g_1}{g_0} - 1; \quad t = \lambda_T - \lambda_0;$$
$$a = 2\pi r_0^2 n_0;$$

here λ_T is the wavelength corresponding to the recording threshold energy E_T of the detector, r_0 is the classical radius of the electron, and n_0 is the electron density of the medium.

We calculate F_∞ by starting with the Boltzmann equation for the energy flux of gamma radiation from a PMMS. We consider only high-energy source gammas ($\lambda_0 < 1$) since they are of the greatest interest in calculating the transmission of thick shields. Then in solving the Boltzmann equation we can use the small-angle approximation [1, 3]. After integrating over r with a weight $2\pi r$ the Boltzmann equation for a PMMS in this approximation goes over into the equation for a plane monodirectional source, and consequently within the framework of the approximation used F_∞ is the dose from a plane monodirectional source. This dose is given by the expression

$$F_\infty(z, \lambda_0) = E_0 g_0 \exp(-\mu_0 z)\left\{\left(1 + \frac{\mu_1 z}{\xi}\right)^{\frac{a}{\mu_1}} + \frac{az\varepsilon}{\xi^2}\left(1 + \frac{\mu_1 z}{\xi}\right)^{\frac{a}{\mu_1} - 1} - 1 + \exp(-\xi t)(1 + \varepsilon t)\frac{(\mu_1 z t)^{\frac{a}{\mu_1}}}{\Gamma\left(1 + \frac{a}{\mu_1}\right)}\right.$$
$$\left. - \frac{\left(\frac{\mu_1 z}{\xi}\right)^{\frac{a}{\mu_1}}}{\Gamma\left(1 + \frac{a}{\mu_1}\right)}\left[\left(1 - \frac{\varepsilon}{\xi}\right)\Gamma\left(1 + \frac{a}{\mu_1}, \xi t\right) + \frac{\varepsilon}{\xi}\Gamma\left(2 + \frac{a}{\mu_1}, \xi t\right)\right]\right\};$$

$$\Gamma(\nu, x)=\int_x^\infty d\omega\omega^{\nu-1}e^{-\omega};\quad \Gamma(\nu)=\Gamma(\nu, 0);\ \xi\approx\frac{1.74}{\lambda_0};$$

$$\varepsilon\approx\frac{0.09}{\lambda_0}+\frac{g_1}{g_0}. \tag{8}$$

Equations (4)-(8) give the required solution for the dose at large distances from a PMMS.

The upper numbers in Table 1 give the dose in water calculated with Eqs. (4)-(8), and the lower values are calculated by the Monte-Carlo method [2]. For $E_0 > 2$ MeV the agreement between the two methods is satisfactory.

Table 2 shows the results of calculating the dose from a plane anisotropic source [$f(\theta') = \cos^n\theta'/4\pi$, $n = 0, 1, 2$] in water ($\mu_0 z = 10$) by Eqs. (1), (4)-(8) (I), by the moments method (II), and by using the Taylor building factors (III). It is clear that the results obtained by the moments method are much more closely approximated by using Eqs. (1), (4)-(8) than by using buildup factors.

Thus it can be concluded that F_{PL}^{D} can be determined relatively simply and reliably by the method described.

LITERATURE CITED

1. U. Fano, L. Spencer, and M. Berger, Transport of Gamma Radiation [Russian translation], Gosatomizdat, Moscow (1963).
2. V. G. Zolotukhin et al., in: Dosimetry and Radiation Shielding [in Russian], Vol. 11, Atomizdat, Moscow (1970), p. 95.
3. V. I. Ogievetskii, Zh. Éksp. Teor. Fiz., 29, 454 (1955).
4. H. Goldstein and J. Wilkins, The Shielding of Nuclear Powered Vehicles [Russian translation], Inost. Lit., Moscow (1961), p. 212.

QUANTITATIVE DETERMINATION OF CHEMICAL ELEMENTS IN MULTICOMPONENT SAMPLES BY PHOTONEUTRON ANALYSIS

A. I. Gutii, D. P. Mel'nichenko, N. P. Mazyukevich, A. M. Parlag, and V. A. Shkoda-Ul'yanov

UDC 543.53:518.6

Many industrial problems require the nondestructive determination of the percentages of chemical elements in samples whose components have very similar physical properties.

The present work is an extension of that reported in [1, 2] and tests the possibility of using a stable method of quantitative analysis of multicomponent mixtures based on experimentally determined photoneutron yields.

We use the scheme of measuring photoneutron yields on a betatron proposed by O. V. Bogdankevich [3], and the mathematical apparatus for solving certain incorrectly formulated problems first proposed by A. N. Tikhonov [4] and subsequently successfully developed in papers by V. G. Shevchenko et al. for determining photonuclear cross sections.

We assume that the sample contains elements with atomic numbers Z_1, Z_2, ..., Z_k for which the photoneutron yields $Y_i(E)$ ($i = 1, 2, \ldots, k$) in a certain energy range are known per unit weight and per unit accelerator current. Suppose the sample is thin enough so that there is practically no absorption of the beam of primary gamma rays in it. In this case we have the equation

$$p_1Y_1(E)+p_2Y_2(E)+\ldots+p_kY_k(E)=Y(E), \tag{1}$$

where p_1, p_2, ..., p_k are the weights of the corresponding chemical elements Z_i in the sample of weight p which have to be determined; Y(E) is the yield of photoneutrons from the sample, and $\sum_{i=1}^{k} p_i = p$.

Since in practice photoneutron yields are determined at a number of point values of the energy E_γ generally larger than the number of unknowns p_1, p_2, ..., p_k, we obtain an overdetermined system of algebraic equations. We write Eq. (1) in the form

$$A\bar{p}=\bar{Y}, \tag{2}$$

where

$$\bar{p}=\{p_1, p_2, \ldots, p_k\}, \quad \bar{Y}=\{Y(E_1), Y(E_2), \ldots, Y(E_n)\};$$

$$A=\begin{bmatrix} Y_1(E_1)\, Y_2(E_1) \ldots Y_k(E_1) \\ Y_1(E_2)\, Y_2(E_2) \ldots Y_k(E_2) \\ \cdots\cdots\cdots\cdots \\ \cdots\cdots\cdots\cdots \\ \cdots\cdots\cdots\cdots \\ Y_1(E_n)\, Y_2(E_n) \ldots Y_k(E_n) \end{bmatrix} (n>k).$$

Since experimentally determined values have a statistical spread it is possible to consider not one but a whole family of possible solutions, which we call formal, satisfying Eq. (1).

Generally speaking instabilities appear in finding a solution $\tilde{p}$ of Eqs. (2) from the known photoneutron yields $Y_i(E)$, Y(E). That is, arbitrarily small variations in $Y_i(E)$, Y(E) lying within the limits of statistical accuracy can give rise to large, and in many cases arbitrarily large, changes in p.

Translated from Atomnaya Énergiya, Vol. 37, No. 5, pp. 421-422, November, 1974. Original letter submitted August 13, 1973.

TABLE 1. Solution of the Problem as a Function of the Regularization Parameter α

α	$\tilde{p}^{\alpha}$		$\nu(\alpha)$
	p_1^{α}	p_2^{α}	
0,000	63,08	—20,77	
0,00005	42,26	—3,61	26,9
0,0001	33,84	3,33	21,78
0,00013	30,95	5,72	16,20
0,00015	29,48	6,92	14,21
0,000152	29,20	7,08	20,97
0,000155	29,15	7,189	7,49
0,000157	28,96	7,348	22,61
0,00016	28,79	7,456	10,77
0,00017	28,29	7,90	11,08
0,0002	26,84	9,09	12,47
0,0003	23,63	11,275	12,45

Methods of constructing an approximate solution are determined by imposing additional requirements which limit the class of solutions to those for which the method is stable. These requirements ensure the extraction of a compact subset from the set of formal solutions, i.e., one such that from any sequence $\{p_n\}$ of this set it is possible to choose a convergent subsequence whose limit is an element (in our case the true solution of system (2) for $\bar{p}$) of that same set [5].

The problem of finding a certain parametrized family of solutions by the method of regularization can be reduced to the problem of finding the absolute minimum of the following smoothing functional [4]:

$$M^{\alpha}(p) = \left\| \frac{1}{\sqrt{\bar{Y}}} (A\bar{p} - \bar{Y}) \right\| + \alpha \| \bar{p} \|^2, \qquad (3)$$

where $1/\sqrt{Y}$ is the weighting function; the first functional in (3) estimates the accuracy of satisfying the equation in the given energy interval $E_1 - E_n$, and the second the "complexity" of the approximation in it. The positive parameter α depends on the accuracy of the measurements and relates it to the complexity of the approximation.

The upper limit of the regularization parameter α is the maximum α for which the solution $\tilde{p}^{\alpha}$ satisfies the requirement

$$| A\tilde{p}^{\alpha} - \bar{Y} | \leqslant \delta\bar{Y},$$

where $\delta\bar{Y}$ is the mean-square deviation of the sum of the random quantities $Y_i(E)$, $Y(E)$ ($i = 1, 2, \ldots, k$).

As noted in [6] $\tilde{p}^{\alpha} \to p$ as $\delta\bar{Y}/\bar{Y} \to 0$. A quasioptimum approximation for $\bar{p}$ is that solution $\tilde{p}^{\alpha}$ for which α satisfies the condition

$$\min_{\alpha} \nu(\alpha) \approx \min_{\alpha n} \frac{\| \tilde{p}^{\alpha_{n-1}} - \tilde{p}^{\alpha_n} \|}{\Delta\alpha_n}.$$

An experiment was performed on a sample consisting of a combination of thin sheets of rhenium and tungsten (up to 20% rhenium). The weights of the components were determined by weighing. Such a sample is promising as an alloy for the electrovacuum industry and for making thermocouples which can be used up to 2500°C.

It should be noted that this mixture is specially chosen, since the atomic numbers of tungsten and rhenium are 74 and 75 and the thresholds for the (γ, n) reaction are 7.46 and 7.39 MeV respectively. In addition these elements have (γ, n) yields and cross sections which are nearly the same because the atomic weights are nearly the same.

The photoneutron yields are obtained for energy steps $\Delta E_{\gamma} = 100$ keV in the 6-21 MeV energy range on a BU-25/30 betatron with an intensity of 30 R/min at a distance of 1 m from the target by a multichannel method [3]. In this case the reference voltage generator and the auxiliary equipment for scanning the accelerator energy enable the maximum energy in the bremsstrahlung spectrum to be maintained to an accuracy of up to 0.5%.

We choose three values of the energy corresponding, for example, to the 92nd, 102nd, and 112th channel numbers of the analyzer. For them Eq. (1) is represented by the system (the yields are in relative units)

$$\begin{gathered} 0.80p_1 + 0.90p_2 = 32.0; \quad 1.20p_1 + 1.49p_2 = 47.0; \\ 1.65p_1 + 2.03p_2 = 59.9, \end{gathered} \qquad (4)$$

where p_1 is the weight of tungsten, p_2 the weight of rhenium, $Y_1 = \{0.80, 1.20, 1.65\}$ is the yield of photoneutrons from tungsten in the 92nd, 102nd, and 112th channels per unit weight, $Y_2 = \{0.90, 1.49, 2.03\}$ is the yield of photoneutrons from rhenium in the 92nd, 102nd, and 112th channels per unit weight, and $Y = \{32.0, 47.0, 59.9\}$ is the yield of photoneutrons from the mixture of tungsten and rhenium.

It should be noted that the relative deviation of the right and left hand sides of system (4) when the true solution determined by weighing is substituted into it ($p_1 = 28.35$, $p_2 = 7.030$) is equal to 10, 5.6, 1.9% for the 92nd, 102nd, and 112th analyzer channels respectively, but even these deviations lie within the limits of $\delta\bar{Y}/\bar{Y}$.

Table 1 shows the parametric solutions of system (4) obtained by the method of regularization for certain regularization parameters α. These data show that the quasioptimum solution corresponds to the solution $\tilde{p}^{\alpha}$ for $\alpha_{\text{quasioptimum}} = 0.155 \cdot 10^{-3}$. In this case the values obtained $p_1 = 29.15$, $p_2 = 7.189$ deviate least on the average from the values $p_1 = 28.35$, $p_2 = 7.03$ obtained by weighing: the deviations are $\delta p_1 = 2.82\%$, $\delta p_2 = 2.26\%$.

For $\alpha = 0$ Eq. (3) is solved by the method of least squares which is unsuited to incorrectly formulated problems. Its instability is shown by the fact that the solution $p_1 = 63.08$, $p_2 = -20.77$ corresponding to $\alpha = 0$ is physically meaningless.

The method of assaying described in the present paper also gave good results for an alloy of tantalum, tungsten, and rhenium used in the manufacture of commercial heating furnaces and for making thermal shields for spacecraft.

In determining the amounts of the components in the two-compound alloy of tungsten and rhenium we did not try to achieve the rapid analysis characteristic of methods using high-current beams. However, even with low-current accelerators the method of analysis will be rapid in comparison with those existing at the present time, not to mention the fact that it is nondestructive.

LITERATURE CITED

1. V. A. Shkoda-Ul'yanov et al., Byul. Izobret., No. 13, 72 (1964).
2. A. M. Parlag et al., Atomnaya Énergiya, 15, No. 2, 146 (1963).
3. O. V. Bogdankevich, Atomnaya Énergiya, 12, No. 3, 198 (1962).
4. A. N. Tikhonov, Dokl. Akad. Nauk SSSR, 151, 501 (1963); 153, 49 (1963).
5. A. N. Tikhonov, Dokl. Akad. Nauk SSSR, 39, 195 (1973).
6. A. N. Tikhonov, in: Calculational Methods and Programming [in Russian], Vol. 8, MGU, Moscow (1967), p. 3.

CORROSION AND ELECTROCHEMICAL BEHAVIOR OF CERTAIN ALLOYS OF URANIUM WITH ZIRCONIUM, NIOBIUM, AND MOLYBDENUM IN AQUEOUS SOLUTIONS

L. I. Gomozov, V. B. Kishinevskii, O. S. Ivanov, A. V. Byalobzhenskii, and V. N. Lukinskaya

UDC 669.017:620.193.23

The corrosion resistance of uranium and its alloys in water has been studied in a number of works (for a survey of these studies, see [1, 2]). The electrochemical behavior of uranium was investigated in [3].

Earlier [4] the favorable influence of such alloying additives as molybdenum, zirconium, and niobium on the corrosion resistance of uranium in water at 100°C was demonstrated. A number of alloys, which show the best results in the indicated work, were selected for further investigation. Their behavior was compared with the behavior of technical-purity uranium (basic impurity 1.5 atomic % carbon). The composition of the investigated alloys is cited in Table 2. The alloys were prepared by argon arc melting from technical purity uranium, iodide zirconium, and 99.5% pure niobium and molybdenum. Then they were homogenized at 1000°C, quenched from the γ-region in oil, and tempered according to the system: at 650°C for 10 min and at 500°C for 100 h. The alloy with 20 atomic % molybdenum was also investigated in the quenched state.

The alloys were tested at the temperatures 90 and 100°C. In view of a number of methodological difficulties, unavoidable in electrochemical measurements in distilled water, we used tenth normal solutions of sodium sulfate or sulfuric acid. As was shown by the control experiments, this had no significant influence on the nature of the curves obtained in comparison with tests in water, which was also noted in [1, 2].

Figure 1 presents the results of a potentiostatic investigation of the alloys, obtained at 90°C on the potentiostat of the Central Laboratory of Automation with exposure at each point from 1 to 3.5 h (depending on the intensity of the corrosion). All the data are cited with respect to a saturated calomel electrode. In the entire region of potentials, the investigated binary alloys U – Mo and U – Zr, as well as the ternary alloy U – Zr – Nb, possess increased corrosion resistance in comparison with uranium, while the ternary alloy U – Mo – Nb even corrodes more rapidly than uranium.

Parallel corrosion tests were conducted at 100°C in media with various pH (Fig. 2). Technical purity uranium exhibited somewhat smaller losses (especially in acid medium) in comparison with electrolytic

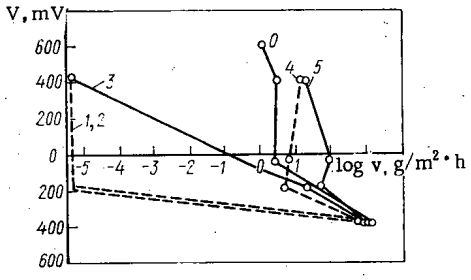

Fig. 1. Potentiometric anodic curves taken in a 0.1 N solution of Na_2SO_4 in an atmosphere of air at 90°C. The numbers next to the curves correspond to the numbers of the alloys cited in Table 1; the curves were taken after preliminary cathodic polarization (10 min at a current density of 160-180 mA/cm^2); v is the rate of corrosion.

Translated from Atomnaya Énergiya, Vol. 37, No. 5, pp. 423-425, November, 1974. Original letter submitted November 20, 1973.

TABLE 1. Chemical Composition of Uranium Alloys Subjected to Tests

Alloy No.	Code designation	Content, atomic %		
		Zr	Nb	Mo
0	Uranium	Unalloyed		
1	Ts-20	20	—	—
2	Ts8N12	8	12	—
3	M-20	—	—	20
4	M5N15	—	15	5
5	M10N10	—	10	10

TABLE 2. Rate of Corrosion ($g/m^2 \cdot h$) of Uranium and Its Alloys at Various Voltages in H_2SO_4 at 90°C in an Atmosphere of Air*

Voltage, mV	Presence of preliminary cathodic polarization	Uranium	Alloys				
			Ts-20	M-20	Ts8N12	M5N15	M10N10
50	Yes	2,74	0,083	1,59	0,112	5,9	92,5
	No	—	—	—	0	0	0,81
200	Yes	2,43	—	2,25	0,084	4,22	53,1
	No	2,93	0,11	1,77	0	0,13	0,31
400	Yes	1420	395	670	775	576	770
	No	1000	117	—	—	—	—

* Duration of experiment 1-3.5 h.

uranium. The stability of the alloys, investigated in the quenched and tempered states, increases in the series U – Zr, U – Mo, U – Zr – Nb. The greatest loss is observed in acid medium, the least in alkaline medium. Part of the samples were preliminarily anodized at 20°C in a saturated solution of chromic acid at a voltage up to 50 V. The anodic oxide film, within the limits of error, had no influence on the corrosion resistance or caused some deterioration of it. Evidently these films were porous.

Thus, direct corrosion experiments confirm the results of potentiostatic investigations: the alloys Ts-20, M-20, and Ts8N12 possess higher corrosion resistance than unalloyed uranium.

Interesting results were obtained in experiments on the use of preliminary cathodic polarization in potentiostatic investigations (see Fig. 1), in order to remove the natural oxide film from the surface of the samples. From the data of Table 2 it is evident that preliminary cathodic polarization (in any case, in a short period of continuing tests) increases the rate of corrosion of the alloys and has practically no influence on the behavior of uranium. Evidently this is associated with the different porosity of the oxide film formed on uranium and its alloys under atmospheric conditions.

Figure 3 shows the curve of the establishment of the static potential on uranium in 0.1 N H_2SO_4 at room temperature (for a sample kept for a long time in air after preliminary polishing). It is characteristic that at first the potential of the sample is shifted in the negative direction, and only after this does it

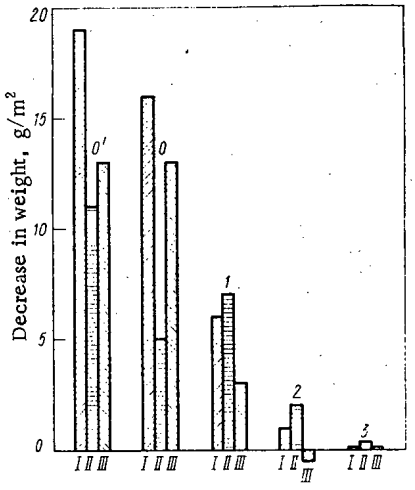

Fig. 2

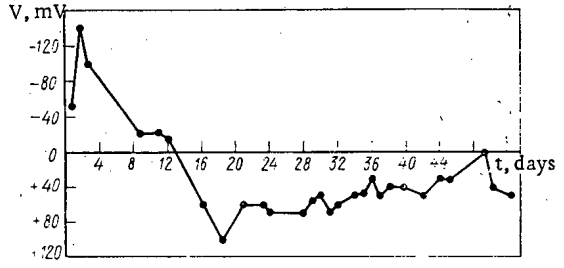

Fig. 3

Fig. 2. Comparison of weight losses of certain alloys in 100 h at 100°C. The numbers of the alloys correspond to Table 1; 0, 0') technical and electrolytic uranium, respectively. Media: I) distilled water; II) 0.1 N solution of H_2SO_4; III) 0.1 N solution of KOH.

Fig. 3. Change in the potential of uranium in 0.1 N H_2SO_4 solution at room temperature (t is the duration of testing).

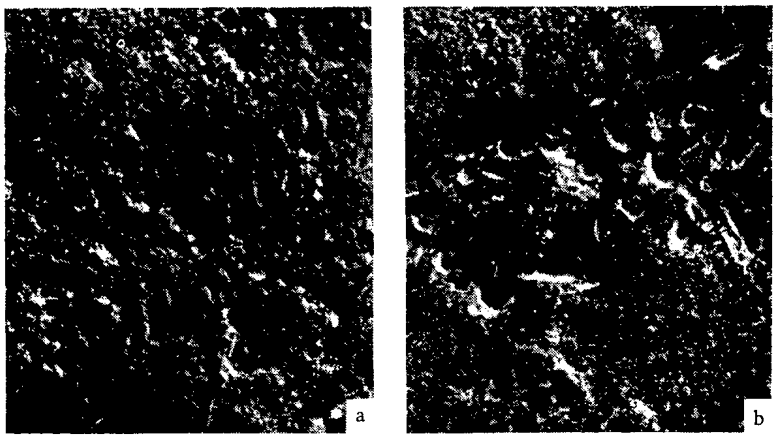

Fig. 4. Surface of a microsection after testing in water at 100°C for 1 h (×2000): a) unalloyed uranium (traces of corroded deposits of U(C, N) of dendrite form); b) alloy Ts-20 (accumulation of corrosion-resistant deposits of zirconium carbide).

begin to be shifted in the positive direction. Evidently, such a shape of the curve is due to the fact that the protective film formed on the surface of a sample during its exposure in air gradually breaks down in the electrolyte. The breakdown of the oxide film is caused by the dissolution of inclusions of uranium carbides, unstable in water. At the boiling point there is a very strong decomposition of UC [5]. A metallographic investigation, conducted on microsections preliminarily prepared, confirmed the predominant breakdown of inclusions of carbides (Fig. 4a), * which disrupts the integrity of the primary oxide film, i.e., acts analogously to cathodic polarization. After breakdown of carbides on the surface of the metal, a secondary oxide film begins to form, which also determines the corrosion behavior of uranium under the given conditions.

In U – Zr or U – Nb alloys, the corresponding carbides are formed, relatively stable in water [6], which was confirmed metallographically (see Fig. 4b). This circumstance is responsible for the conservation of a passive oxide film on the surface of the samples, inhibiting corrosion for some time (see Table 2). Hydrogen depolarization, breaking down the primary oxide film, activates the surface of the metal, which leads to an acceleration of corrosion at the initial stage of the process. It has been noted that without preliminary cathodic polarization, a substantial dispersion of the corrosion data is observed; this is due to the different duration of the exposure of the samples in air after mechanical treatment before the beginning of the experiment, the quality of the treatment, and, consequently, the different state (strength) of the "atmospheric" film. The use of preliminary cathodic polarization reduces the dispersion of the data.

In a potentiodynamic† investigation of the anodic behavior of uranium and the alloys under consideration, the following results were obtained. Under the investigated conditions (tenth normal sulfuric acid at 90°C), deaeration of the solution (purging with argon) has no influence on the nature of the potentiodynamic curve for uranium (Fig. 5A) and the alloy M10N10 (see Fig. 5C). Such behavior is due to the large volume content of α-uranium in the alloy M10N10 in comparison with the other investigated alloys [7]. In the case of the remaining alloys, deaeration facilitates the process of dissolution from the active state (see Fig. 5B, portion a); moreover, the potential changes by almost 0.5 V. Under conditions of deaeration (atmosphere of argon), the potentiodynamic curves of uranium and its alloys practically coincide (see Fig. 5A-C). The presence of two passive regions on the potentiodynamic curves is due to the formation of various oxides [3]. These oxides may be UO_2 (on the portion b) and UO_3 (on the portion d).

Thus, potentiostatic and corrosion investigations demonstrated the advisability of the alloying of uranium with zirconium, niobium, and molybdenum for increasing its corrosion resistance in water at 100°C. Damage to the original (formed in air) oxide film on uranium as a result of the breakdown of uranium carbides in water was detected. It was shown that in the case of uranium and the alloy M10N10, deaeration of a solution of 0.1 N H_2SO_4 by replacement of the air atmosphere by argon does not influence the shape

*The photographs presented in Fig. 4 were taken with a scanning electron microscope.
†The potentiodynamic curves were taken on the potentiostat of the Central Laboratory of Automation, using mechanical development. The rate of shift of the potential was 100 mV in 6 min.

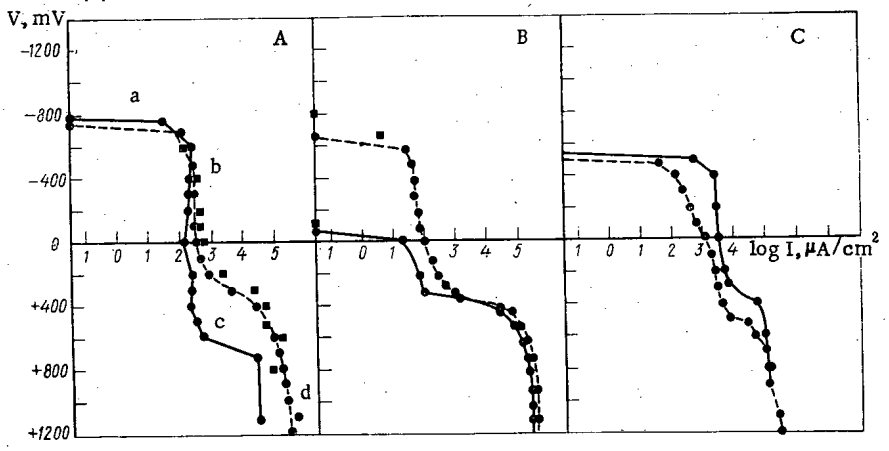

Fig. 5. Potentiodynamic anodic curves for uranium and its alloys in a 0.1 N solution of H_2SO_4 at 90°C [I) current density, V) potential]: A) unalloyed uranium; B) alloy Ts-20 (the alloys M20, Ts8N12, M8N12, and M5N15 give an analogous shape of the curves); C) alloy M10N10; ——) in an atmosphere of air; ---) in an atmosphere of argon; ■) data obtained in a 0.1 N solution of Na_2SO_4 in an atmosphere of air.

of the potentiodynamic curves. For the remaining alloys, an atmosphere of air shifts the polarization curve on the region of active dissolution into a more positive region of potentials, which is evidence of the passivating role of oxygen for these alloys.

LITERATURE CITED

1. V. V. Gerasimov, Corrosion of Uranium and Its Alloys [in Russian], Atomizdat, Moscow (1965).
2. W. Wilkinson, Uranium Metallurgy, V. II, Uranium Corrosion and Alloys, New York – London (1962).
3. E. G. Shapovalov and V. V. Gerasimov, At. Énerg., 27, No. 4, 289 (1969).
4. V. B. Kishinevskii, L. I. Gomozov, and O. S. Ivanov, in: Physical Chemistry of Alloys and Refractory Compounds with Thorium and Uranium [in Russian], Nauka, Moscow (1968), p. 81.
5. Reactor Materials, 6, No. 3, 1 (1963).
6. L. I. Gomozov et al., At. Énerg., 31, No. 3, 279 (1971).
7. O. S. Ivanov et al., Phase Diagrams and Phase Transformations of Uranium Alloys [in Russian], Nauka, Moscow (1972).

EXCITATION OF ACOUSTIC OSCILLATIONS IN A NUCLEAR REACTOR WITH A CIRCULATING GASEOUS FUEL

V. A. Denisov

UDC 621.039.51.514

The question of the excitation of acoustic oscillations in the core of a nuclear reactor with a circulating gaseous fuel has been investigated in [1, 2] using numerical methods. In such an investigation, in order to obtain a qualitative picture of the phenomenon it is necessary to carry out a large number of computer calculations, each of which requires a considerable expenditure of machine time. In connection with this, it makes considerable sense to investigate the indicated problem analytically, which has also been done in the present study using the method of perturbation theory.

A mathematical model of the core of a nuclear reactor of small dimensions with circulating gaseous fuel is described by a system of differential equations [1]:

$$\begin{gathered}\frac{dN}{dt}=\frac{k-\beta}{l}N+\sum_i \lambda_i C_i;\ C_i=\text{const};\\ k=k_0+\alpha\int_0^H[\rho(x,\ t)-\rho_0(x)]\,\Phi(x)\,dx;\\ \frac{\partial\rho}{\partial t}+\frac{\partial}{\partial x}(\rho w)=0;\\ \rho\frac{\partial w}{\partial t}+\rho w\frac{\partial w}{\partial t}+\frac{\partial P}{\partial x}=0;\\ \rho c_v\left(\frac{\partial T}{\partial t}+w\frac{\partial T}{\partial x}\right)+P\frac{\partial w}{\partial x}=AN\rho F(x);\\ P=R\rho T\end{gathered} \tag{1}$$

with the boundary conditions

$$\begin{gathered}T(t,\ x=0)=T_{\text{in}}=\text{const};\\ P(t,\ x=0)=P_{\text{in}}=\text{const};\\ P(t,\ x=H)=P_{\text{out}}=\text{const}.\end{gathered} \tag{2}$$

Here, in distinction from [1], in the equation of motion of the fuel we do not take account of the hydraulic losses due to friction, which stabilize the system [1, 2], and more rigorously write the energy equation. We linearize Eqs. (1) and (2) in the neighborhood of the stationary solution, we apply a Laplace transformation with respect to the time t, and we eliminate the neutron temperature and density. We write the obtained system in the form of a matrix equation

$$A\frac{du}{dy}+MB\frac{du}{dy}+Cu+MDu+Ksu-M\varphi(s)\,RF(y)\int_0^1 u\Phi(y)\,dy=0 \tag{3}$$

with the boundary conditions

$$\begin{gathered}u_2(s,\ y=0)=0;\ u_3(s,\ y=0)=0;\\ u_3(s,\ y=1)=0.\end{gathered} \tag{4}$$

Here we introduce the following notation:

Translated from Atomnaya Énergiya, Vol. 37, No. 5, pp. 426-428, November, 1974. Original letter submitted January 14, 1974.

$$u=\begin{pmatrix}u_1\\u_2\\u_3\end{pmatrix};\quad A=\begin{pmatrix}\frac{1}{m}&0&0\\0&0&m\\\varkappa n&0&0\end{pmatrix};\quad B=\begin{pmatrix}0&m&0\\m&0&0\\0&0&m\end{pmatrix};$$

$$C=\begin{pmatrix}\frac{d}{dy}\left(\frac{1}{m}\right)&0&0\\0&0&0\\\frac{dn}{dy}&0&0\end{pmatrix};$$

$$D=\begin{pmatrix}0&\frac{dm}{dy}&0\\\frac{dm}{dy}&0&0\\0&-\alpha_1F(y)&\varkappa\frac{dm}{dy}\end{pmatrix};$$

$$K=\begin{pmatrix}0&1&0\\1&0&0\\0&0&1\end{pmatrix};\qquad R=\begin{pmatrix}0&0&0\\0&0&0\\0&1&0\end{pmatrix};$$

$$\varphi(s)=\frac{\alpha_1\alpha_2}{1+\alpha_3 s};$$

$$u_1=\frac{\Delta w}{C_{\text{in}}};\quad u_2=\frac{\Delta\rho}{\rho_{\text{in}}};\quad u_3=\frac{\Delta P}{P_{\text{in}}};\quad m=\frac{w_0(y)}{w_{\text{in}}};$$

$$n=\frac{P_0(y)}{P_{\text{in}}};$$

$$\alpha_1=\frac{AN_0\rho_{\text{in}}H(\varkappa-1)}{P_{\text{in}}w_{\text{in}}};\quad \alpha_2=\frac{l\alpha\rho_{\text{in}}H}{\beta_{\text{ef}}};$$

$$\alpha_3=\frac{lc_{\text{in}}}{\beta_{\text{ef}}H};\quad \xi=\frac{\beta-K_0}{\beta};\quad \beta_{\text{ef}}=\beta\xi;$$

$$\varkappa=\frac{c_p}{c_v};\quad M=\frac{W_{\text{in}}}{c_{\text{in}}};\quad y=\frac{x}{H}.$$

The parameters α_1, α_2, α_3, and ξ characterize, respectively, the stationary power of the reactor, the density coefficient of reactivity, the ratio of the time constant of variation of the neutron density to the period of the acoustic oscillations, and the importance of the delayed neutrons [3]. The subscript "zero" denotes a variable in the stationary regime; s is the parameter of Laplace transformation. The variables m and n are determined from the stationary equations, which can be transformed into the system

$$\frac{dm}{dy}=\frac{\alpha_1F(y)}{m(\varkappa n-M^2m)};\quad \frac{dn}{dy}=-M^2\frac{dm}{dy} \tag{5}$$

with initial conditions

$$m(y=0)=1;\quad n(y=0)=1. \tag{6}$$

We note that the functions F(y) and Φ(y) are positive and F(y) $\leq$ 1.

Let the parameter α_1 be of order unity. Then all the coefficients of Eq. (3) and of order unity, and the parameter M, the Mach number at the inlet of the core, is 10^{-2}, i.e., M $\ll$ 1. Then we seek the solution and the eigenvalues of the boundary-value problem (3)-(4), using perturbation theory, in the form of series in powers of the small parameter M:

$$u=u_0+Mu_1+M^2u_2+\ldots;\quad s=s_0+Ms_1+M^2s_2+\ldots$$

In the zeroth approximation (M = 0) the matrix equation (3) reduces to a self-adjoint second-order equation:

$$\frac{d}{dy}\left[my\frac{du_{30}}{dy}\right]-\frac{s_0^2}{\varkappa}u_{30}=0 \tag{7}$$

with boundary conditions

$$u_{30}(y=0)=u_{30}(y=1)=0. \tag{8}$$

According to [4], the eigenvalues s_0 of the boundary-value problem (7)-(8) are pure imaginary ($s_0 = j\omega_0$) i.e., the system is found on the stability boundary. The question of the excitation of oscillations for M $\ll$ 1 is solved according to the first approximation: if Re $s_1 > 0$, then acoustic oscillations are excited in the system.

Restricting ourselves to the first approximation, we neglect terms with M^2, and in Eq. (3) we take

$$\frac{dn}{dy}=0;\quad n\equiv 1;\quad \frac{dm}{dy}=\frac{\alpha_1 F(y)}{\varkappa m};\quad m(y=0)=1.$$

Applying the method of perturbation theory [5], † we obtain

$$s_1=\frac{v^*Au_0\Big|_0^1+\int_0^1\left[v^*B\frac{du_0}{dy}+v^*Du_0\right]dy-\varphi(s_0)\int_0^1 v^*RF(y)\int_0^1\Phi(y)\,u_0\,dy\,dy}{\int_0^1 v^*ku_0\,dy},\tag{9}$$

where v* is defined by

$$-\frac{d}{dy}(v^*A)+vC+v^*Ks_0=0.\tag{10}$$

Solving Eq. (10) with boundary conditions $v_3^*(0)=v_3^*(1)=0$; $v_1^*(0)=0$, we obtain $v_1^*=0$; $v_2^*=(\varkappa du_{30}/dy)/s_0$; $v_3^*=u_{30}$. It is evident that $\int_0^1 v^*ku_0dy=\int_0^1[-\varkappa m/s_0^2(du_{30}/dy)^2+u_{30}^2]dy>0$, and the sign of Re s_1 is determined by the numerator in Eq. (9). We substitute $s_0=j\omega_0$ in it, and we calculate its real part. After transformations using Eq. (7), we find that the sign of Re s_1 is determined by the sign of the equation

$$Q=-\int_0^1\left[\frac{\varkappa m\frac{dm}{dy}}{\omega_0^2}\left(\frac{du_{30}}{dy}\right)^2-\frac{\varkappa\left(\frac{dm}{dy}\right)^2}{\omega_0^2}u_{30}\frac{du_{30}}{dy}+(\varkappa-1)\frac{dm}{dy}u_{30}^2\right]du-\frac{\alpha_1\alpha_2}{(1+\alpha_3^2\omega_0^2)\,\omega_0^2}\int_0^1 Fu_{30}\,dy\int_0^1\Phi\frac{d^2u_{30}}{dy^2}\,du.\tag{11}$$

From an analysis of Eq. (11) we can draw certain conclusions about the excitation of acoustic oscillations.

We consider the particular case in which the reactor operates at constant power [N(t) = const], i.e., the power feedback to the reactivity can be disconnected. The second term in Eq. (11) is then absent. If the neutron-density distribution over the height of the core is constant, i.e., F(y) = const, then

$$Q=-\int_0^1\varkappa\frac{dm}{dy}u_{30}^2\,dy<0.$$

In the case $F(y)\neq$ const it is difficult to exactly estimate Q, but we can obtain a sufficient condition in order that $Q<0$. The integrand is a quadratic form with respect to the variables u_{30} and du_{30}/dy. Evidently, $Q<0$ if

$$\left(\frac{dm^2}{dy}\right)<4m\omega_0^2\frac{\varkappa-1}{\varkappa}.\tag{12}$$

It is easy to verify that for α_1 of order unity, this inequality holds, i.e., acoustic oscillations are not excited in the reactor at constant power.

We show that in the general case, when N(t) ≠ const, acoustic oscillations can arise in the reactor. This is possible only when the second term in Eq. (11) is negative. We estimate the sign of this term, when ω_0 is the first natural frequency. Then, the eigenfunction u_{30} is positive in the interval (0, 1) and vanishes only at the ends of this interval. From Eq. (7) we have $d/dy[m(y)(du_{30}/dy)]=-(\omega_0^2/\varkappa)u_{30}<0$ for $0<y<1$, i.e., $m(y)(du_{30}/dy)$ is a decreasing function. From the equations of statics, it follows that m(y) is an increasing function; then du_{30}/dy is a decreasing function and, hence, $d^2u_{30}/dy^2<0$. Thus, the first integral in the second term of Eq. (11) is greater than zero, and the second integral is less than zero, i.e., the entire second term is less than zero and makes a positive contribution to the quantity Re s_1. This can lead to the condition Re $s_1>0$, i.e., to the excitation of the first harmonic of the acoustic oscillations. Hence, the cause of the excitation of acoustic oscillations is the existence of power feedback to the reactivity.

The magnitude of this feedback is determined by the parameter α_2 characterizing the density coefficient of reactivity; its increase can lead to the excitation of acoustic oscillations (there is an increase

†Unlike work [5], the matrix equation (3) is multiplied not by u*, but by v*, defined by Eq. (10).

in the positive contribution to Re s_1, see Eq. (11)). On the other hand, the increase in the parameter α_3 promotes the stabilization of the system. Since the parameters α_2 and α_3 enter into only the second term of Eq. (11), we have that, owing to their selection, we can always satisfy the condition Re $s_1 < 0$, in principle, i.e., we can make a reactor stable with respect to acoustic oscillations.

LITERATURE CITED

1. V. D. Goryachenko and E. F. Sabaev, At. Énerg., 24, No. 4, 375 (1968).
2. V. A. Denisov, in: Questions in Atomic Science and Technology. Series "Dynamics of nuclear power apparatus," No. 4 [in Russian], TsNIIatominform, Moscow (1973), p. 47.
3. V. D. Goryachenko, At. Énerg., 21, No. 1, 3 (1966).
4. G. Sansone, Ordinary Differential Equations [Russian translation], Vol. 1, Izd. Inostr. Lit., Moscow (1953).
5. L. Collatz, Eigenvalue Problems [Russian translation], Nauka, Moscow (1968).

PERTURBATION THEORY FOR PROCESSES OF ISOTOPE IRRADIATION

S. A. Nemirovskaya and A. P. Rudik

UDC 621.039.554

Calculations of the production of new isotopes by irradiation in nuclear reactors have received great attention in recent times [1-4] and depend on a large number of constants, when the chain of irradiated isotopes is relatively long. Since in some cases all the constants are known only with poor accuracy, the question arises how the results of the calculations depend upon the degree to which the initial constants are known. The problem is solved in the present paper with the aid of a mathematical method according to which the Hamiltonian and conjugated functions [5] are introduced as shown in [6, 7] for processes of isotope irradiation. For the sake of simplicity we consider the simplest chain of obtaining ^{238}Pu from ^{237}Np [4]. The method can be easily generalized to chains with any number of isotopes.

Let us denote the concentrations of the isotopes ^{237}Np, ^{238}Np, and ^{238}Pu by x^1, x^2, and x^3, respectively. The process of obtaining ^{238}Pu from ^{237}Np by irradiation with a flux of neutrons having the spectral hardness parameter γ [4] and the thermal neutron flux U can be described by the following system of equations [8]:

$$\begin{aligned}\frac{dx^1}{dt} &= -U(\sigma_1+\gamma I_1)\,x^1 \equiv f^1;\\ \frac{dx^2}{dt} &= U(\sigma_1+\gamma I_1)\,x^1-[U(\sigma_2+\gamma I_2)+\lambda_2]\,x^2 \equiv f^2;\\ \frac{dx^3}{dt} &= \lambda_2 x^2-U(\sigma_3+\gamma I_3)\,x^3 \equiv f^3.\end{aligned} \tag{1}$$

when the time of irradiation is T, the amount of ^{238}Pu formed after a sufficiently long exposure is $x^3(\infty) = x^2(T) + x^3(T)$ and can be expressed by the following integral

$$-x^3(\infty) = -\int_0^T [f^2(t)+f^3(t)]\,dt \equiv -\int_0^T f^0(t)\,dt \equiv J. \tag{2}$$

The dependence of $x^3(\infty)$ upon changes in any of the constants α in equation system (1) is given by the following expression of [7]:

$$\Delta_\alpha x^3(\infty) = -\Delta\alpha \int_0^T \frac{\partial \mathcal{H}}{\partial \alpha}\,dt \equiv -\Delta J, \tag{3}$$

where

$$\mathcal{H} = \sum_{i=0}^{i=3} \psi_i f^i;\quad \frac{d\psi_i}{dt} = -\frac{\partial \mathcal{H}}{\partial x^i},$$

with $\psi_0 = -1$; the conjugated functions ψ_i satisfy the transversality conditions [5, 7].

We restrict our considerations to the cases considered in [4], i.e., the self-shielding of the resonance absorptions is assumed to be immaterial. The resonance integrals I_1, I_2, and I_3 are independent of the concentrations x^1, x^2, and x^3. We obtain the following Hamiltonian $\mathcal{H}$ for the example under consideration:

$$\begin{aligned}\mathcal{H} = U\{(\sigma_1+\gamma I_1)\,x^1-(\sigma_2+\gamma I_2)\,x^2-(\sigma_3+\gamma I_3)\,x^3\}-\psi_1 U(\sigma_1+\gamma I_1)\,x^1+\psi_2\{U(\sigma_1+\gamma I_1)\,x^1\\ -[U(\sigma_2+\gamma I_2)+\lambda_2]\,x^2\}+\psi_3[\lambda_2 x^2-U(\sigma_3+\gamma I_3)\,x^3].\end{aligned} \tag{4}$$

Translated from Atomnaya Énergiya, Vol. 37, No. 5, pp. 428-429, November, 1974. Original letter submitted January 29, 1974.

TABLE 1. Results of the Calculation of the Quantity $\left(\frac{\Delta J}{J}\right)_\alpha = \frac{\Delta\alpha \int_0^T \frac{\partial \mathcal{H}}{\partial \alpha} dt}{J(T)} = \frac{\Delta\alpha}{\alpha} F_\alpha(T)$

T (year)	$F_\alpha(T)$			
	F_{Σ_1}	F_{Σ_2}	F_{Σ_3}	F_{λ_2}
0,25	+0,873	$-0{,}547\cdot10^{-1}$	−0,187	$+0{,}401\cdot10^{-1}$
0,50	+0,740	$-0{,}556\cdot10^{-1}$	−0,376	$+0{,}416\cdot10^{-1}$
0,75	+0,600	$-0{,}559\cdot10^{-1}$	−0,553	$+0{,}420\cdot10^{-1}$

The Hamiltonian of Eq. (4) depends upon σ_i and I_i only through the combination $\Sigma_i = \sigma_i + \gamma I_i$. Thus, only Σ_i (i = 1, 2, 3) and λ_2 are taken as α. The corresponding derivatives of $\mathcal{H}$, which appear in Eq. (3), are

$$\frac{\partial \mathcal{H}}{\partial \Sigma_1} = Ux^1[1-\psi_1+\psi_2];$$
$$\frac{\partial \mathcal{H}}{\partial \Sigma_2} = -Ux^2[1+\psi_2]; \quad (5)$$
$$\frac{\partial \mathcal{H}}{\partial \Sigma_3} = -Ux^3[1+\psi_3]; \quad \frac{\partial \mathcal{H}}{\partial \lambda_2} = x^2[\psi_3-\psi_2].$$

We describe as an example the results of calculations made with the following values of the constants [4]: $U = 10^{14}$ neutrons/cm$^2\cdot$sec; $\gamma = 0.15$; $\sigma_1 = 170$ barn; $I_1 = 946$ barn; $\sigma_2 = 2070$ barn; $I_2 = 880$ barn; $\sigma_3 = 500$ barn; $I_3 = 150$ barn ($I_3 = 3420$ barn was assumed in [4] in accordance with the data which were available at that time); and $\lambda_2 = 0.693/T_{1/2} = 0.321$ days^{-1}. The initial conditions are

$$x^1(0)=1; \quad x^2(0)=x^3(0)=\psi_1(T)=\psi_2(T)=\psi_3(T)=0.$$

The results of the calculations made for three T values are listed in Table 1.

The method described in the present paper can be easily applied to complicated problems for which no analytic solution exists. It is then possible to obtain general formulas for $F_\alpha(T)$ and, hence, to avoid solving equation system (1) for each $\Delta\alpha$.

LITERATURE CITED

1. M. A. Bak et al., Atomnaya Énergiya, 23, No. 6, 561 (1967).
2. V. M. Gorbachev et al., Basic Characteristics of the Isotopes of Heavy Elements [in Russian], Atomizdat, Moscow (1970).
3. A. S. Krivokhatskii and Yu. V. Romanov, Production of Transuranium and Actinoid Elements by Neutron Irradiation [in Russian], Atomizdat, Moscow (1970).
4. A. D. Galanin et al., Atomnaya Énergiya, 31, No. 3, 277 (1971).
5. L. S. Pontryagin et al., Mathematical Theory of Optimal Processes [in Russian], Fizmatgiz, Moscow (1965).
6. T. S. Zaritskaya et al., Atomnaya Énergiya, 26, No. 5, 432 (1969).
7. A. P. Rudik, Nuclear Reactors and Principles of the Pontryagin Maximum [in Russian], Atomizdat, Moscow (1967).
8. A. D. Galanin, Theory of Nuclear Reactors Operated with Thermal Neutrons [in Russian], Atomizdat, Moscow (1959).

ALBEDO AND COMPOSITION OF ABSORBED ENERGY FOR A TISSUE-EQUIVALENT SLAB IRRADIATED BY NEUTRONS

A. A. Dubinin, G. M. Obaturov, V. A. Rykov, and V. A. Shalin

UDC 539.109

In dosimetric and radiobiological studies, it is important to know the spatial and energy distribution of neutrons within and on the surface of the body (phantom). This is necessary to obtain other macro- and micro-dosimetric quantities such as absorbed dose, LET, specific energy, etc. and also the correct measurement of dose when using detectors having a sensitivity which depends, as a rule, on the energy of the radiation.

Data has been presented [1] from calculations of the fluxes and spectra of neutrons and capture γ-radiation in a tissue-equivalent slab 30 cm thick for normal and isotropic incidence of neutrons with energies from thermal to 10 MeV. The calculations used the ROZ-5 program [2]. The composition of the tissue-equivalent material was chosen in accordance with the recommendations of the ICRU [3]: H, 10.2%; N, 3.5%; C, 12.3%; O, 72.9%. On the basis of the results of the calculations, the following quantities were obtained: flux and current albedo; neutron capture probability; fraction of kinetic energy absorbed in the slab; the energy of capture γ-radiation in the reactions $^1H(n, \gamma)^2H$ and $^{14}N(n, \gamma)^{15}N$ and of protons in the reaction $^{14}N(n, p)^{14}C$ absorbed in the slab, and also the ratio of the absorbed-energy components to the total absorbed energy.

The fraction of the kinetic energy absorbed in the slab for incident neutrons of the k-th group was calculated from

$$\eta_k = 1 - \frac{\sum_{j=k}^{26} I^-_{j,k}(0)\,\bar{E}_{n,j} + \sum_{j=k}^{26} I^+_{j,k}(h)\,\bar{E}_{n,j}}{I^+_{k,k}(0)\,\bar{E}_{n,k}}, \quad (1)$$

where $I^-_{j,k}(0)$ and $I^+_{j,k}(h)$ are the currents of reflected and transmitted neutrons in the j-th energy group; $\bar{E}_{n,j}$ and $\bar{E}_{n,k}$ are the average kinetic energies of neutrons in the j-th and k-th groups.

As is clear from Fig. 1, the flux albedo* a_4 for normal incidence (curve 1) is greater than for isotropic incidence (curve 1'); in addition, $a_4 > 1$ for $E_n < 100$ keV. This is explained in the following way: for normal incidence $\Phi^+(0) = I^+(0) = 1$;

$$I^-(0) = \frac{1}{4\pi}\int \Phi^-(0,\ \theta)\cos\theta\sin\theta\,d\theta\,d\varphi \leqslant \Phi^-(0),$$

where the equality is realized for normal distribution of the reflected flux $\Phi^-(\theta)$. It is then clear that for normal incidence, where the contribution of neutrons directed at small angles $(\pi/2 - \theta)$ to the slab is large, the flux $\Phi^-(0)$ can be greater than $\Phi^+(0)$ for given $I^-(0)$. For isotropic incidence, a_4 would be equal to A_4 if the distribution of reflected neutrons were also isotropic. Some increase of a_4 in comparison with A_4 is explained by a deviation of reflected neutron distribution from isotropic.

The neutron current albedo, on the other hand, is greater for isotropic than for normal incidence since the probability for reflection of neutrons which are incident at grazing angles is greater than for neutrons incident at right angles.

*The notation used here is the same as that in the book by T. A. Germogenova et al., Neutron Albedo, Atomizdat, Moscow (1973).

Translated from Atomnaya Energiya, Vol. 37, No. 5, pp. 429-431, November, 1974. Original letter submitted February 4, 1974.

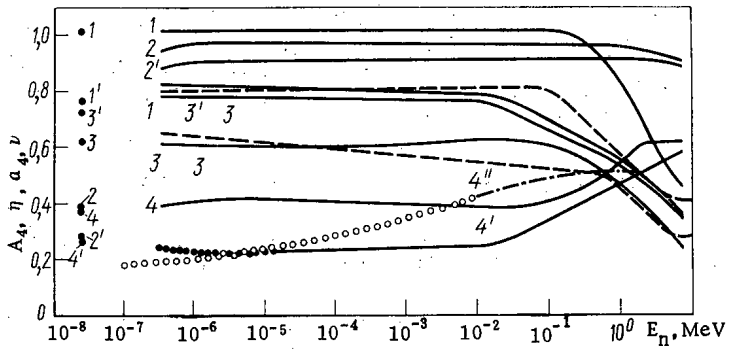

Fig. 1. Flux albedo a_4 (1) and current albedo A_4 (3); neutron capture probability ν (4) and fraction η of neutron kinetic energy absorbed in the slab (2) as a function of E_n for normal (1-4) and isotropic (1'-4') incidence; 4") neutron capture probability for a cylinder 30 cm in diameter [5]: ∘∘∘ and •••) extrapolated data; ——) present data; ---) data from [4]; -·-·-) data from [5].

For comparison, data is given in Fig. 1 for neutron current albedo in both cases of incidence calculated in [4] (dashed lines 3 and 3'). The data obtained and that of Nagarajan are in satisfactory agreement.

Curves 2 and 2' vary little with energy and this means that if one knows the current of incident neutrons one can determine the average absorbed dose from recoil nuclei,

$$D_{rn} = \eta \int I_n(E_n) E_n dE_n. \tag{2}$$

The capture probability ν_j is higher for normal irradiation. The curve 4" was obtained by Dennis [5] for the neutron capture probability in the case of normal incidence on a cylindrical phantom. The marked difference between our data and that of Dennis is explained first by the irradiation geometry and second by the arbitrariness of the extrapolation in [5] for neutron energies $E_n < 10$ keV.

The absorbed energy from capture γ-radiation in the reactions $^1H(n, \gamma)^2H$ and $^{14}N(n, \gamma)^{15}N$ and from protons in the reaction $^{14}N(n, p)^{14}C$, which is shown in Fig. 2 was calculated from

$$E_{\gamma j} = \nu_j \left(\frac{\Sigma_{\gamma H}}{\Sigma} E_{\gamma H} + \frac{\Sigma_{\gamma H}}{\Sigma} E_{\gamma N} \right) - \sum_{i=1}^{13} [I^{+}_{\gamma i, j}(h) + I^{-}_{\gamma i, j}(0)] E_{\gamma i}; \tag{3}$$

$$E_{\gamma i} = \nu_j \frac{\Sigma_{pN}}{\Sigma} E_{pN}; \quad \Sigma = \Sigma_{\gamma H} + \Sigma_{\gamma N} + \Sigma_{pN}, \tag{4}$$

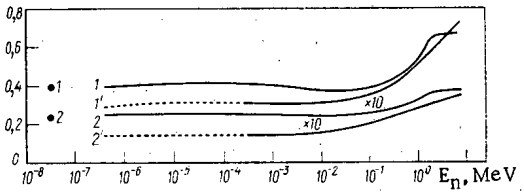

Fig. 2

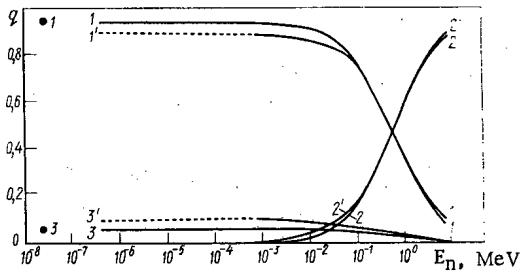

Fig. 3

Fig. 2. Absorbed energy: 1-1') from capture γ-radiation; 2-2') from protons of the $^{14}N(n, p)^{14}C$ reaction for normal (1-2) and isotropic (1'-2') distribution of incident neutrons; ---) extrapolated data.

Fig. 3. Fraction q of various components in the total absorbed energy; 1-1') from capture γ-radiation; 2-2') from neutrons; 3-3') from protons in the reaction $^{14}N(n, p)^{14}C$ for normal (1-3) and isotropic (1'-3') distribution of incident neutrons; ---) extrapolated data.

where $\Sigma_{\gamma H}$, $\Sigma_{\gamma N}$, and Σ_{pN} are the macroscopic cross sections for the reactions $^{1}H(n, \gamma)^{2}H$, $^{14}N(n, \gamma)^{15}N$, and $^{14}N(n, p)^{14}C$; $E_{\gamma H}$, $E_{\gamma N}$, and E_{pN} are the energies of the γ-rays and protons in the respective reactions, which are 2.23, 4.5, and 0.62 MeV; $I^{+}_{\gamma i,j}$ and $I^{-}_{\gamma i,j}(0)$ are the γ-ray currents for the i-th group; ν_j is the capture probability.

The kinetic energy of the j-th group absorbed in the slab (energy of recoil nuclei), E'_{nj}, was calculated from

$$E'_{nj}=E_{nj}-\sum_{i=j}^{26}[I^{-}_{i,j}(0)+I^{+}_{i,j}(h)]\,E_{ni}. \quad (5)$$

The total absorbed energy is

$$E_j=E'_{nj}+E_{\gamma i}E_{pj}. \quad (6)$$

It is clear from Fig. 3 that the main contribution to the absorbed energy for incident neutrons with energies above ~1 MeV is made by recoil nuclei, and for $E_{nj} \leq 0.5$ MeV it is made by γ-rays independently of irradiation conditions – normal or isotropic neutron incidence. This conclusion is of great significance for personnel neutron dosimetry since both kinds of irradiation are encountered in practice.

LITERATURE CITED

1. G. M. Obaturov et al., in: Neutron Monitoring for Radiation Protection Purposes, IAEA, Vienna (1973), SM-167/79.
2. V. I. Zhuravlev et al., Preprint, IPM AN SSSR, Moscow (1972).
3. Report of Intern. Comm. on Radiological Units and Measurements, Handbook 62, USNBS, Washington (1956).
4. P. Nagarajan and K. Krishan, Health Phys., 17, 323 (1969).
5. J. Dennis, AERE-R4365, Harwell (1964).

THE POSSIBILITY OF USING PHENOLFORMALDEHYDE RESIN FOR INSTRUMENTAL NEUTRON ACTIVATION ANALYSIS OF ROCKS

D. I. Leipunskaya, M. A. Kolomiitsev,
V. I. Drynkin, B. V. Belen'kii,
V. Yu. Dundua, and N. V. Pachuliya

UDC 543.08

Instrumental neutron activation analysis (INAA) is now used to solve many geological problems. The development of irradiation techniques including powerful nuclear reactors, and of measurement techniques based on multichannel analyzers and germanium – lithium detectors, and the use of computers to process the complex gamma spectra, enable us to make rapid determinations of twenty or more elements in a sample [1]. This type of analysis often requires prolonged irradiation of samples: the integral neutron fluxes can reach $n \cdot 10^{19}$ neutrons/cm^2. However, problems concerning optimum packing of the analysis samples and standards have hitherto remained unsolved.

In the irradiation of test material in a reactor, the packing is usually made of aluminum, graphite, quartz, or polyethylene. Each of these materials has its own peculiar disadvantages: for example, aluminum cannot be obtained in a sufficiently pure state, and it undergoes the nuclear reaction $^{27}Al(n, \alpha)^{24}Na$; it is difficult to fabricate packing from graphite owing to its mechanical weakness; quartz is often contaminated with impurities and is a brittle material; and polyethylene does not possess sufficient thermal and radiation stability [2]. Therefore, as a rule, the specimens are repacked in inactive material after irradiation and before measurement of the activity. This is particularly necessary when the irradiation is by high integral neutron fluxes.

Owing to the high activity of the packing material and of the analysis sample itself, the procedure of preparing the samples for measurement is difficult and requires special equipment. Furthermore, the weight of the original specimen can alter during irradiation (owing to the action of radiation and temperature), leading to additional uncontrolled errors.

TABLE 1. Element Content of Rocks

Element	Concentration, %
Aluminum	$4 \cdot 10^{-3}$—$2 \cdot 10^{1}$
Sodium	$1 \cdot 10^{-3}$—$1{,}5 \cdot 10^{1}$
Cerium	$1 \cdot 10^{-4}$—$1{,}6 \cdot 10^{-2}$
Chromium	$1 \cdot 10^{-3}$—$2 \cdot 10^{-2}$
Europium	$2 \cdot 10^{-6}$—$6 \cdot 10^{-4}$
Lanthanum	$1 \cdot 10^{-3}$—$1 \cdot 10^{-2}$
Scandium	$1 \cdot 10^{-5}$—$3 \cdot 10^{-3}$
Samarium	10^{-3}
Thorium	$1 \cdot 10^{-5}$—$2 \cdot 10^{-1}$
Manganese	$4 \cdot 10^{-4}$—$2 \cdot 10^{-1}$
Iron	$2 \cdot 10^{-2}$—$1 \cdot 10^{1}$
Cobalt	$2 \cdot 10^{-5}$—$5 \cdot 10^{-3}$
Cesium	$1 \cdot 10^{-5}$—$1 \cdot 10^{-4}$
Hafnium	$3 \cdot 10^{-6}$—$6 \cdot 10^{-3}$
Rubidium	$1 \cdot 10^{-2}$—$1 \cdot 10^{-1}$
Tantalum	$1 \cdot 10^{-4}$—$3 \cdot 10^{-3}$
Uranium	$1 \cdot 10^{-4}$—$3 \cdot 10^{-3}$

Kolomiitsev et al. [3, 4] have shown the possibility of synthesizing phenolformaldehyde resol resin (PFR) with a low level of activating impurities and of using it as a binder for comparison standards in neutron activation analysis. In [4] they gave the actual composition and impurity element contents of PFR. In this article we shall study the properties of PFR as a universal packing material for INAA of various rocks with different elemental compositions and impurity element contents. We analyzed specimens of granite gabbro-diorite, basalt, trap-rock, and graphite.

The specimens were prepared for analysis as follows. In a vessel 8 mm in diameter and 5-6 mm high, pressed from activation-purity PFR, we placed a precisely-weighed powdered sample of rock. The vessel was then filled to the brim with an 80% alcoholic solution

Translated from Atomnaya Énergiya, Vol. 37, No. 5, pp. 431-432, November, 1974. Original letter submitted February 8, 1974.

of PFR in the resol stage and was placed in a drying cupboard where it was kept for 2-3 h at 60°C so that the solvent slowly evaporated. Then the temperature was raised to 100 ± 10°C and maintained there for 10-15 h to convert the resol to resite (C-stage resin). The total weight of PFR in the specimen was 400-500 mg.

Now PFR in the resol stage possesses high adhesion both to the material of the vessel and to powdered rock. An alcoholic solution of resol wets rock powder, so that the solidified specimens are sealed airtight. The ultimate form of such a specimen is a tablet of vitreous (glassy) polymer in which the test powder is encapsulated. These monolithic specimens are thermostable up to at least 250-300°C and radiation-stable up to $n \cdot 10^{19}$ nuetrons/cm^2, and are easy to free from surface contaminants.

To estimate the level of possible impurities, using the same technique we prepared "blanks" of pure PFR. To determine the impurity elements which form short-lived isotopes on activation, we irradiated the blanks in a reactor under a neutron flux of $1.3 \cdot 10^{13}$ neutrons/cm$^2 \cdot$ sec for 20 min, or, in the case of longer-lived isotopes, for 20 h. We measured the activity by means of germanium – lithium detectors and multichannel analyzers at 30 min intervals and 5 days after irradiation. The specimens were accompanied by standards made of solid solutions of the elements in PFR.

To detect impurities we investigated PFR specimens synthesized in various batches. We performed the experiment with the aim of establishing possible variations in the impurity element contents between different batches of PFR. We found that the contents of such impurity elements as iron, sodium, manganese, chromium, mercury, bromine, and gold can display severalfold differences. For experimentation with real rocks, we chose that batch of PFR which contained the maximum amount of impurity elements.

In the experiments we compared the results of measurements of the spectra of specimens packed in PFR with those of specimens packed for irradiation in a polyethylene film, then in filter paper and aluminum foil, and before measurement repacked in inactive material. We found that the spectrometric pattern was not altered by the PFR. Not only the analytical lines, but also the background counts for the whole energy spectrum remained unchanged.

Table 1 lists the concentrations of various elements in the rocks, found by the INAA method. For the element concentrations given in this table, no interference was found from the impurity elements in the PFR.

In preparing the standards we first estimated the homogeneity of the distribution of elements in the PFR. For this purpose we determined the concentrations of the elements in several tableted standards. The concentrations of various elements contained in the PFR-based standards ranged from $n \cdot 10^{-5}$ to $n \cdot 10^{-8}$ g per gram of resin. We found that in all the cases the concentrations of the elements in the standards were the same within the error of determination, which was 1-2%. The geometrical shapes of the standards did not alter after irradiation (the same was observed by Kolomiitsev et al. [3]). The mechanical strength was fairly high after irradiation with integral neutron fluxes of up to $n \cdot 10^{19}$ neutrons/cm^2.

Thus from these results we can draw the conclusion that by using PFR to pack rock samples we can carry out INAA without repacking before measuring the activity, even after prolonged irradiation up to 10^{19} neutrons/cm^2. Furthermore, by using PFR we can impart a definite geometrical shape to the powdered rock specimens; this is very important in measuring the activity with the aid of germanium—lithium detectors. The analysis method is greatly simplified. The use of PFR-based comparison standards enables us to irradiate them for a long time together with the rock samples. As in the case of PFR packed test specimens, there is no need to repack the standards after irradiation.

LITERATURE CITED

1. R. Allen, J. Radioanal. Chem., 6, 115 (1970).
2. G. Bowen and D. Gibbons, Radioactivation Analysis [Russian translation], Atomizdat, Moscow (1967).
3. M. A. Kolomiitsev et al., At. Énerg., 35, No. 3, 191 (1973).
4. M. A. Kolomiitsev et al., Ibid., No. 5, 348.

TRACK AUTORADIOGRAPHY FOR SEALING TESTS ON AMPULES CONTAINING TRANSURANIUM ELEMENTS

V. G. Polyukhov, G. D. Lyadov, and V. N. Syuzev

UDC 778.347:621.039.548

Transuranium element production requires prolonged irradiation of tubes containing starting materials in a reactor [1, 2]. This means that there is a high probability that the sealing will fail, which can lead to loss of valuable products and contamination of the heat-transfer medium in the first loop. Tubes may be monitored for sealing during irradiation continuously by means of a delayed-neutron monitor and also periodic sampling of the peak carrier.

It is usual to irradiate several tubes together in a reactor, so the basic problem is to observe leakage. For this purpose, the tubes are periodically extracted from the reactor for monitoring of the states of the outsides (a visual examination in hot cells and also by analysis of water extracts on an alpha spectrometer).

Visual examination does not unambiguously indicate failure of the sealing, especially in the initial stages; again, the surface of the ampules may be coated with a friable layer of corrosion products, which hinders evaluation. The water wash method does not enable one to establish the position or size of the flaw.

To locate flaws and estimate their size by track autoradiography, a defective ampule is placed in a glass tube of diameter 11.5 ± 0.5 mm; appropriate exposure (from 1 to 2 h) enables one to produce a visible image of the damaged shell. Then the tube is washed with nitric acid and etched in 5% hydrofluoric acid for 10 min at 20°C; the method has been tested on an 0-38 ampule containing ^{252}Cf [3].

Visual examination of the surface revealed two defects of diameter about 1 mm and one defect of diameter 3-4 mm, at distances of about 220 and 135 mm respectively from the bottom end. Water washing confirmed that the damage extended through the casing. To eliminate possible contamination of the casing by ^{252}Cf, the ampule was washed three times with distilled water and carefully wiped with alcohol. After that, two track autoradiographs were recorded with glass tubes. The surface of the ampule was additionally cleaned before exposure of the second tube. The two autoradiographs were identical, so there was clearly no appreciable residual contamination of the surface by ^{252}Cf. Figure 1 shows one of the track autoradiographs from the active part of the tube.

Then the ampule was replaced in the reactor, where it was irradiated for 30 effective days, after which it was extracted and again autoradiographed.

The resulting autoradiographs showed that the damage lay at one side of the active part, and in both cases the position and size of the damaged zone were almost identical. However, in the latter case the area of extensive damage as revealed by the autoradiograph was much more extended. The damage to the casing was seen on the autoradiograph as numerous spots of diameter 1-3 mm representing accumulations of tracks, which occupied up to 24% of the surface of the active part.

To obtain more detailed information on the distribution of the damage along the tube, the autoradiographs were photometered with an MF-4 photometer, before which the autoradiographs had been annealed to eliminate the radiation-induced coloring of the glass by the gamma rays.

Translated from Atomnaya Énergiya, Vol. 37, No. 5, pp. 432-433, November, 1974. Original letter submitted February 15, 1974.

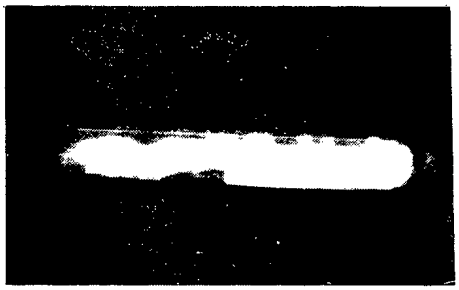

Fig. 1. Track autoradiograph of an 0-38 ampule.

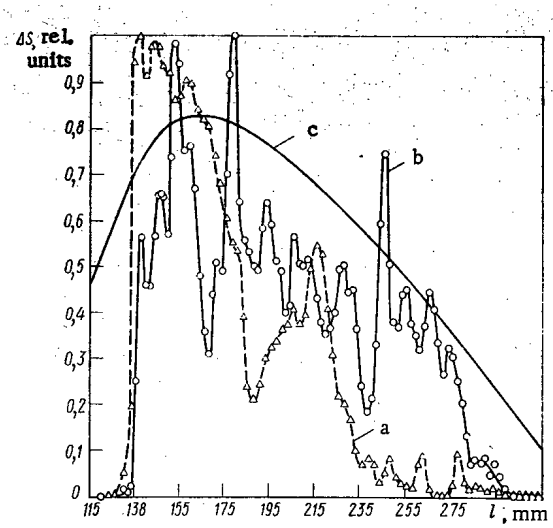

Fig. 2. a and b) Track density distributions on autoradiographs; c) ^{252}Cf distribution in the 0-38 ampule.

Curves a and b of Fig. 2 show the photometry results; here we also give the distribution of ^{252}Cf along the active part (curve c of Fig. 2), which was recorded by neutron scanning in a hot cell. The curves of Fig. 2 show that the damage was most extensive on the part containing the most ^{252}Cf. In the latter period of irradiation, there was rapid extension of the damage to the entire area of the casing (curve b). This is clear, in particular, from the occurrence of prominent peaks in the parts 150-160 and 240-280 mm, as well as the increase in the relative density of the peaks in the 240-280 mm part. Also, new peaks appeared in the 160-210 mm part. Subsequent metallographic studies showed that the thickness of the casing had been reduced by about 50%. Previous evidence [4] indicated that the thickness reduction is related to erosion due to irradiation. Our results would appear to confirm this.

Then track autoradiography can be used to identify sites of damage and to evaluate the size of them, as well as to record the distribution along a tube containing a transuranium element.

LITERATURE CITED

1. E. Hyde, J. Perlman, and G. Seaborg, in: Nuclear Parameters of Heavy Elements. Issue 1: The Transuranium Elements [Russian translation], Atomizdat, Moscow (1967), p. 60.
2. V. A. Davidenko et al., Atomnaya Énergiya, 33, No. 4, 845 (1972).
3. V. Ya. Gabeskiriya et al., Preprint NIIAR P-110, Melekess (1971).
4. V. G. Polyukhov et al., Atomnaya Énergiya, 33, No. 3, 773 (1972).

USE OF NEUTRON ACTIVATION RADIOGRAPHY TO DETERMINE NEUTRON FLUX DISTRIBUTION

L. V. Navalikhin, E. S. Flitsiyan, N. A. Kryzhenkova, and A. A. Kist

UDC 543.53+621.386.8

At the present time, neutron generators are widely used in elemental analysis in the procedures of research and industrial laboratories and also in the field.

One of the practical difficulties of their use for elemental analysis of material is the spatial inhomogeneity of the flux in proportion to separation from the generator target. Quantitative measurements of this gradient indicate that for a spatially extended target the values of the drop in density even at a distance of 15 mm are much greater than the values of all other errors of the neutron activation method without exception [1].

Because of this, it is of interest to determine what effect the inhomogeneity factor of the flux has on the accuracy of the results of neutron activation analysis for direct calibration in its various modifications, particularly for simultaneous joint irradiation of sample and standard, for separate irradiation using rabbits and simultaneous beam monitoring, and also for cyclic activation.

Flux variation for an extended target and source has been investigated theoretically [2-4]. The special case of identical linear dimensions of source and irradiated sample shows that calibration involving joint irradiation leads to considerable error in the direction of markedly overestimated or underestimated results depending on the relative location of sample and standard. The nature of the variation in the error in this case [1] is well described by the relation

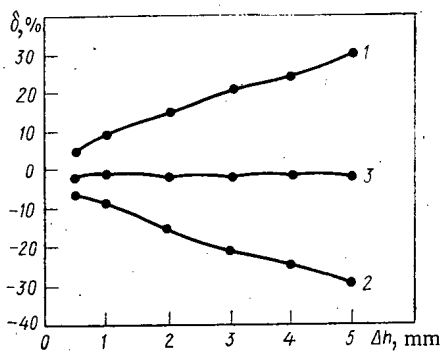

Fig. 1

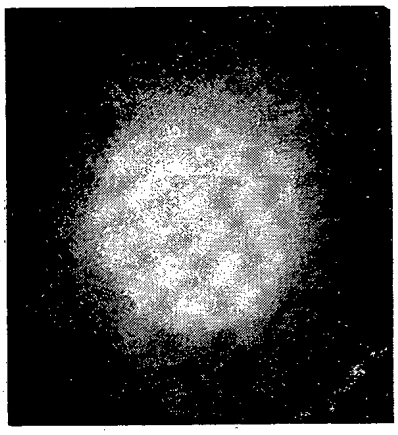

Fig. 2

Fig. 1. Variation of calibration error for various positions of sample with respect to the standard.

Fig. 2. Flux distribution along the diameter of a copper disk located directly at the generator target.

Translated from Atomnaya Énergiya, Vol. 37, No. 5, pp. 434-435, November, 1974. Original letter submitted February 22, 1974.

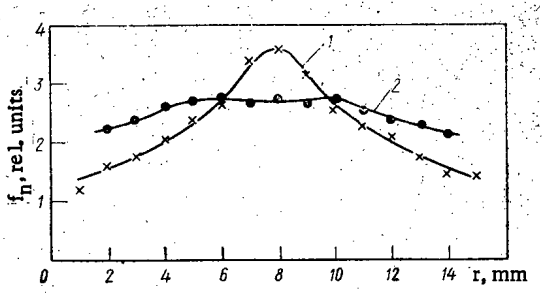

Fig. 3. Photogram of flux distribution over surface of a container: 1) continuous irradiation; 2) irradiation in 10 5-min cycles.

$$\delta = 1 - \frac{h_2 - h_1}{h_4 - h_3} \frac{\ln h_4/h_3}{\ln h_2/1}, \quad (1)$$

where $h_4 - h_3$ and $h_2 - h_1$ are respectively the sample and standard thicknesses, and h_1 and h_3 are respectively the distances from generator target to standard and sample.

For identical standard and sample thicknesses, the calibration error is

$$\delta = 1 - \frac{\ln h_4/h_3}{\ln h_2/h_1}. \quad (2)$$

The variation of calibration error is shown in Fig. 1 for the assumed conditions where $\Delta h_{st} = \Delta h_s$. Curves 1 and 2 demonstrate the calibration errors for two different positions of the standard with respect to the sample. Curve 3 shows the decrease in calibration error for the case where the calibration is carried out with two standards, one before and one behind the sample. This kind of sandwich calibration makes it possible to reduce the magnitude of the error in analysis sharply while avoiding the introduction of any corrections whatever for the gradient.

Equations (1) and (2) were derived under the assumption of equal radii for standard and sample. However, this condition is not always achieved, and it is therefore of interest to analyze the form of the flux density dependence along a section of the sample parallel to the generator target. In addition to calculations based on Eq. (1), the flux density distribution was studied experimentally by means of neutron-activation autoradiography.

A copper plate (circle) 40 mm in diameter was selected as a probe. The plate was irradiated for 0.5 h with a flux of fast neutrons, allowed to cool to allow for complete decay of the short-lived ^{62}Cu activity, and exposed for 12 h in contact with RT-6 x-ray film to produce an autoradiograph. The RT-6 film was selected because of its high sensitivity with sufficiently good resolution. The exposure was chosen in accordance with the low threshold sensitivity of the photographic material, which amounts to 10^6 disintegrations per unit area. The developed film was photometrized to obtain a photogram of the flux distribution over the area of the plate. The autoradiograph of the plate is shown in Fig. 2. The flux density falls sharply as one moves away from the center of the copper disk. Neglect of this factor can lead to large errors in analysis. However, the calibration error is sharply reduced by use of the sandwich calibration, with its value reaching a minimum in the case of identical sample and standard dimensions.

Another generally accepted type of sample irradiation in a neutron generator is the use of pneumatic devices for transport of the sample to the source and to measuring equipment. In this instance, as a rule, the samples and standards are irradiated separately and beam instability is taken into account by the introduction of a monitoring factor of a different kind. Neutron autoradiography was also used to evaluate the calibration accuracy in this case.

A copper cylinder in the shape of the container in which samples are irradiated was subjected to the effects of a neutron flux for an hour, and after the required cooling its surface was pressed into a plane. The copper sheet thus obtained was exposed in contact with an x-ray film for 12 h. A photogram of the flux distribution over the lateral surface of the container is shown in Fig. 3. In this case activation of the sample surface also occurs nonuniformly, which can lead to a large error. For powder samples or standards, the uniformity of sample distribution along the container is of great importance. With nonuniform distribution of a sample, the derived values for activities may vary over wide limits even for standard, homogeneous powdered samples. As follows from the photogram, this error rises sharply with an increase in linear dimensions because of redistribution of mass. Special systems of rotation are used [5] for irradiation of samples in the field of an inhomogeneous flux of neutrons. The use of such systems considerably smooths out the flux nonuniformity but greatly complicates the design of pneumatic systems to deliver

the samples. In addition, such design separates the sample from the target with a resulting decrease in the sensitivity of the analysis.

It was determined that irradiation over several cycles where the sample repeatedly passes through the channel of the pneumatic system approximates irradiation using the system of sample rotation. A photogram is shown in Fig. 3 of the flux density distribution for a sample irradiated over 10 5-min cycles. The photogram in Fig. 3 clearly indicates how the degree of smoothing of activation nonuniformity depends on the number of cycles.

LITERATURE CITED

1. N. A. Kryzhenkova et al., in: Nuclear-Physics Methods for the Analysis of Matter [in Russian], Atomizdat, Moscow (1971), p. 301.
2. K. A. Petrzhak and M. A. Bak, Zh. Tekh. Fiz., 25, No. 4, 636 (1955).
3. F. Crawford, Rev. Scient. Instrum., 24, No. 7, 552 (1953).
4. M. M. Agrest and M. Z. Maksimov, Zh. Tekh. Fiz., 28, No. 6, 1345 (1958).
5. A. Barvinski and L. Gurski et al., Isotopenpraxis, No. 2, 52 (1968).

THE PRECIPITATION OF PLUTONIUM DIOXIDE FROM CHLORIDE MELTS

V. F. Gorbunov, G. P. Novoselov, and S. A. Ulanov

UDC 546.799:541.48-143

In certain processes of processing of nuclear fuel, various compositions of fluoride salts containing plutonium are formed. The extraction of plutonium from these salts involves great difficulties.

In this work an attempt was undertaken to develop a pyrochemical method of extraction of plutonium from mixtures of fluorides of the alkali and alkaline earth metals. The method is based on the precipitation of plutonium dioxide from a fluoride melt, using the exchange interaction of plutonium tetrafluoride with metal oxides in a salt melt.

It is known that in the interaction of uranium and thorium tetrafluorides with oxides of certain metals in a medium of fluoride melts, sparingly soluble uranium and thorium dioxides are precipitated from the melt [3, 4]. Plutonium trifluoride is stable in molten mixtures of lithium, beryllium, zirconium, and thorium fluorides in contact with beryllium, zirconium, and thorium oxides; however, in the presence of NiO, plutonium is precipitated in the form of a $PuO_2 - ThO_2$ solid solution [5].

We studied the precipitation of plutonium dioxide from melts of $LiF - NaF - PuF_4$ with oxides of calcium and aluminum at the temperature 800°C. Analytical grade lithium and sodium fluorides were used; they were melted in a eutectic ratio. Plutonium tetrafluoride, produced by the hydrofluorination of plutonium dioxide, was introduced into the melt. Analytical grade calcium and aluminum oxides were preliminarily calcined in air at the temperature 1000°C for 1 h.

The experiments with melts were conducted in a glove box in an atmosphere of purified argon in nickel crucibles. Weighed portions of calcium or aluminum oxides were successively introduced into the salt

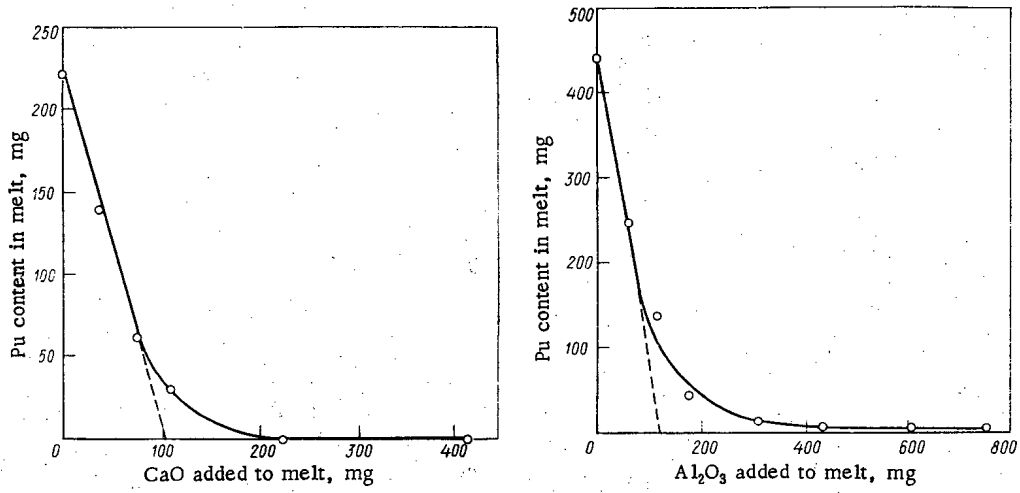

Fig. 1. Precipitation of plutonium from a melt of $LiF - NaF - PuF_4$ with calcium and aluminum oxides (initial weight of melt 60 g).

Translated from Atomnaya Énergiya, Vol. 37, No. 5, pp. 435-436, November, 1974. Original letter submitted February 28, 1974.

melt. The melt was mixed for 2 h, and after an hour of standing, samples of the melt were collected with a small nickel spoon. The samples were dissolved in nitric acid and plutonium determined radiometrically (according to the α-radiation). The results of the experiments are cited in Fig. 1.

The linear portion of the curves of the precipitation of plutonium with calcium and aluminum oxides have a slope corresponding to the stoichiometric reaction:

$$PuF_4 + 2CaO = PuO_2 + 2CaF_2;$$
$$3PuF_4 + 2Al_2O_3 = 3PuO_2 + 4AlF_3.$$

At the equivalence point of these reactions, the plutonium concentration in the melt is evidently determined by the solubility of plutonium dioxide. When the oxide precipitant is added in excess relative to the stoichiometry of the indicated reactions, i.e., when the concentration of oxygen ions in the melt is increased, the plutonium concentration decreases in accord with the requirement of constancy of the solubility product. In the presence of excess calcium oxide, the plutonium concentration is lowered to a value of less than $5 \cdot 10^{-4}$% by weight, which permits virtually complete isolation of plutonium from the melt. In the presence of aluminum oxide the plutonium concentration is lowered to $1.2 \cdot 10^{-2}$% by weight and remains constant during subsequent addition of the oxide. Evidently, the constant value of the plutonium concentration is reached at a concentration of aluminum oxide in the melt corresponding to its solubility and indicates the absence of sorption of plutonium dioxide on aluminum oxide. The relatively high concentration of plutonium in the presence of aluminum oxide can be explained by the fact that part of the oxygen ions in the melt are in oxyfluoride anions of aluminum.

LITERATURE CITED

1. G. P. Novoselov, I. N. Kashcheev, and Yu. D. Dogaev, At. Énerg., 28, No. 1, 49 (1970).
2. S. Katz and G. Cathers, Nucl. Appl., 5, No. 1, 5 (1968).
3. W. Grimes et al., Radioisotopes in the Physical Sciences and Industry, Vienna, IAEA (1962), p. 575.
4. J. Shaffer et al., Nucl. Sci. and Engng., 18, No. 2, 177 (1964).
5. C. Bamberger et al., J. Inorg. Nucl. Chem., 33, No. 3, 767 (1971).

NEUTRON RESONANCES IN OSMIUM ISOTOPES IN THE 4-300 eV RANGE

T. S. Belanova, A. G. Kolesov,
V. A. Safonov, and S. M. Kalebin

UDC 621.039.556

The transmissions of highly enriched samples of $^{186-190,191}$Os in the 4-300 eV range were measured at the SM-2 reactor by the time of flight method (Table 1). A neutron burst was formed with a selector having three synchronously revolving rotors suspended in a magnetic field [1]. The neutrons were detected by a set of helium counters. The resolution of the spectrometer was 70 nsec/m.

We have identified the resonance levels. In addition to the known levels [2, 3] we have observed 25 new levels for all the osmium isotopes. The energies of the resonances are given in Table 2.

The authors thank S. I. Sukhoruchkin for posing the present problem, and A. A. Belyaev for kindly placing the set of osmium isotopes at our disposal.

TABLE 1. Composition of Osmium Samples

Sample No.	Sample wt., mg	Percentages of osmium isotopes						
		184	186	187	188	189	190	192
1	169,73	<0,05	42,1	9,6	17,9	9,2	10,5	10,7
2	132,36	<0,05	0,8	18,1	42,2	25,3	7,8	5,8
3	181,2	<0,05	0,5	0,5	80,1	10,3	5,9	2,7
4	188,1	<0,05	<0,05	0,4	2,9	79,8	13,9	3,0
5	255,13	<0,05	<0,05	<0,05	0,9	4,0	89,9	5,2
6	339,22	<0,05	<0,05	<0,05	0,3	0,6	2,3	96,8

TABLE 2. New Levels Observed in Present Work

E_0, eV					
^{186}Os	^{187}Os	^{188}Os	^{189}Os	^{190}Os	^{192}Os
19,45±0,07	18,20±0,07	25,7±0,1	71,6±0,4	28,40±0,10	23,03±0,09
21,28±0,08	20,80±0,07	33,45±0,15	77,8±0,5		36,17±0,15
24,71±0,09	21,00±0,08	57,3±0,3	183±2		43,9±0,2
25,31±0,10	26,31±0,10	149,5±1,4	224±3		95,7±0,7
99,1±0,7	69,1±0,4	165±2	294±4		115,8±1,1
163±2	97,4±0,7	176±2			126,0±1,2
202±3	172±2	253±4			
	211±3	279±4			
	246±4				

Translated from Atomnaya Énergiya, Vol. 37, No. 5, p. 437, November, 1974. Original letter submitted May 27, 1974.

LITERATURE CITED

1. S. M. Kalebin et al., "Neutron chopper with three synchronously revolving rotors suspended in a magnetic field," Preprint NIIAR P-131, Dimitrovgrad (1972).
2. H. Jackson et al., Phys. Rev., 124, 1142 (1961).
3. V. P. Vertebnyi et al., Ukr. Fiz. Zh., No. 14, 1967 (1969).

INFORMATION

THE BRUNO LEUSCHNER ATOMIC POWER STATION IN THE GERMAN DEMOCRATIC REPUBLIC*

V. V. Gur'ev

In October of this year the German Democratic Republic celebrated its jubilee. In the 25 years existence of this country great achievements have been made in economics, and the republic has become one of the first ten industrially-developed nations in the world.

National nuclear power has developed vigorously in the GDR within the framework of socialist economic integration. The first exploit in this field was the creation of the experimental-industrial Reinsberg nuclear power station brought into service in 1966.

At the present time the large Nord nuclear power station is being constructed in the GDR, also with the help of the Soviet Union; this will consist of four successively introduced power units of 440 MW (el.) each. The two first units of the nuclear power station Nord-1 are being built on the basis of the Soviet water-cooled, water-moderated VVÉR-440 reactors with an electrical power of 440 MW each. The first unit was introduced into service in 1973 and the second is planned for 1974.

Recently the stations were named after the famous antifascist Bruno Leuschner.

Some of the most important criteria in choosing the site for the Bruno Leuschner nuclear power station (close to Greifswald) were: the fact that this region contained hardly any large power sources, the favorable meteorological conditions, and the large supply of drinking and industrial water with a salt content of no more than 0.7%. In accordance with general planning, the principal axis of the nuclear power station territory is directed from east to west, as has been generally accepted in recent years in the GDR in connection with the unit construction of thermal power stations.

The main parts of the Bruno Leuschner nuclear power station envisaged by the general plan are as follows:

1) the principal power installation, situated in the reactor, machine, ventilation, and other buildings (including the water supply);

2) technological auxiliary installations, including chemical water purification, deactivation systems, health and laboratory facilities, a compressor unit, reserve current supplies, oil and gas facilities;

3) administrative and other auxiliary buildings.

The main building of the principal power installation, together with the buildings containing special systems and services, constitutes a single technological complex, the optimized arrangement of which corresponds to the needs of both the first (already operating) and the second units of the nuclear power station.

As fuel the station uses slightly-enriched uranium dioxide, placed in the cassettes of an active zone 2.5 m high and 3 m in diameter. Altogether the active zone of the reactor holds 349 hexagonal cassettes (of these 312 are fuel elements and 37 contain control and emergency rods). These are arranged in a

*Abstract composed from data published in Kernenergie, 17, No. 7, 189-244 (1974).

Translated from Atomnaya Énergiya, Vol. 37, No. 5, pp. 439-441, November, 1974.

triangular lattice in steps of 147 mm. The gage size of each cassette is 144 mm. Apart from the control and emergency rods, a solution of boric acid may be introduced into the active zone of the reactor along special conduits in the event of an emergency.

Each power unit of the nuclear power station is built on the two-circuit principle. In the first water circuit, operating at a pressure of 125 atm, apart from the reactor, there are six circulation loops; in each loop is a pump, a steam generator, and two cut-off valves. The diameter of the main pipe is 500 mm.

Saturated steam passes from the steam generator at a pressure of 44 atm into two turbogenerators of the K-220-44 type with a power of 220 MW each; water cooling of the stator and hydrogen cooling of the rotor are provided. The power factor of the turbogenerator is 0.85. Industrial sea-water is fed to the turbogenerators directly from the Greifswalder – Bodden bay.

The following are the main parameters of the first unit of the Bruno Leuschner nuclear power station:

Number of reactors	2
Thermal power of each reactor, MW	1375
Electrical power of each reactor, MW	440
Number of turbine systems	4
Power of each turbogenerator, MW	220
Pressure in the second circuit, atm	44
Efficiency of the nuclear power station (gross)	32.2
Number of circulation loops in the second circuit	6
Number of fuel cassettes in the reactor	312
Number of control and safety rods in the reactor	37
Flow of coolant, m^3/h	40500
Temperature of coolant, °C	
at the inlet	268.8
at the outlet	299.0
Pressure of the coolant, atm	
average in the reactor	125
calculated	140
losses in the reactor	2.78
Fuel enrichment, %	
initial	2.5
subsequent chargings	3.5
Fuel burn-up, MW·days/ton	28600
Power intensity of active zone, kW/liter	84.5
Velocity of control rods, cm/sec	
normal	2
emergency	20-30
Range of power regulation, %	
manual	0-105
automatic	3-105
Number of rechargings per campaign	3
Power of reactor with natural circulation, %	15
Maximum cooling rate, °C/h	30
Content of boric acid, g/kg	
normal	0-8
emergency	up to 12

Particular attention is paid in the nuclear power station to water preparation and water supply in order to compensate for losses in the second circuit, shut-down cooling, accidental leaks, and so forth. The flow rate of the main installation is up to 130 m^3/h. The filters of the complete desalination system are successively filled with a weakly-acid cation exchanger (CA20), a strongly-acid cation exchanger I(KPS), a weakly-basic anion exchanger AD41, a strongly-acid cation exchanger II (buffer layer and KPS), and a basic anion exchanger (SBW). This combination of layers in the filters ensures a salt content at the outlet corresponding to an electrical conductivity of no more than 1.7 $\mu\Omega^{-1}$/cm and a dry residue of ~0.1 mg /liter.

The installation is monitored, serviced, and controlled (regulated) from a central panel. The regeneration of the filters is carried out automatically by a timed program.

The system of chemical water purification consists of five units. The purpose of the first of these with a flow rate of 20 tons/h to each unit of the nuclear power station, is that of preparing and purifying the water of the first circuit; the second, with a flow rate of 40 tons/h to two units, is used for reprocessing the water of the first circuit; the third, with a flow rate of up to 6 tons/h per unit, feeds the first circuit if any uncontrollable water leaks occur; the fourth, with a flow rate of 40 tons/h to two units, supplies the borided solution; the fifth, with a flow rate of 37 tons/h to two units, feeds the second circuit.

Provision is made for the reprocessing of the radioactive water by two methods: ionic purification (first, second, fourth, and fifth units), and evaporation (third unit).

The nuclear power station is also furnished with an installation for purifying the highly-active gases with a delivery of up to 7.5 nm^3/h of gas; this is used during operations and while the fuel is being recharged.

Also incorporated are principal electrical radial circulation pumps of the GTsÉN-310 type with hermetically-sealed electrical drives, auxiliary electrical pumps of the VTsÉN-315 type, PGV-180 steam generators, volume compensators with electrical heating (96 elements of 4 kW each), a cut-off armature with an electrical drive, evaporators, ion-exchange filters, and other equipment of Soviet production which have been fully attested in other nuclear power stations.

Great attention has been paid to the reliability of the electrical supply, the biological and radiation shielding, nuclear safety, and dosimetric monitoring, so as to ensure as far as possible the safe operation of the nuclear power station.

According to the degree of reliability needed, all the equipment is divided into several categories. The first category includes the control and safety mechanisms, the oil pumps of the turbines, the monitoring and regulating systems, i.e., equipment which will permit hardly any interruption of electrical supply in either normal operation or emergency situations. In individual cases there may be interruptions of no more than 1 sec in order to switch in the reserve supply sources.

The equipment of the second category (feed-maintenance pumps of the first circuit, pumps for introducing the boric solution, air blowers, certain parts of the turbogenerator, pumps for the cooling circuits of the GTsÉN-310 type, and so on) allows the electrical supply to be disconnected for up to 3 min. The third category – ordinary electrical equipment – places no special demands upon the electrical supply.

In accordance with the foregoing, the nuclear power station employs the following forms of electrical supply: 6 kV, 50 Hz for electric motors of 200 kW and over (through a 6/0.4 kV transformer); 380/220 V, 50 Hz for electric motors of powers up to 220 kW, illumination, and welding operations; 6 kV and 380/220 V, 50 Hz for equipment of the first category; 220 V dc for systems not allowing any interruption of supplies.

Biological shielding from the γ and neutron radiation of the reactor and the first circuit correspond to world standards and ensure normal working of the staff. All the rooms in the nuclear power station are divided into three categories: strictly-limited zone, partly-restricted zone, and normal zone.

In developing the basic principles of nuclear safety, the designers of the Bruno Leuschner nuclear power stations have made use of the vast experience accumulated in the construction of Soviet nuclear power stations with water-cooled, water-moderated reactors, and also experience from other countries.

The basic criteria for the nuclear safety of nuclear power stations corresponding to world standards were formulated as follows after discussion between the corresponding special organizations of the GDR and USSR:

1) in choosing a site for a nuclear power station, not only should the characteristics of the location be considered systematically and in all due complexity, but attention should also be paid to the essential characteristics of the power station itself, with due allowance for accumulated experience;

2) the nuclear power station should be so designed that the harmful effects of radiation should be less than that demanded by the national general-government norms;

3) the construction of the active zone and the first circuit, even in extreme cases, should not allow the melting of the fuel or substantial ejections of radioactive products;

4) if in an unforeseen case a large ejection of activity should occur, the service staff should be able to localize and completely eliminate the consequences of the accident in the immediate surroundings of the nuclear power station.

These criteria were established earlier when building nuclear power stations in the USSR and were also employed when designing and constructing stations in the GDR, Bulgaria, Hungary, Czechoslovakia, Finland, and others.

The main radioactivity in installations with water-cooled, water-moderated reactors is concentrated in the fuel fission products, i.e., in the fuel elements; hence the chief problem of nuclear safety in the nuclear power stations lies in the continuous maintenance of the circulation systems and auxiliary installations, as well as electrical and transport technology, in a proper working state, which may be effected by previously-instructed and practically-experienced personnel. Repair and servicing operations in the nuclear power stations may be divided up in the following way on a percentage basis: 33% centralized assembly; 22% operations in inactive centralized workshops; 8.5% operations in active centralized workshops; 18% current servicing of the second circuit and auxiliary systems; 18.5% current servicing of the first circuit and recharging equipment. More than 60% of the mechanical operations in servicing may be carried out in a centralized manner; preparations may be made for the assembly of active equipment in the same way.

In accordance with intergovernmental scientific and trade agreements between the GDR and the USSR, the nuclear fuel for the Bruno Leuschner nuclear power station (as in the case of the first Reinsberg nuclear power station) is supplied by the USSR in the form of cassettes completely ready for installation in the water-cooled water-moderated VVÉR-440 reactor.

The staff of the first unit of the nuclear power station are distributed in the following way: 25% engineers, 10% skilled workmen, 65% workers of various qualifications. Some 41% of the staff had experience in working with power equipment before the erection of the nuclear power station. Instructing and raising the qualifications of the nuclear power station staff is an extremely important problem, and in accordance with established requirements consists of the following: general theoretical training; the perfection of knowledge in the field of nuclear power and nuclear power stations, water-cooled water-moderated reactor installations, hygiene, and radiation shielding; special theoretical knowledge, knowledge of the specific technology of VVÉR-440 reactors, control and servicing procedures; general practical experience of work not only in nuclear but also in ordinary thermal power stations; special practical experience of direct work on the VVÉR-440. Staff of the Bruno Leuschner nuclear power station received this experience while training in the first unit of the Novovoronezh nuclear power station. Leading personnel received four weeks training and the operators of the power station ten weeks. Chief study was devoted to the behavior of the VVÉR-440 under steady and transient operating conditions, and in deepening understanding in particular parts of the reactor installation.

Further training of the nuclear power station staff will take place in the first unit of the nuclear power station.

While the first unit of the Bruno Leuschner nuclear power station was being constructed, a great deal of experience was gained in the organization of work relating to the construction and use of large unified nuclear power stations containing water-cooled water-moderated reactors.

IX BALATON SYMPOSIUM ON ELEMENTARY PARTICLE PHYSICS

I. A. Radkevich

The Balaton symposia on elementary particle physics have been held since 1965 and are organized by the Hungarian Academy of Sciences in the framework of the Bratislava—Budapest—Trieste—Vienna—Zagreb collaboration. Each symposium is generally concerned with a specific topic in elementary particle physics. At the Ninth Symposium (June 11-18, 1974), problems of hadron interactions were discussed with the main emphasis being on hadron formation in leptonic interactions. The chairman of the organizing committee was Professor G. Pochek (VNP).

A. B'yalas (Cracow) in his report "Diffraction dissociation as the shadow of production processes" discussed the phenomenological requirements for the process of pionization (a property of multiparticle production from nuclei). A model was presented in which the leading particle and pionization are dynamically independent of each other and diffraction dissociation is the correlation between them. The following conclusions were drawn:

Diffraction dissociation reflects the correlation between leading particles and the formation of clusters in nondiffractive collisions. It has two structural components arising from the two component structure of the correlation;

If the momentum transfer is conserved, then the scaling part of diffraction dissociation responsible for the long range correlation has some structure like the nondiffractive transfer;

Experiments on nuclei with hadrons and leptons play a decisive role in understanding the processes of elementary particle interactions;

Diffractive interference of virtual particles may not occur.

In his report "Neutral currents, the present and the future," M. Gourdain (Paris) remarked that to gain knowledge about neutral currents, it is important to study the deeply inelastic interactions of charged leptons with protons. As is well known, the inclusive cross section for this interaction is dominated by the amplitude for one photon exchange. However, if neutral currents exist, then a contribution from virtual vector boson exchange must manifest itself. On the basis of theoretical analysis one draws the conclusion that in lepton and antilepton scattering in the symmetric case of one photon exchange a charge asymmetry must appear. This conclusion has not been verified experimentally because of the paucity of experimental data.

The main goal of N. Zovko's (Yugoslavia) theoretical analysis of the electromagnetic form factors of the nucleon, kaon and pion, was to get information from experimental data supporting the attractive idea, stemming from the Venetian model, of the existence of a series of vector mesons.

On the basis of his semiphenomenological analysis, N. Zovko came to the conclusion that the theoretical explanation of the totality of existing experimental data requires the existence of a series of new vector mesons.

The Czech theorist S. Dubnichka (Dubna) related his proposed model for the pion form factor. Using the phase representation for the electromagnetic pion form factor and an intelligent parametrization of the phase, he found a simple formula for the form factor which describes all experimental data in the interval $-2.02\ (\mathrm{GeV}/c)^2 \le t \le 4.4\ (\mathrm{GeV}/c)^2$. The agreement with existing experimental data and the correct predictions tends to substantiate the correctness of the proposed model.

Translated from Atomnaya Énergiya, Vol. 37, No. 5, pp. 441-442, November, 1974.

A series of theoretical papers were devoted to the problem of hadronic annihilation of positrons and electrons and in particular to attempts at explaining the so-called energy crisis in which the experimentally measured energy of charged particles produced in the annihilation is substantially less than the initial energy of the colliding leptons. It is assumed that either neutral particles carry off considerably more energy than was supposed based on simple, essentially phenomenological ideas or that in the collision process narrow beams of forward going charged particles are formed which are difficult to resolve experimentally. The difficulty for theory to explain the weak dependence of the mean hadron multiplicity on the energy of the annihilating leptons was pointed out.

R. Phillips (England) in a review talk on two body scattering examined the totality of experimental data on the total, elastic and inelastic, cross sections of pp scattering. According to data from the CERN colliding rings, the cross sections rise slowly with energy while the ratio of elastic to the total cross section remains constant and equals ~0.175. A dip at $t \approx 0.15$ $(GeV/c)^2$ and ~1/3 $(GeV/c)^2$ is evident in the differential cross section.

A review talk by M. Eichorn (USA) surveyed results on the total cross sections of $\pi^{\pm}$-, $K^{\pm}$-meson, protons, and antiprotons on protons and deuterons. The main conclusions of research performed at IFVÉ (Serpukov) were confirmed. The results obtained at Batavia can be summarized in the following way: the total cross section for pp interactions grows to 43 mbarns; the total cross section for protons on antiprotons continues to decrease with increasing energy up to 200 GeV with the speed of fall gradually decreasing; however, clear indication of rising cross sections with increasing energy have been seen for all processes studied $\pi^{\pm}p$, $K^{\pm}p$, pd, $\bar{p}d$, $\pi^{\pm}d$; the difference between particle and antiparticle cross section decreases with increasing energy in accordance with theoretical predictions. New results from experiments studying the production of particles ($\pi^{\pm}$-, $K^{\pm}$-mesons, protons, antiprotons, deuterons, and antideuterons) in proton – nucleus interactions at center of mass angles near 90° were also presented. The experiment was performed in an external proton beam. Tungsten was used for a target. The measurements were performed at 200, 300, and 400 GeV in the transverse momentum region of 0.7-9 GeV/c. Analysis of the dependence of cross sections on $X = 2P_{\perp}/\sqrt{3}$ shows that the universal dependence of the inclusive cross section on X (simple exponent) occurs only in the region $X \approx 0.40$. These results are in good agreement with data from the CERN intersecting storage rings.

The hadron production cross section dependence on atomic number of the target nucleus at large momentum transfers and primary energies of 300 GeV was also studied at Batavia.

Hadron production at 77 mrad (laboratory coordinate system) was compared for targets of tungsten, titanium, and beryllium. This angle corresponds for an angle of 88° in the center of mass system of the proton and nucleus. In measuring the produced particles a magnetic spectrometer with two Cerenkov counters and a hadron calorimeter was used. The ratio of cross sections for hadron production for titanium and tungsten with respect to the production cross section on beryllium is proportional to $A^{1,1}$ (with $P_{\perp}$ = 4 GeV/c) and increases with increasing transverse momentum to the nucleon $P_{\perp}$.

Cronin et al. reported on the results of a search for a long-lived penetrating negative particle with mass from 1 to 8 GeV, formed in the collision of 300 GeV protons with a lead target. The search was motivated by some indications from CERN that such a particle might exist. The measurements are performed on a μ-meson spectrometer set for a momentum transfer of $P_{\perp}$ = 2.38 GeV/c which is the same as CERN's. The separation factor from μ-meson was 10^5. After all corrections were made, the 90% confidence lower limit on the production cross section for such a particle is $5.4 \cdot 10^{-39}$ $cm^2/(GeV/c)^2$.

R. Avakian reported on the characteristics of the Erevan electron accelerator polarized photon beams and their use in experiments on photoproduction of elementary particles. The beam polarization approaches 90%, and polarized beams of γ-rays have been achieved with energies close to the limiting accelerator energies. The asymmetry in the photoproduction of π^0-mesons on hydrogen was measured in the γ-ray energy interval of 0.9-1.65 GeV. For π^+-mesons, measurements were performed in the 0.9-1.2 GeV region. The asymmetry measurements contradict Walker's well-known theory and are in better agreement with Moorhouse's predictions (Berkeley).

The report "Study of the reaction $\pi^- d \rightarrow p\Delta^-$ (1236) (Δ^--backward) at 1.68 GeV/C" presented one of the newest experiments performed by a group of physicists from ITEF (USSR) in the study of particle interactions at large momentum transfers. The production reaction for backward $\Delta^-(1236)$ isobar productions is very difficult to study because of its small cross section but this study was greatly stimulated by theoretical calculations done at ITEF on the basis of which the numerical value of the cross section and

its energy dependence were predicted. The predictions were made before the experiment began. The measurements were performed on the ITEF 3-meter magnetic spectrometer. The backward production cross section for the $\Delta^-(1236)$ isobar turned out to be 247 ± 87 mbarns$(GeV/C)^2$ which is close to the theoretical prediction.

D. Cary et al. studied inclusive π^0-meson production cross sections in pp interactions in the 50-400 GeV primary energy region with transverse momentum $P_\perp$ from 0.3 to 4 GeV/C. It was shown that the invariant π^0-production cross section can be factorized as the product of two functions $f(X_R) \cdot g(P_\perp)$, where X_R is a new "radial" variable equal to the ratio of the π^0-meson momentum to its maximum value: $X_R = P^* / P^*_{max} = 2P^* / \sqrt{S}$.

At fixed $P_\perp$ the invariant cross section grows with increasing primary momentum and at $P_\perp$ = 2 GeV/C the ratio of cross sections at 250 and 50 GeV/C is equal to ~25. At the same time the function $g(P_\perp)$ changes by almost five orders of magnitude as $P_\perp$ goes from 0.5 to 3.0 GeV/C independent of primary energy. It has also been shown that, based on the data, the radial function $f(X_R)$ and the function of the transverse momentum $g(P_\perp)$ are universal functions in the kinematical parameter interval studied. The following expressions are proposed for the analytic description of the functions: $f(X_R) \approx (1 - X_R)^{-4}$; $g(P_\perp) \approx (P_\perp^2 + 0.86)^{-4,5}$.

The author thanks R. Avakian, S. Dubnichka, F. Echu, M. Muradyan, and particularly A. Tyapkin for assistance in the preparation of the material.

SOVIET — FRENCH SEMINAR ON CORE DIAGNOSIS AND SAFETY OF FAST REACTORS

Yu. E. Bagdasarov

The Seminar took place on June 9-14 in Cadarache. The Soviet delegation visited the Rapsodie reactor, the Phoenix atomic power plant, and the sodium racks of Cadarache. The Seminar discussed problems associated with the general approach to the safety of sodium-cooled fast reactors, design and operation methods of core monitoring, consequences of fuel element leaks, methods of leakage indication and on-line determination of defective fuel bundles, specific problems encountered in working with leaky fuel elements, methods of detecting defective fuel elements with the aid of labeled gases, systems and equipment for fast data acquisition and processing and reactor control, and many others. The reports of Soviet scientists met with great interest, especially those describing the operation and experimental research with BR-10, BOR-60, and BN-350 reactors and on methods of detecting faulty fuel bundles. Interesting papers have been presented by French participants.

Super-Phoenix Reactor. The French Atomic Energy Commission devotes much consideration to the design and development of the high-power fast reactor Super-Phoenix with an electrical output of 1200 MW. The technological design has been completed and is now being coordinated with the industry. The reactor construction is to be started in 1975 and its first run is being planned for 1980. After carefully considering the various concepts of the first-circuit design, the French scientists decided to use the integral design version. One of the most important advantages of this version is that it is much more satisfactory from the point of view of safety.

The most important distinguishing features of the Super-Phoenix reactor are:

1. Elimination of the pantograph (folding arm) and use of a direct reloading mechanism: the main reason for this change is the danger of large stresses which can occur during fuel discharge as a result of swelling of structural materials.
2. Elimination of graphite from the upper ends of fuel bundles and in-core shields to prevent safety element leakage, interaction of graphite with sodium, and carbonization of reactor materials.
3. Different construction of the top reactor cover and special insulation of this cover from the argon blanket: the insulation has the form of a flat bundle of many layers of tightly pressed stainless steel gauze lined with sheet steel; the insulation passed many tests in the sodium racks.
4. Replacement of micromodular steam generators by large tank steam generators with a thermal power of about 750 MW (one per loop). Two types of steam generators are being developed: one with twisted Incoloy pipes (evaporator and superheater in one vessel) and with straight pipes with separate vessels for the evaporator (Croloy piping) and superheater (316 steel piping). Models of steam generators are tested in special test stands for water leakage into the sodium circuit. The basic reasons for replacing the micromodular steam generators by tank-type steam generators were the complicated operation and high cost of the former.
5. Introduction of automatic control (as is known, the Phoenix reactor is manually controlled).

Phoenix Reactor. During the visit of the Soviet delegation the atomic plant operated at nominal power providing steam with rated parameters. In the course of operation 24 core triggerings occurred at different power levels, the triggering signals being, as a rule, false.

Translated from Atomnaya Énergiya, Vol. 37, No. 5, pp. 443-444, November, 1974.

Experimental cooling of the reactor by normal air circulation in the jacket space indicated a power removal of about 9 MW. Experiments on temperature distribution in the reactor proved that the ratio of the average (over all active fuel bundles) heating in the core to heating in the reactor is 1.15. Measurement of temperature distribution in the reactor vessel (according to readings of approximately 30 thermocouples) indicates a uniform distribution with respect to the angular distribution of the coolant used for reactor vessel cooling. Experimental tests indicated that no hydrodynamic reactivity effects are present in the Phoenix reactor. Since the reactor pressure cannot be varied significantly, the absence of barometric effects has been established indirectly.

The state of the reactor core is monitored as follows:

1. Two thermocouples mounted over each fuel bundle inside a jacket tube ~12 mm in diameter monitor the bundle temperature; the thermocouples can be replaced if necessary. The thermocouples operate very satisfactorily. No breakdowns have been noted. The reading of thermocouple indications, data processing, calculation of the desired parameters, and comparison with preset limits are carried out at 3 sec periods with the aid of two computers. The generation of appropriate alarm signals is foreseen. The time constant of the thermocouples is about 4 sec. The thermocouple tubes are placed at the center of 20 mm tubes mounted about 100 mm from the cap of each active fuel element bundle. Tubes 20 mm in diameter carry sodium to a system which monitors the integrity of fuel element jackets. The sodium is drained off through tubes with a diameter of of about 8 mm. The monitoring system is located in a special plug; sodium flows to a two-stage sample distributor which makes it possible to take three kind of samples: a mixed sample from all fuel bundles, a sample from any three bundles, and a sample from any individual bundle. Behind the distributor (below the sodium layer) is mounted an electromagnetic pump which directs the samples to a delayed-neutron detector. The arrival of one sodium sample to the detector takes about 10 sec; the time of a single measurement at one location is 2 sec, the entire core can be checked in groups of three fuel bundles in about 47-60 min.

2. For acoustic monitoring, the Phoenix reactor is fitted with 21 test sockets in eleven of which waveguides have been already installed. The metal waveguides have open bottom ends and a pick-up and amplifier mounted in the top end of each waveguide. The waveguides are protected by jackets welded at the bottom to the waveguide so that only the waveguide end is open; the top of each jacket (beyond the reactor cap) is fastened through a seal to the waveguide body. The space between the waveguide and its jacket is filled with an inert gas. All transverse disturbances originating in sodium or in the reactor structure are thus cushioned by the jacket. The acoustic system of the Phoenix reactor will be put into operation after experiments in the Rapsodie reactor are completed.

3. Monitoring with a reactivity meter and generation of an alarm signal when the reactivity deviates by 10^{-4} $\Delta k/k$ is also foreseen. This system will be probably replaced as the operating experience indicates that the system is sometimes triggered when one pump is stopped.

Safety Evaluation and Control in Atomic Power Plants with Fast Reactors. The principal points of interest (in particular, in the Super-Phoenix reactor) are the following:

1. The safety system should consist of two independent systems each of which acts on one half of the total number of safety rods, i.e., all circuits, control units, and power supplies should be separated in space. Failure of one system to operate should shut down the reactor in not more than 1 sec and keep it in a cold subcritical state as long as the system remains inoperative.

2. A shielding jacket must be provided around the reactor vessel so that the state of the vessel can be continuously monitored; the sodium in the reactor must not be allowed to fall below the core top and below the intermediate heat exchanger outlet. Residual heating should be removed by several independent means.

3. The prevention of core breakdown should be based on detection of failures in each individual fuel bundle, overall core monitoring, and correlation between the two signals. The monitoring system should include measurement of integral reactivity parameters, monitoring of delayed neutrons and of the activity of fission products in the reactor gas cushion, acoustic detection of boiling, reading of fuel bundle temperature with the aid of two thermocouples at the outlet of each bundle, monitoring of delayed neutrons in each fuel bundle. An attempt will be made in the Super-Phoenix reactor to reduce the time constant of thermocouples and to add a device for computing the reactivity balance.

4. All boxes must be designed to be able to confine the results of core explosion and melting. For example, in the Super-Phoenix reactor the maximum core condensation as a result of pump breakdown and simultaneous loss of emergency protection (the worst possible case) causes an influx of reactivity equal to 60 dollars/sec. The primary-circuit box contains the basic reactor vessel, the shielding vessel, and a hermetic metal "cover" which can withstand pressures of up to 3 atm. In order to confine radioactivity in case of reactor cover leaks, the box is fitted with a hermetic metal hood.
5. To prevent ignition of radioactive sodium, the latter is separated from air by means of two strong leakproof barriers: in addition, all sodium circuits must be located in an inert medium.
6. The plant should suffer no damage in case of seismic shocks of strength n, and radioactive safety must not be affected by shocks of strength n + 1 (n = 7 for the Super-Phoenix reactor).
7. To prevent dangerous consequences of aircraft crashes, the safety shields will be surrounded by a concrete shell.

CONFERENCES AND SEMINARS ORGANIZED BY THE ALL-UNION ASSOCIATION "IZOTOP"

A seminar and exhibition of Application of Isotopes and Radioisotopic Techniques in the Food, Textile, and Machine Construction Industries was held in Smolensk on April 24-25, 1974 by the Moscow Regional Branch of the All-Union Association "Izotop" in cooperation with the Smolensk Center of Scientific and Technical Information. Papers have been read by representatives of ten industrial enterprises and scientific institutes. The exhibition included various isotopic devices, examples of radioisotopic engineering products, and radiation protection equipment.

A seminor on Radioisotopic Inspection Methods and Results of Their Application in the Building Industry was organized in April, 1974 in Voroshilovgrad by the Kiev Regional Branch of the "Izotop" Association, in cooperation with the Ukrainian and Voroshilovgrad Administrations of the Scientific and Technical Division of the Building Industry, the Voroshilovgrad Branch of the Research Institute of the Building Industry, and the Voroshilovgrad Territorial Center of Scientific Information. Twenty-three reports have been presented and discussed on the application of commercial radioisotopic instruments and devices in the building industry.

The participants learned about the introduction of isotopic methods of inspecting the quality of soil compaction in the foundations of buildings and constructions in the Voroshilovgradtyazhstroi complex, and visited the laboratory of the Ukrainian Gosstroi and the main building laboratory of the Voroshilovgradtyazhspetsstroi complex. The Seminar has been accompanied by demonstration of special films and an exhibition of radioisotopic and electronic equipment supplied by the "Izotop" Association.

The Fifth Ural Scientific and Practical Conference on the Use of Radiation Techniques in Medicine took place in Sverdlovsk in May, 1974. The Conference proceedings were conducted in six sections on radiological techniques, experimental radiology, clinical radiodiagnosis, isotopes in endocrinology, isotopes in oncology and hematology, and the use of radiations in oncology.

A seminar on the Application of Radioisotopic Techniques in Planning of Automatic Technological Processes, organized by the Tashkent Branch of the "Izotop" Association and the Kazakh Institute of Scientific and Technical Information, was held in May, 1974 in Alma-Ata. The Seminar was attended by 55 specialists of 37 planning organizations. The participants visited the Alma-Ata Cotton Complex at which radioisotopic devices are successfully employed.

A seminar on the Present Uses and Future Prospects of Radioisotopic Techniques in the Chemical and Metal Industries has been organized by the Sverdlovsk Regional Branch of the "Izotop" Association, the Krasnoyarsk MNU-10 SUMNRT, and the Krasnoyarsk Center of Scientific and Technical Information in May, 1974 in Krasnoyarsk. The Seminar was attended by 37 specialists of four scientific research institutes and 15 industrial enterprises; reports have been made about the successful application of radioisotopic techniques at the Krasnoyarsk Aluminum Plant, the Achinsk Aluminum Oxide Plant, at which more than 150 radioisotopic devices are presently used, and the Krasnoyarsk Paper and Pulp Mills.

A seminar on the Application of Radioisotopic Methods and Devices in the Chemical and Metallurgical Industries, organized by the Kiev Republican Branch of the "Izotop" Association in cooperation with the Erevan Special Design Bureau of Automation and the Armenian Institute of Scientific and Technical Information, was held in Erevan in May, 1974. The Seminar was attended by 88 specialists of the chemical, metallurgical, and other branches of the industry of the Armenian SSR, by leading Party workers of the Republic, and by representatives of scientific and design institutions.

Translated from Atomnaya Énergiya, Vol. 37, No. 5, pp. 444-445, November, 1974.

The participants have been given the necessary information about devices and equipment supplied by the "Izotop" Association, exchanged opinion on the application of isotopes, and familiarized themselves with the operation of such instruments at the Polivinilatsetat Erevan Factory, where nearly 90 different radiosotopic instruments are presently successfully employed.

A seminar on the Application of Radioisotopic Methods and Devices in Machine Building has been organized by the Kiev Republican Branch of the "Izotop" Association together with the Moscow Regional Branch, the Tbilisi Scientific-Research Institute of Electron and Ion Technology, and the Georgian Scientific-Research Institute of Scientific and Technical Information and Engineering Economy in Tbilisi in May, 1974. The Seminar was attended by 146 representatives of various organizations of the Georgian SSR. Thirteen papers and reports have been presented and discussed. An accompanying exhibition included new radioisotopic devices, dosimetric, radiometric, and electronic physical instruments, as well as various radiation safety devices.

A seminar on Industrial Applications of Radioisotopic Engineering was held by the Sverdlovsk Regional Branch of the "Izotop" Association together with the West-Ural Center of Scientific and Technical Information in Perm' in June, 1974. Twenty specialists of industrial organizations attended the Seminar.

A seminar and exhibition on the theme "Practical application and future prospects of radioisotopic methods and devices in the industry" has been organized by the Sverdlovsk Regional Branch of the "Izotop" Association and the Krasnoyarsk MNU-10 SUMNRT in June, 1974.in Novosibirsk. The Seminar was attended by more than 100 specialists who heard ten reports. An accompanying exhibition included various radioisotopic devices and electronic physical instruments; 70% of the exhibited devices have been purchased by various Novosibirsk organizations.

The Second All-Union Seminar on Radioisotopic Methods and Devices in Hydraulic Engineering and Land Reclamation, organized by the State Atomic Energy Commission of the USSR, the Ministry of Land Reclamation and Water Economy, the "Izotop" All-Union Association, the A. N. Kostyakov All-Union Scientific-Research Institute of Hydraulic Engineering and Land Reclamation, and the Atomic Energy Pavilion of the Exhibition of Achievements of the National Economy of the USSR, was held in June, 1974 in Moscow. Specialists of various research institutions, planning organizations, and of the USSR and Ukrainian Gosstroi participated in the proceedings. Forty-four papers have been presented for discussion. New radioisotopic devices and instruments used in hydraulic engineering and land reclamation have been demonstrated.

A seminar on the Application of PGP-2, GGP-1, and NIV-2 Radioisotopic Devices was held in Ostashkov in June, 1974. The Seminar was organized by the Moscow Regional Branch of the "Izotop" Association and the Highway Construction and Maintenance Administration of the USSR.

The participants learned about the application of these devices and observed them in operation.

A seminar on Automatic Fire-Prevention Systems was held in Moscow in June, 1974. The Seminar was organized by the Moscow Regional Branch of the "Izotop" Association and the Moscow City and Regional Fire-Prevention Administration. The Seminar was attended by 400 people (mostly engineers, chief mechanics, and power engineers). The RUOP-1 system has been demonstrated.

A seminar on the Application of Isotopes and Isotopic Devices in Food Factories was held by the "Izotop" All-Union Association together with the Ministry of Food Industry of the USSR on the grounds of the Exhibition of the Achievements of the National Economy in Moscow in June, 1974.

The Seminar was inaugurated by the Deputy Minister of the Food Industry of the USSR, N. V. Oreshkin. He commended the fruitful work of the "Izotop" Association and the SUMNRT in the introduction of radioisotopic methods to the food industry and recommended to expand the application of commercially produced radioisotopic devices in the sugar, canning, butterfat, pastry, brewing, baking, liquor, and wine industries. The speakers told about the application of radioisotopic techniques in their enterprises.

INFORMATION: CORRESPONDENCE

INSTRUMENTS OF THE "IZOTOP" ALL-UNION ASSOCIATION AT THE INTERNATIONAL LEIPZIG FAIR

V. A. Dolinin

More than 9000 exhibitors from 60 countries all over the world took part in the International Leipzig Spring Fair. Most prominent were the exhibits of the German Democratic Republic, Czechoslovakia, the Polish People's Republic, the Federal Republic of Germany, and the USSR.

This was the 52nd time the Soviet Union participated in the International Leipzig Fair. The Soviet exhibition (with a total floor area of nearly 9000 m^2) has been arranged by 19 foreign trade associations including the "Tekhsnabéksport."

More than half a million people visited the Soviet exhibition during the Fair duration.

The "Izotop" All-Union Association demonstrated the following instruments:

1. The GRP1-1 (single-channel) and GRP2-1 (two-channel) general-purpose industrial gamma relay for automation of various industrial processes; these relays are intended to replace older types of gamma relays. In contrast to other Soviet and foreign gamma relays, these relays are based on digital data processing techniques and uses integrated circuits. This improves their operating characteristics (such as speed, reliability, and sensitivity) and parameter stability.

2. The SURM-2 level indicator intended for positional control of the level of liquid and free-flowing materials (including highly inflammable and explosive materials) in tanks, reservoirs, compartments, cesspools, and other containers on merchant vessels, and in other reservoirs of general industrial use.

3. Various types of radioisotopic static-electricity neutralizers which prevent the accumulation of electrostatic charges on materials undergoing various technological treatments.

4. The AZhR-1 x-ray radiometric analyzer for measuring the concentration if iron-group elements. The AZhR-1 is used for rapid analysis of powdered samples of ores and their products for the content of iron, manganese, and certain other elements of the iron group, and can also be used in geological explorations, mining and enriching enterprises, in metallurgy, etc.

5. The BDBSZ-1eM ("Vorya") basic detector block intended for detection and spectrometry of γ-quanta and charged particle fluxes in the following energy ranges: 1 to 10 MeV for α-particles, 0.05 to 3 MeV for β-radiation, and 0.03 to 3 MeV for γ-radiation.

6. The YaGRS-4 ("Medeya") general-purpose gamma-resonance spectrometer for measuring the spectra of γ-resonance absorption and the energy spectra of γ-sources. The instrument is designed for use in research and industrial laboratories.

7. The UIM2-1eM ("Aktiniya") count-rate meter for measuring the average pulse count rate and for generating an alarm signal when the rate of pulses arriving from standard α, β, γ, and neutron radiation detectors exceeds a preset count rate.

8. The Laboratory model of the UIM2-1eM meter used in various branches of science and industry for dosimetry and monitoring radioactive radiations.

Translated from Atomnaya Énergiya, Vol. 37, No. 5, p. 446, November, 1974.

9. The AI-256-6 multichannel pulse-height analyzer for the analysis of periodic and statistical pulse amplitude distributions and the distributions of instantaneous values of continuous processes in physical, biophysical, chemical, and other investigations.

10. The DRGZ-1 dosimeter for measuring the average exposure dose rate of continuous and pulsed x-ray and γ-radiations. The instrument is used in dosimetric laboratories of scientific-research institutes and various industrial laboratories.

11. The 2323-01 ("Biota") gas radiometer for calibration and verification of β-active gas radiometers in standards laboratories and in industrial enterprises, and also for measuring the concentration (specific bulk activity) of ^{41}Ar, ^{85}Kr, ^{133}Xe, and their mixtures in the atmosphere. The instrument operation is based on measuring the current of an ionization chamber filled with air containing gaseous radioactive impurities. The analyzed gas, whose concentration or total specific activity is measured, is let into the ionization chamber through a built-in blower or through an external air intake system. A potential difference (1250 V) between the central electrode and housing of the ionization chamber causes a current flow which is measured by and electronic circuit. The instrument is capable of measuring radioactive gas concentrations in the range $5 \cdot 10^{-10}$ to $2.5 \cdot 10^{-5}$ Ci/l. The "Biota" radiometer has been awarded a Gold Medal of the International Leipzig Spring Fair in 1974.

Considerable interest among specialists has been aroused by the DRGZ-1, GRP2-1 and GRP1-1, SURM-2, "Aktiniya," "Voriya," and AZhR-1 instruments of which the DRGZ-1 ("ARAKS") gamma dosimeter has been sold.

In the course of the Fair negotiations have been conducted on signing trade agreements with the "Isocommertz" and "Elektrotechnik Exportimport" Companies (GDR).

INAUGURATION OF THE EXHIBITION HALL OF THE "IZOTOP" ALL-UNION ASSOCIATION IN KHABAROVSK

V. A. Dolinin

The "Izotop" All-Union Association has opened its new branch and demonstration hall in Khabarovsk. The Khabarovsk Regional Branch of the "Izotop" Association is a specialized organization whose task is the introduction of radioisotopic methods and instruments into the national economy of Eastern Siberia, the Far East, the Kamchatka Oblast', and Sakhalin. The prime aim of the new demonstration hall is the popularization and dissemination of leading experience in the use of radioisotopic methods and devices in various branches of the national economy.

Colorful posters, circuits, and tables displayed in the exhibition hall visualize the methods used for isotope production, their properties, the possibilities and economical effects of their application in industry, agriculture, medicine, and scientific research. The visitors can familiarize themselves with models of radioisotopic samples and labeled compounds, radioisotopic control devices, level gages, densimeters, thickness gages, moisture meters, electrostatic neutralizers, radiometric propecting equipment, instruments for gamma flaw detection and nuclear-physics analysis of the composition of various materials, and to learn about the design and use of radiation protection devices used in handling radioactive materials. The exhibition hall serves as a visualized catalog of the devices supplied by the Khabarovsk Branch of the "Izotop" Association.

Consultations, reference and advertising literature, lectures, motion pictures about the advances in atomic science and engineering all serve as a link between the Branch and local industrial and scientific organizations. But this does not exhaust the tasks of the demonstration hall. Specialists of the exhibition hall will carry out local studies at the various interested enterprises.

An entirely new service offered by the Khabarovsk Branch is the supply of equipment on a trial basis. This service consists in that in agreement with the given enterprise, the Branch organizes the supply, assembly, adjustment, and experimental operation of radioisotopic instruments, even financing these measures if necessary. If the results are satisfactory and the instruments are accepted, the enterprise reimburses the Branch for the equipment and services supplied. On the basis of experience gained, the enterprise can decide whether to expand the use of radioisotopic instruments or not. Such services are now being given to several enterprises and have produced concrete positive results.

The materials exhibited in the demonstration hall testify to the possibilities of widespread use of radioisotopic engineering in the national economy of the Eastern Siberia, the Far East, the Kamchatka Oblast', and Sakhalin.

The demonstration hall of the Khabarovsk Branch of the "Izotop" Association will serve as a large lecture hall for specialists of the national economy whose task is to point out the practical applications of "peace atoms."

Translated from Atomnaya Énergiya, Vol. 37, No. 5, pp. 446-448, November, 1974.

Fig. 1. Exhibition hall of the Khabarovsk Branch of the "Izotop" Association.

The Plenum/China Program.

An event of singular importance for international science and technology.

Following closely upon the appearance of the first scientific periodicals in China since the Cultural Revolution, Plenum proudly announces the publication of authoritative, cover-to-cover translations of the major, primary journals from China, under the Plenum/China Program imprint.

These authoritative journals contain papers prepared by China's leading scholars and present original research from prestigious Chinese institutes and universities.

In addition to the biomedical and geoscience journals listed for 1974, the Plenum/China Program will publish cover-to-cover translations of periodicals in physics, chemistry, computer science, automation, mathematics and the engineering disciplines. The translations will be prepared by a large team of experts selected especially for the program, and each journal will be under the direct supervision of an outstanding authority in the field.

The first issue of each of the translation journals will be published in early 1974, and, as with our Russian periodicals under the Consultants Bureau imprint, the translations of the Chinese journals will be available within six months following the appearance of the original Chinese edition.

Subscriptions are now being accepted. Examination copies will be available in early 1974.

available in 1974

	Subscription Rates*
Acta Botanica Sinica (2 issues)	$ 75
Acta Entomologica Sinica (2 issues)	$ 55
Acta Geologica Sinica (2 issues)	$ 75
Acta Geophysica Sinica (1 issue)	$ 27.50
Acta Microbiologica Sinica (2 issues)	$ 55
Acta Phytotaxonomica Sinica (4 issues)	$125
Acta Zoologica Sinica (4 issues)	$125
Chinese Medical Journal (12 issues)	$195
Geochimica (4 issues)	$110
Kexue Tongbao—Scientia (6 issues)	$ 90
Scientia Geologica Sinica (4 issues)	$125
Vertebrata PalAsiatica (2 issues)	$ 60

forthcoming

Acta Astronomica Sinica (2 issues)

Acta Biochimica et Biophysica Sinica (2 issues)

Acta Mathematica Sinica (4 issues)

Genetics Bulletin (4 issues)

Huaxue Tongbao—Chemical Bulletin (6 issues)

*These prices are for the 1973 Chinese volumes which will be published in translation during 1974. Prices somewhat higher outside the U.S.

plenum

PLENUM PUBLISHING CORPORATION
227 West 17 Street, New York, N.Y. 10011
In United Kingdom 8 Scrubs Lane, Harlesden, London, NW10 6SE, England